Energy Yield Optimization of a Large-Scale PV Power Plant in Self-Consumption Mechanism

Mehmet Şenol

Submitted to the
Institute and Graduate Study and Research
In partial fulfillment of requirements for the degree of

Doctor of Philosophy
in
Electrical and Electronics Engineering

Eastern Mediterranean University
February 2017
Gazimağusa, North Cyprus

Approval of the Institute of Graduate Studies and Research

_____

Prof. Dr. Mustafa Tümer
Director

I certified that this thesis satisfies the requirements as a thesis for the degree of Doctor of Philosophy in Electrical and Electronics Engineering.

_____

Prof. Dr. Hasan Demirel
Chair, Department of Electrical and Electronics Engineering

We certify that we have read this thesis and that in our opinion it is fully adequate in scope and quality as a thesis for the degree of Doctor of Philosophy in Electrical and Electronics Engineering.

_____

Prof. Dr. Osman Kükrer
Supervisor

Examining Committee

1. Prof. Dr. Uğur Atikol _____
2. Prof. Dr. Osman Kükrer _____
3. Prof. Dr. Belgin Emre Türkay _____
4. Prof. Dr. Tanay Sıdkı Uyar _____
5. Prof. Dr. Şener Uysal _____

ABSTRACT

The objective of this thesis is to optimize the design parameters of a large scale photovoltaic power plant in order to find its optimal size having the lowest payback period. A methodology is proposed to guide the investors and technical staff in the design of such a system, with core emphasis on self-consumption policy. A flowchart of the process, that uses site survey, system components, associated costs, meteorological data, load analysis, is created. A three-step algorithm is developed in order to solve the optimization problem that searches for the PV plant size having the lowest payback period. The first phase of the algorithm is to minimize the energy fed into the grid for free of charge. In other words the self-consumption is maximized. The decision variables such as the tilt angle of the PV modules, number of PV modules connected in series across a string, number of strings connected to an inverter and the number of inverters are calculated in this phase. The second phase involves maximizing the occupied land area and determining layout of the PV plant. The layout is based on consecutive PV blocks in the installation area. Number of rows and columns in a PV block are obtained in this phase. Last phase is based on the calculation of the optimal size of the PV plant, which has the lowest payback period, by using an iterative approach. Net present value analysis is used as a supplementary tool in order to allow the investor to make better judgment on the project.

A case study is carried out in Cyprus International University campus in order to support the proposed methodology. The lowest payback period is achieved at 6.18 years with the total installed capacity of 712 kW_P. The payback period results

calculated by the proposed algorithm and PV*SOL Premium, which is one of the most commonly used PV planning software in the PV market, for each increment in the PV plant size are compared. The difference between the payback periods obtained from the proposed algorithm and PV*SOL Premium is 1.79% on average and 0.34% at the optimum PV plant capacity.

According to the case study, a 712 kW_p self-consumption PV plant can be installed on 9055 m^2 of land area. The initial investment cost is calculated as € 1,063,700. The system can consume 97.92% of its own annual production while only 2.08% of the annual PV energy generation is exported to the grid. The system reaches a self-sufficiency ratio of 25.02%. The net present value is calculated as € 7,091,000.

Keywords: Solar energy, large-scale PV power plant, non-incentivized self-consumption, design optimization.

ÖZ

Bu tezin amacı, büyük ölçekli fotovoltaik (FV) enerji santralinin tasarımını optimize etmektir. Öz tüketim politikasını temel alarak, böyle bir sistemin tasarımında yatırımcılara ve teknik personele rehberlik etmek için bir yöntem geliştirilmiştir. Bu bağlamda tüm süreci gösteren ve saha araştırması, sistem bileşenleri ile ilgili maliyetler, meteorolojik veriler, yük analizi konularını kapsayan bir akış şeması oluşturulmuştur. En düşük geri ödeme süresi olan FV santralini bulmak için üç adımdan oluşan bir optimizasyon algoritması geliştirilmiştir. Algoritmanın ilk aşaması, şebekeye ücretsiz olarak verilen ancak ekonomik karşılığı olamayan enerjiyi en aza indirgemektir. Bir başka değişle öz tüketimi en üst seviyeye çekmektir. FV modüllerinin eğim açısı, bir dizi boyunca seri bağlanmış FV modül sayısı, bir eviriciye bağlı dizi sayısı ve evirici sayısı gibi karar değişkenleri bu aşamada hesaplanır. İkinci aşamada, kullanılan arazinin hesaplanıp, FV santralinin yerleşimi belirlenir. Bu aşamada bir FV bloğunda bulunan yatayda ve dikeyde yerleştirilen modül sayıları belirlenir. Son aşamada ise tekrarlanan bir yaklaşım kullanılarak, en düşük geri ödeme süresi olan FV santralinin optimum büyüklüğünü hesaplanır. Net bugünkü değer analizi, yatırımcının projeyle ilgili daha iyi karar vermesine olanak tanıyacak şekilde geri ödeme süresi analizi ile birlikte kullanılır.

Önerilen metodolojiyi desteklemek için bir üniversite kampüsü için durum çalışması yapılmıştır. En düşük geri ödeme süresini olan 6.10 seneyi veren FV santralinin optimum kapasitesi 712 kWp olarak hesaplanmıştır. FV santralinin büyüklüğündeki her artış için önerilen algoritma ile hesaplanan geri ödeme süresi sonuçları PV*SOL Premium yazılımından elde edilen sonuçlar ile karşılaştırılmıştır. Önerilen

algoritmanın sonuçları ile PV*SOL Premium yazılımından elde edilen sonuçlar arasında yalnızca %3'lük bir fark olduğu görülmüştür.

Yapılan durum çalışmasına göre, 9055 m^2 arazi üzerine öz tüketim prensibi ile çalışan 712 kW_p gücünde bir FV tesisi kurulabilmektedir. Sistemin ilk yatırım maliyeti 1.06.700 € olarak hesaplanmıştır. Sistem, kendi yıllık üretiminin %97,92'sini tüketebilirken, yıllık PV enerjisinin yalnızca %2,08'ini elektrik şebekesine verilmektedir. Sistem, %25,02'lik kendi kendine yeterlilik oranına ulaşmaktadır. Net bugünkü değer 7.091.000 € olarak hesaplanmıştır.

Anahtar Kelimeler: Güneş enerjisi, büyük ölçekli FV santrali, teşviksiz öz tüketim, tasarım optimizasyonu.

To my Family

ACKNOWLEDGEMENT

First of all, I would like to express my sincere gratitude to my supervisor Prof. Dr. Osman Kükrer. His support and guidance helped me during the research phase as well as the writing of this thesis. His timely feedback and perceptive comments contributed greatly to getting my goals accomplished.

Besides my supervisor, I would also like to thank the examining committee members; Prof. Dr. Uğur Atikol, Prof. Dr. Belgin Emre Türkay, Prof. Dr. Tanay Sıdkı Uyar and Prof. Dr. Şener Uysal for their contribution and constructive criticism. Their comments help me to widen my research in various perspectives.

I would like to thank Assoc. Prof. Dr. Serkan Abbasoğlu who provided me an opportunity to study in the renewable energy field. I thank him for his continuous guidance and mentorship in the last decade of my life.

I would like to express my sincere appreciation to my colleague Asst. Prof. Dr. Neyre Tekbıyık Ersoy for her comments and technical support.

I am very thankful to Asst. Prof. Dr. Öykü Akaydın for being a constant source of motivation and for supporting me mentally throughout this grueling process.

Last but not least; I would like to express my gratitude to my family and friends for supporting me and for sharing my joy and sadness throughout my academic studies and my life in general.

TABLE OF CONTENTS

ABSTRACT iii

ÖZ v

DEDICATION vii

ACKNOWLEDGEMENT viii

LIST OF TABLES xi

LIST OF FIGURES xii

LIST OF SYMBOLS xv

ABBREVIATIONS xxii

1 INTRODUCTION 1

1.1 Review of World's Energy Sources 1

1.2 Solar Energy in the World 7

1.3 Electrical Power in Northern Cyprus 8

1.4 Overview of Solar Energy Support Schemes 12

1.5 Thesis Objective 17

1.6 Organization of the Thesis 18

2 SELF-CONSUMPTION POLICIES 19

2.1 Characteristics of the Self-Consumption Policies 19

2.2 Complementary Support Schemes 23

2.3 Self-Consumption Scheme Variants and Challenges 26

3 LARGE SCALE PV SYSTEM DESIGN ASPECTS 30

3.1 Site Survey for PV Power Plant 30

3.2 Electricity Consumption of the Facility 31

3.3 Meteorological Data Collection 34

3.4 Component Selection for PV Power Plants 36
3.4.1. PV Array 36
3.4.2. Inverters 39
3.4.3. Other Components 41
3.5 Mounting System 66
3.6 Grid Connection and Permit Process 68
3.7 Plant Layout Design 69
3.8 Costs Associated with PV Plants 72
4 METHODOLOGY 76
4.1 Structure of the Methodology 76
4.2 The Objective Function 79
4.3 Design Constraints 83
4.4 Design Parameters 91
5 CASE STUDY AND RESULTS 108
5.1 Structure of the Methodology 108
6 CONCLUSIONS AND FUTURE WORK 123
6.1 Conclusions 123
6.2 Future Work 125
REFERENCES 126

LIST OF TABLES

Table 1: Allowed capacity additions by year 10

Table 2: Main types of the solar energy support schemes (Dusonchet & Telaretti, 2015). 13

Table 3: Main characteristics and definitions of PV self-consumption scheme (IEA-PVPS, 2016). 20

Table 4: Self-consumption mechanism applied in Northern Cyprus 22

Table 5: Major support schemes in Europe 24

Table 6: Major support schemes in net-metering compensation model 25

Table 7: Parameters to be measured in a PV system 59

Table 8: Distribution transformer ratings 63

Table 9: Overview of the main factors affecting the performance of the PV system and the referred international standards for optimizing the energy production 64

Table 10: Nomenclature for equation (20) 73

Table 11: Decision variables 80

Table 12: PV module and inverter parameters 84

Table 13: Seasonal optimum tilt angles for different locations 89

Table 14: Cost components with definitions, units and weights 105

Table 15: Specifications of the PV modules (Yingli Green Energy Holding Company) 112

Table 16: Specifications of the inverters (SMA Solar Technology AG) 113

Table 17: Miscellaneous parameters of the PV system 114

Table 18: Simulated PV plant sizes 115

LIST OF FIGURES

Figure 1: Global primary energy consumption in 2014 and 2015. 1

Figure 2: Primary energy consumption by fuel in 2015. 3

Figure 3: Global CO_2 emissions from 1965 to 2015. 5

Figure 4: Evolution of the total installed PV capacity between 2005 and 2015. 7

Figure 5: Evolution of electricity generation and consumption in Northern Cyprus... 9

Figure 6: Historical support schemes in the PV market (IEA-PVPS, 2015). 14

Figure 7: Connection of the metering units in FiT compensation model 15

Figure 8: Connection of the metering units in PPA compensation model. 16

Figure 9: Connection of the metering units in self-consumption compensation model. 17

Figure 10: Main self-consumption business models. 21

Figure 11: Self-consumption models in different regulatory environments. 23

Figure 12: Regulatory scheme durations in Europe 28

Figure 13: Daily consumption and PV energy generation profile 32

Figure 14: Typical implementation of battery combined DSM in PV applications .. 34

Figure 15: Single-line diagram of an on-grid PV system 36

Figure 16: String and main DC cables in a PV array (MCS, 2012). 42

Figure 17: Upstream and downstream short-circuit currents in a string 46

Figure 18: Upstream and downstream short-circuit currents in between strings 47

Figure 19: Current levels for determining circuit breaker or fuse characteristics (Schneider Electric, 2015) 50

Figure 20: Steps for selecting LPS in PV systems 53

Figure 21: Recommended PV panel cabling method (Schletter Solar-Montagesysteme, 2014) 55
Figure 22: Rolling sphere method versus protective angle method (DEHN + SÖHNE, 2014) 55
Figure 23: Isolated (left) and non-isolated (right) LPS (Charalambous et al., 2013) 56
Figure 24: Earth termination system (DEHN + SÖHNE, 2014)..... 57
Figure 25: Flowchart of the proposed process to determine the optimal PV plant size 77
Figure 26: A typical accrued cash flow diagram of a PV power plant 82
Figure 27: PV block and available PV area dimensions 88
Figure 28: Equation tree of the optimization algorithm..... 92
Figure 29: Illustration of latitude, hour angle and declination angle (Kalogirou, 2009) 93
Figure 30: Representation of solar angles (Kalogirou, 2009) 94
Figure 31: Beam, diffuse and ground reflected irradiance..... 95
Figure 32: PV blocks installed in the available area 101
Figure 33: Electricity consumption of the University campus in years 2012-2015. 109
Figure 34: Daily electricity consumptions in a typical weekday, Saturday and Sunday 110
Figure 35: Evolution of electricity tariff for the universities in Northern Cyprus ... 111
Figure 36: Percent energy lost, self-consumption and self-sufficiency rates..... 116
Figure 37: Trends in the unit cost of the PV power plant investment 117
Figure 38: The change in PBP with respect to the installed PV capacity 118
Figure 39: Amount of PV energy injected into the grid and the change in payback period with respect to the installed PV capacity 119

Figure 40: Comparison of the PBPs of the projects with and without the land cost 120

Figure 41: Comparison of payback periods obtained from the proposed algorithm and PV*SOL Premium 121

Figure 42: Net present value and payback period 122

LIST OF SYMBOLS

A_{ac}	Cross-sectional area of AC cables (m^2)
A_{bl}	Area occupied by a PV block (m^2)
A_{dc}	Cross-sectional area of the DC main cable (m^2)
A_{loan}	Annual loan payment (€)
A_{max}	Maximum permissible area for the PV power plant (m^2)
A_{str}	Cross-sectional area of the string cables (m^2)
A_{tot}	Total area occupied by the PV power plant (m^2)
A_{tot_ini}	Initial value for the area occupied by the PV power plant (m^2)
C_{ac}	Unit cost of AC cables (€/m)
C_{dc}	Unit cost of DC main cables (€/m)
C_{EQ}	Equipment cost (€)
C_i	Unit cost of inverters (€/kW_p)
$C_{initial}$	Initial investment cost of the PV power plant (€)
C_L	Land cost (€/m^2)
C_{Lb}	Labor cost (€/kW_p)
C_{loan}	Amount of the loan (€)
C_{LPS}	Unit cost of the lightning protection system (€/kW_p)
C_{LPS_t}	Total cost of the lightning protection system (€)
C_{MS}	Unit cost of mounting system (€/kW_p)
C_{MS_t}	Total cost of mounting system (€)
C_{MV}	Unit cost of medium voltage cables (€/m)
C_{OM}	Operating and maintenance cost (€)

C_{PD}	Unit cost of over-current protection devices and the electric distribution boards (€/kW$_p$)
C_{PD_t}	Total cost of over-current protection devices and the electric distribution boards (€)
C_{per}	Grid permit cost (€)
C_{PV}	Unit cost of PV modules (€/kW$_p$)
C_{str}	Unit cost of string cables (€/m)
C_{TP}	Transportation cost (€)
C_{Tr}	Total cost of the medium voltage transformer (€)
$CIF(y)$	Annual cash in-flows (€)
D	Total distance between two successive PV blocks (m)
D_1	Mounting support clearance (m)
D_2	Depth of a PV block (m)
$d(y)$	Yearly degradation in the module's output power (%)
E_{pl_h}	Hourly energy produced by the PV power plant (kWh)
E_{pl_y}	Yearly energy produced by the PV power plant (kWh)
e_t	Electricity tariff (€/kWh)
EF_h	Hourly energy fed into the grid (kWh)
EF_y	Yearly energy fed into the grid (kWh)
EG_h	Hourly energy from the grid (kWh)
EG_y	Yearly energy from the grid (kWh)
f	Inflation rate (%)
G	Global horizontal irradiance (W/m^2)
G_B	Beam irradiance on horizontal surface (W/m^2)

G_D	Diffuse irradiance on horizontal surface (W/m^2)
g_e	Annual growth rate of the electricity prices (%)
g_m	Annual growth rate of the O&M cost (%)
G_t	Global irradiance on a tilted surface (W/m^2)
$\bar{H}$	Monthly average daily total irradiation (J/m^2)
h	Hour angle (°)
H_{bl}	Height of a PV block (m)
$\bar{H}_D$	Monthly average daily diffuse irradiation (J/m^2)
h_{ss}	Sunset hour angle (°)
h'_{ss}	Sunset hour angle on a tilted surface (°)
$\bar{H}_t$	Monthly average daily total radiation on a tilted surface (J/m^2)
i	Discount (interest) rate (%)
I_b	PV string design current (A)
i_f	Inflation adjusted interest rate (%)
I_{i_max}	Maximum DC input current (A)
I_{i_out}	Nominal AC output current (A)
I_{M_mpp}	Module current at MPP (A)
I_{M_sc}	Short circuit current of a module (A)
$I_{M\_sc\_max}$	Maximum short circuit current of a module (A)
I_{MV}	Current carried by medium voltage cables (A)
I_n	Nominal operating current of a protection device (A)
I_z	Current carrying capacity of a cable (A)
k_{ac}	Electrical conductivity of AC cables $\left(\frac{\text{m}}{\Omega \cdot \text{mm}^2}\right)$
k_{dc}	Electrical conductivity of the DC main cable $\left(\frac{\text{m}}{\Omega \cdot \text{mm}^2}\right)$

k_{str}	Electrical conductivity of the string cables $\left(\frac{\mathrm{m}}{\Omega \cdot \mathrm{mm}^2}\right)$
K_t	Clearness index
L	Latitude (°)
L_A	Maximum permissible length of the southern side of the area (m)
L_{ac}	Wiring length of AC cables (m)
L_{bl}	Length of a PV block (m)
L_{dc}	Simple wiring length of the DC main cable (m)
L_h	Hourly energy consumption (kWh)
L_{MV}	Wiring length of medium voltage cables (m)
L_{PV}	Length of the PV modules (m)
L_{str}	Simple wiring length of the string cables (m)
N_{bl}	Number of PV blocks
N_c	Number of columns in a PV block
N_i	Number of Inverters
N_{i_ini}	Initial value for the number of inverters
N_{i_max}	Maximum value for the number of inverters
N_p	Number of PV strings connected to an inverter
N_{p_max}	Maximum number of PV strings connected to an inverter
N_{PV_t}	Total number of PV modules in the PV power plant
N_r	Number of rows in a PV block
N_s	Number of PV modules connected in series across each string
N_{s_max}	Maximum number of PV modules connected across a string
N_{s_min}	Minimum number of PV modules connected across a string
P_{i_max}	Maximum DC input power (kW)

P_{i_out}	Rated AC output power (kW)
P_{in}	Output power of a PV array (kW)
P_{L_ac}	Power loss across AC cables (kW)
P_{L_dc}	Power loss across the DC main cable (kW)
P_{L_MV}	Power loss across medium voltage cables (kW)
P_{L_str}	Power loss across the string cables (kW)
P_{M_op}	Actual power output of a PV module (kW)
P_{M_STC}	Nominal power of a PV module under STC (kW_p)
P_{out}	Power produced by an inverter (kW)
P_{pl}	Power produced by a PV power plant (kW)
R_B	Beam radiation tilt factor
$\bar{R}_B$	Monthly mean beam radiation tilt factor
R_{MV}	Resistivity of the medium voltage cables (Ω/km)
saf	Shading factor (%)
SC_h	Hourly self-consumed energy (kWh)
SC_y	Yearly self-consumed energy (kWh)
sof	Soiling factor (%)
sp_{size}	Specific land-use of the PV power plant (m^2/kW_p)
T_A	Ambient temperature (℃)
T_c	Coldest possible day in a year (℃)
T_h	Warmest possible day in a year (℃)
T_M	Module temperature (℃)
V_{i_max}	Maximum DC input voltage (V)
$V_{i\_mpp\_max}$	Maximum MPP voltage (V)

$V_{i\_mpp\_min}$	Minimum MPP voltage (V)
V_{i_out}	Nominal AC output voltage (A)
V_{LV}	Voltage at the low voltage side of the transformer (V)
V_{M_mpp}	Module voltage at MPP (V)
$V_{M\_mpp\_max}$	Maximum MPP voltage of a PV module (V)
$V_{M\_mpp\_min}$	Minimum MPP voltage of a PV module (V)
V_{M_oc}	Open circuit voltage of a module (V)
$V_{M\_oc\_max}$	Maximum open-circuit voltage of a PV module (V)
V_{MV}	Voltage at the medium voltage side of the transformer (V)
W_A	Width of the available PV area (m)
W_{bl}	Width of a PV block (m)
W_{PV}	Width of the PV modules (m)
y	year
Z_s	Azimuth angle of the PV modules (°)
α	Solar altitude angle (°)
α_{sc}	Temperature coefficient of I_{M_sc} (%/°C)
β	PV module tilt angle (°)
β_{oc}	Temperature coefficient of V_{M_oc} (%/°C)
γ	Temperature coefficient of P_{M_STC} (%/°C)
δ	Declination angle (°)
η_i	Efficiency of the inverter (%)
η_{mppt}	Efficiency of the MPP tracker (%)
η_{tr}	Efficiency of the transformer (%)
θ	Incidence angle (°)

ρ_G	Surface reflectance (albedo)
ϕ	Zenith angle (°)

ABBREVIATIONS

DHI	Diffuse horizontal irradiance
DNI	Direct normal irradiance
DSM	Demand side management
DSO	Distribution system operator
FiP	Feed-in-premium
FiT	Feed-in-tariff
GHI	Global horizontal irradiance
IRR	Internal rate of return
KIB-TEK	Cyprus Turkish Electricity Authority
LCOE	Levelized cost of energy
LPS	Lightning protection system
LV	Low voltage
MCB	Miniature circuit breaker
MCCB	Molded case circuit breaker
MPP	Maximum power point
MPPT	Maximum power point tracker
Mtoe	Million tonnes of oil equivalent
MV	Medium voltage
NOCT	Nominal operating cell temperature
NPV	Net present value
PBP	Payback period
PPA	Power purchasing agreement
PR	Performance ratio

PV	Photovoltaics
RCD	Residual current device
ROI	Return on investment
SF	Sizing factor
SPD	Surge protection device
STC	Standard test conditions

Chapter 1

INTRODUCTION

1.1 Review of World's Energy Sources

Since the industrial revolution, world's total primary energy consumption trend has never changed. The continuous growth of the world's population, having greater accessibility to health, food and transport services, increased electrification and improvements in living standards play critical role in the rise of world's energy demand. After the recession in 2009, the global primary energy consumption has continued to rise. It increased only by 1% in 2015. This value is well below the last 10 year average of 1.9%. Figure 1 summarizes the primary energy consumption in years 2014 and 2015. Oil prices fell sharply in 2015 and the oil market responded to them.

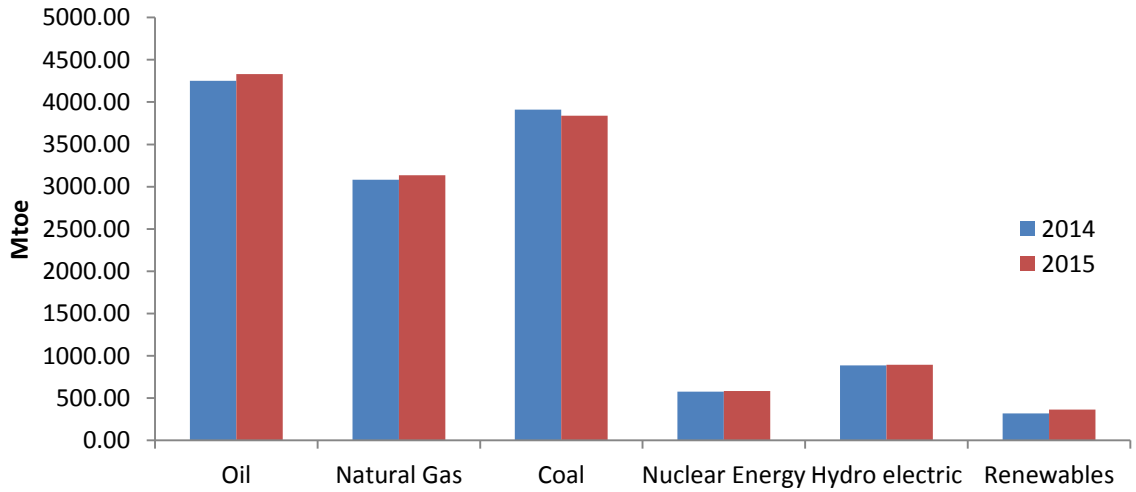

Figure 1: Global primary energy consumption in 2014 and 2015.

The fall in oil prices stimulated a solid growth in the worldwide oil consumption. The oil consumption grew by 80 Mt in 2015 which is equivalent to 1.9 million barrels per day. Ever since 1999, this has been the first increase in the consumption of oil. With a 1.9% increase in 2015, global oil consumption reached a 32.9% share as of end 2015. Similar to the case of oil, natural gas consumption grew by 1.7% in 2015. This growth corresponds to 54 million tonnes of oil equivalent (Mtoe). Natural gas consumption in the world reached a 23.8% share as of end 2015. Unlike oil and natural gas, global coal consumption fell sharply, recording a 1.8% decline in 2015. The global coal consumption decreased to 29.2% share as of end 2015. The two primary reasons driving this change in coal consumption can be analyzed on the supply and demand sides. On the supply side, the strong growth of US shale gas suppressed coal production within the US power market. On the demand side, the recession in the Chinese economy and the change in the structure of the Chinese industry reduced the global coal consumption (BP, 2016).

Despite the remarkable changes in global fossil fuel consumptions, nuclear energy and hydroelectric consumptions were rather static. The demand for nuclear energy and hydroelectricity grew by 1.3% and 1.0% respectively. The fastest growing source of energy in 2015 was renewable energy growing by 15.2%. Renewable energy sources in the power market grew by 48 Mtoe and as of end 2015 they reached 2.8% of the global primary energy consumption (BP, 2016). Figure 2 shows the primary energy consumption by fuel.

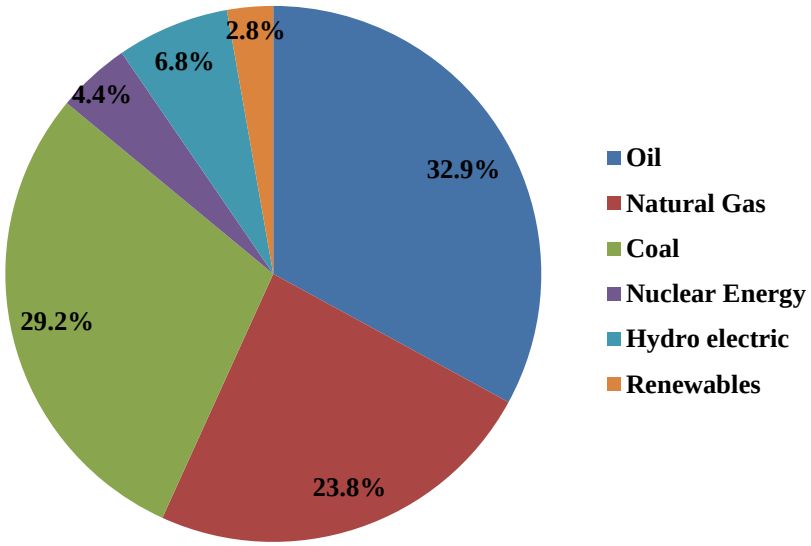

Figure 2: Primary energy consumption by fuel in 2015.

World's fuel mix involves a wide range of diverse options. Fossil fuels are historically the most important fuel type. Fossil fuels account for 76% of the global electricity production in 2015 (REN21, 2016). Tremendous investments have been made on fossil fuel since the industrial revolution. The use of fossil fuels has formed large part of our daily lives; hence it is projected that they will continue dominating the world's fuel mix by 2035 (BP, 2016). Though, the fossil fuels are historically important, its high usage has raised environmental and health concerns globally. The correlation between anthropogenic emissions of greenhouse gasses and global warming is very clear. Emission of gases from fossil fuels has had a great impact on the ecosystem (IPCC, 2015). It is foreseen that the current budget for CO_2 emission for 2100 will be used up by 2040; a major strategy that can help in avoiding to quadruple investments in low carbon or renewable energy (IEA, 2014). There has been a global call to avoid a 2° warmer world by the end of this century. In order to avoid the 2° increase in the atmospheric temperature, the countries of the world have agreed to speed up the transition from higher carbon intensity sources to cleaner ones

in the 21st session of the United Nations Climate Change Conference (COP21) in Paris (IRENA, 2016).

Energy transitions have happened before. Historically, a better performing fuel has always replaced a fuel which has a lower energy density. Energy transition takes a long period of time. From wood to coal and to oil, the dominant energy source has changed several times in the last 200 years. Wood used to be the dominant fuel until the coal overtook it at the end of the 19th century. Similarly oil became dominant in mid-20th century and it is still the most popular fuel today in the world (World Economic Form, 2013).

In recent years, the energy transition tends to follow a path through decarbonization. In spite of the fuel subsidies and falling prices in fossil fuel markets, the renewable energy based economy continued to accelerate in 2015. The investment in modern renewable energy capacity exceeded $265 billion by doubling the investment in fossil fuel based power generation systems (REN21, 2016). Together with the energy transition from coal to cleaner sources and the relatively slow increase in the energy demand, the growth rate of CO_2 emissions stalled in 2015. Carbon dioxide emissions increased just by 0.1% in 2015. This can be considered as the slowest growth rate since 1990, if the 2.1% decrease in the emissions in 2009 is excluded. The evolution of the CO_2 emissions in the last fifty years is illustrated in Figure 3. Accordingly, it can be seen that the global CO_2 emissions have risen by three times since 1965 (BP, 2016).

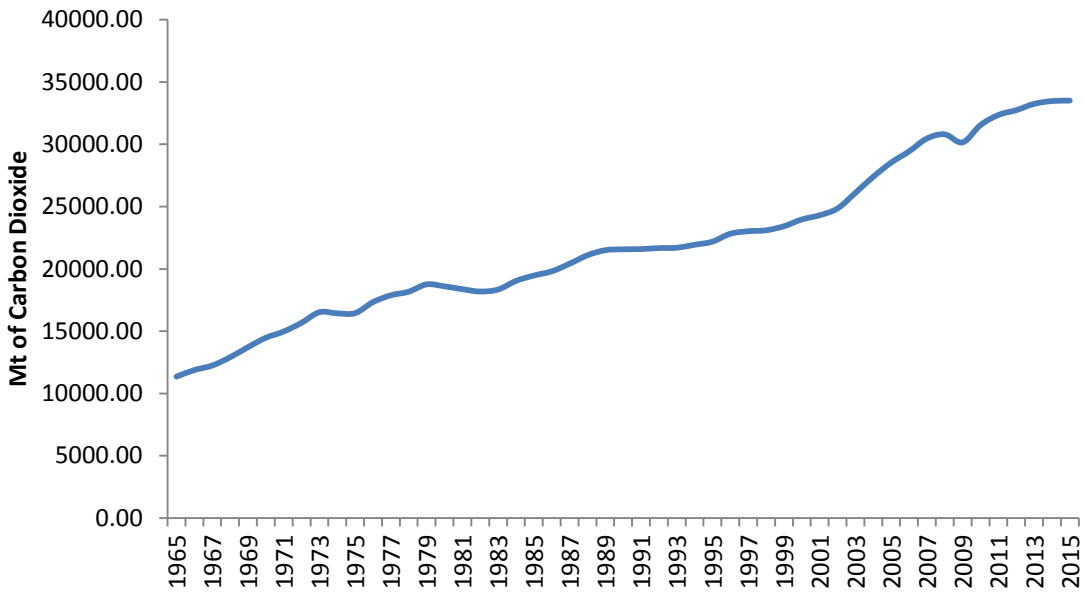

Figure 3: Global CO_2 emissions from 1965 to 2015.

International Panel of Climate Change (IPCC) states that 65% of the human related greenhouse gas emissions are CO_2 from fossil fuel burning and other industrial uses. The rest of the emissions are methane (CH_4), CO_2 from forestry and agriculture, nitrous oxide (N_2O) and fluorinated gases covered under the Kyoto protocol (IPCC, 2015). In addition to those greenhouse gases, there are other primary air pollutants originated from fossil fuel burning. Nitrogen oxides (NO_x), sulfur dioxide (SO_2), carbon monoxide (CO), black carbon and volatile organic matters (VOC) are the primary pollutants which cause air pollution by disturbing the air quality (IEA, 2016). CH_4, NO_x, SO_2, CO and black carbon emissions are almost entirely energy related with energy production and use. On the other hand, only two third of the VOC emissions are energy related. CH_4, NO_x and black coal emissions are 1.5 times higher compared to the 1970s levels. CO and VOC emissions have declined in recent years, but they are still slightly over the 1970s levels. SO_2 is the only pollutant that has generally deceased since 1970 (IPCC, 2014).

In light of the above statements, the number of the countries with renewable energy policy targets has increased from 45 to 173 over the last decade. Regulatory policies in the power sector cover 87% of the world's population. Most of these policies target the modern renewables such as wind, solar, geothermal, hydropower and biofuels (REN21, 2016).

Although each location in the world has its advantage to use indigenous renewable resources, globally the most widely accepted renewable energy resources, excluding hydropower, are wind and solar energy. In terms of cumulative installed capacity at the end of 2015, wind energy leads the renewable energy market, excluding hydropower, with a share of 55% followed by solar PV with 29% (REN21, 2016). The slowdown in the European PV market finally ended after the fourth successive year since 2011. The European PV market grew by 15% in 2015. This corresponds to 8.2% of the newly grid connected PV systems across Europe. The UK took the first place with 3.7 GW of added capacity. On the other hand, with 50.6 GW worldwide installed capacity, PV market continued growing by setting a new record in 2015 (EPIA, 2016). The majority of the global capacity additions took place in China and Asia-Pacific countries. Many countries around the world have already made commitments to decrease their emission levels. Hence, they have made voluntary pledges to increase their renewable energy capacities. Even in the worst case scenario, the solar PV power generation will continue to increase in the coming years (UNEP, 2015).

1.2 Solar Energy in the World

Studies have revealed that at each instant, the earth surface receives approximately 1.8×10^{11} MW of power from solar radiation which is much more than the total global consumption of power.

A review of solar energy policies implemented in different European countries (European Commission, 2015) is a clear indication of acceptance of clean energy from the sun. There are two popular and unique methods for electrical power generation: solar PV and concentrated solar thermal. In 2015, solar PV accounts for the largest share of growth in renewable-based generation (28%), followed by wind power (17%) in terms of installed power capacity (REN21, 2016). On the other hand, concentrated solar thermal power capacity grew only by 11% which was the half of the growth in 2014. Figure 4 depicts the evolution of the total global installed solar PV capacity from 2003 to 2015 (BP, 2016).

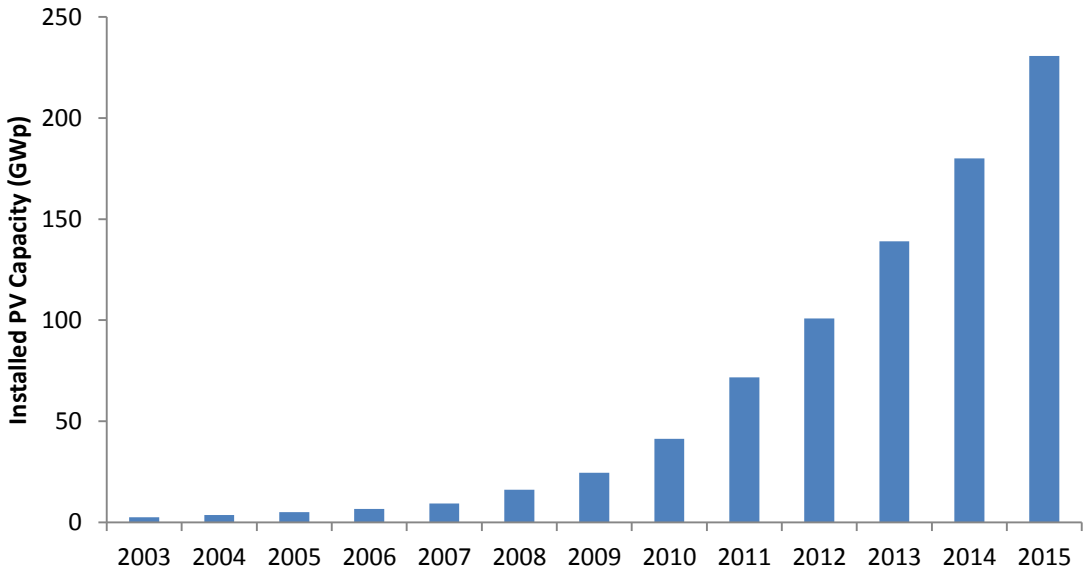

Figure 4: Evolution of the total installed PV capacity between 2005 and 2015.

When both of the solar energy technologies are compared, solar PV is the mature and financially viable options for power generation (IEA-ETSAP and IRENA, 2013). Solar PV could harness the sun's energy to provide large-scale, domestically secure, and environmental-friendly electricity. From the economic point of view, PV systems have become attractive in recent years. PV modules have faced the largest price drop in recent years and the global module price index is now less than 0.6 €/W_p for both wafer based and thin film technologies in European market (Fraunhofer ISE, 2015). The enticing and reliability features of PV systems are modularity, low maintenance and operation cost, low weight, and environmental cleanliness. Mostly, individual capacity of PV modules range from 100 W to 330 W. Several thousands of such PV modules need to be connected in order to get the MW range of power from PV system, thereby, requiring significant land area for the deployment of a large-scale PV. Studies indicate that the total area required for a MW scale PV power plant ranges from 30 MW/km^2 to 33 MW/km^2 (NREL, 2013).

1.3 Electrical Power in Northern Cyprus

The power system in Northern Cyprus is isolated and very small. However, nearly all of the electrical energy is supplied by conventional fossil fuel fired thermal plants. The lack of indigenous fossil fuels in Northern Cyprus makes the supply of energy expensive. Therefore, alternative renewable energy sources are expected to play a significant role in the energy mix of Northern Cyprus in the near future. In this context, the use of photovoltaics for direct conversion of solar energy into electricity has become a viable option considering the climatic conditions of Northern Cyprus. Annual electricity consumption and production of Northern Cyprus is illustrated in Figure 5. According to the data obtained from KIB-TEK, the electricity consumption

has grown by 4.8% per year (KIB-TEK, 2015). Figure 5 also shows the electrical power generation which is slightly over the consumption.

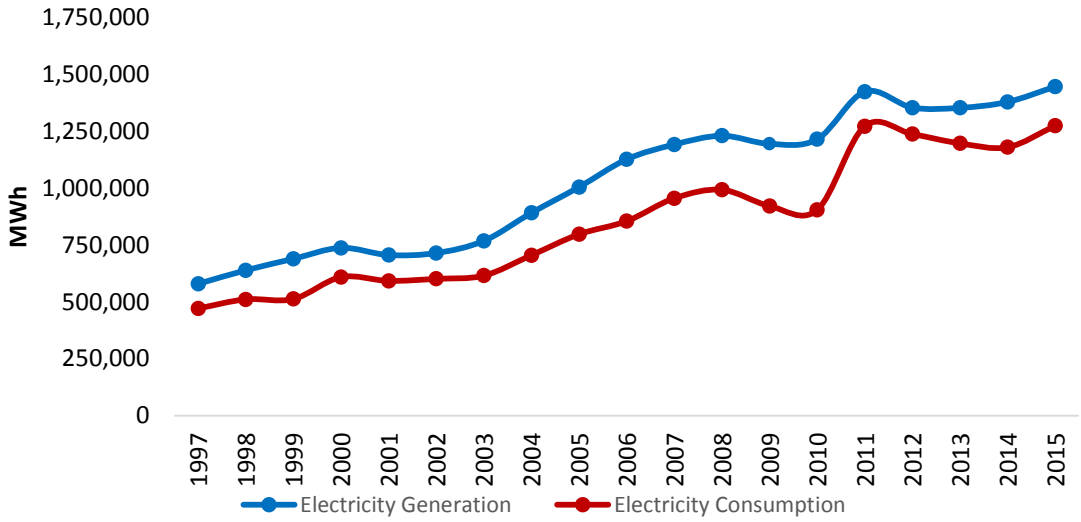

Figure 5: Evolution of electricity generation and consumption in Northern Cyprus.

99.81% of the generated electricity by KIB-TEK was produced by burning fuel oil in steam turbines and diesel generators. The contribution of solar energy to the energy mix of Northern Cyprus was only 0.14%. The remaining 0.19% of the demand was taken from Southern Cyprus (KIB-TEK, 2015).

Late 2000s saw acceptance of the need to use clean energy sources to reduce the dependency on the imported fossil fuels. Therefore, the Renewable Energy Law was passed by the parliament in 2011. After long discussions, the Renewable Energy Implementation and Inspection Regulation took its current state in November 2015 in the fourth major trial. A Renewable Energy Board has been established in the Ministry of Economy and Energy. The Board has been assigned some duties including accepting and approving the grid connected renewable energy projects and driving policies related with renewable energy.

A yearly capacity limit for PV systems is announced by the Renewable Energy Board in the beginning of each year. The established capacities for PV system additions since 2014 have been stated in Table 1.

Table 1: Allowed capacity additions by year

	2014	**2015**	**2016**
Residential	5 MW_p	2 MW_p	2 MW_p
Non-Residential	10 MW_p	5 MW_p	5 MW_p

Although a 29 MW_p capacity addition has been announced in the last three years, only a small number of applications have been made to the Renewable Energy Board. In this period, 819 subscribers applied to the Board for 16 MW_p of PV capacity additions in total. Nearly 7.7 MW_p of PV projects have been approved and 5.5 MW_p are allowed for grid connection since the Board was activated. 2.4 MW_p of the projects with grid connection permit is installed by residential consumers. The remaining 3.1 MW_p is installed by the subscribers who are using commercial, industrial, education and tourism tariffs. The rest of the applications were rejected due to several reasons such as lack of documents and inappropriate designs. The projects approved by the Board are entitled to receive an installation permit certificate. This certificate is valid for a year and the applicant has to complete the project in this timeframe.

According to the Regulation, only the facilities which are KIB-TEK subscribers are allowed to install a grid connected distributed energy generation system. This excludes the companies that are willing to construct renewable energy plants for commercial purposes.

The facilities are separated into two as residential and non-residential subscribers. Residential subscribers are able to sell the electrical energy they produce by renewable sources to KIB-TEK. Here, the electrical energy supplied by the residential subscribers is used to offset the electricity supplied by KIB-TEK to the residential consumer during the billing period. If the consumption is higher than the production, the subscriber only pays for the difference. However, if the consumer produces more electrical energy than he consumes, the extra generation is stored in his account as credits and these credits are used in the following months. Residential subscribers are allowed to install maximum 5 kWp (for single phase power) and 8 kWp (for three-phase power) of solar PV systems.

On the other hand, non-residential subscribers (commercial, industrial, tourism etc.) are not allowed to use the net metering service. Instead of getting benefit from the net metering service, the subscribers have to comply with the rules of self-consumption. Self-consumption is a service for non-residential subscribers to connect a renewable energy system, with a capacity corresponding to his consumption, to the grid. However, KIB-TEK does not pay anything for the non-consumed electricity which is fed into the grid. Therefore, the size of the photovoltaic system has to be well adjusted in order to prevent the excessive injections to the grid. Since the grid injections have no economic value, sizing a renewable energy system that has minimum grid injection is very important in terms of system financing. Additionally, the system sizing has a direct impact on the first cost and therefore the pay-back period of the investment.

Nicosia, the capital of Northern Cyprus, is known to have abundant sunlight. Located in the Eastern Mediterranean, it enjoys a daily average annual solar radiation of 5.2

kWh/m^2 (Abbasoğlu, 2011). This positions Northern Cyprus as a fertile location for conversion of solar energy to electricity and other applications.

Currently, the largest solar PV power plant in Northern Cyprus is operated by the Electricity Authority of Northern Cyprus (KIB-TEK); with an investment cost of €3.7 million by the European Union, it began operations in 2011, and produced 1950 MWh and 2,150 MWh in 2012 and 2013, respectively. The 1.27 MW_p power plant sits at Serhatköy. Besides this, Cyprus International University constructed totally 1.1 MW_p power plants at four different regions in its campus. This is followed by Middle East Technical University's 1 MW_p power plant in its Northern Cyprus Campus.

1.4 Overview of Solar Energy Support Schemes

In order to promote solar energy, various support schemes have been developed so far all around the world. Although the renewable energy support scheme was developed in the USA, Germany was the first country that initiated a program dedicated to solar energy. The aim of these programs was replacing PV panels on the rooftops. After the success of the 1,000 and 100,000 rooftop PV programs in 1990 and 1999 respectively, the global PV installed capacity started to rise by the aid of the new legislations and tariffs. Belgium, Denmark, Germany, Greece, Italy, Luxemburg, Poland and Spain are the first countries who embraced a feed-in-tariff scheme in the second half of the 1990s (European Commission, 2013). Solar energy support schemes can be analyzed under two main categories. These are price regulations and total installed capacity regulating mechanisms. Moreover, the support schemes can either focus on the investment or the energy generation. Table 2 summarizes the main types of solar energy support schemes.

Table 2: Main types of the solar energy support schemes (Dusonchet & Telaretti, 2015).

	Price Regulating Schemes	Installed Capacity Regulating Schemes
Investment Supporting Schemes	• Investment Subsidies • Tax Incentives • Soft Loans / Leasing	• Tender Schemes
Energy Generation Supporting Schemes	• Feed-in-Tariff • Net Metering • Self-Consumption • Green Certificates	• Renewables Obligation

Investment subsidies, tax incentives and soft loans are the most frequently applied investment supporting schemes. A financial subsidy such as a predetermined percentage of the initial cost of the investment is granted to the investor in order to build a renewable energy system. In the tax incentive mechanism, the investor benefits from various tax exemptions or tax credits. Fiscal incentives such as soft loans and leasing are typically applied in PV projects in order to finance the investments. Loans which are below the market interest rate are provided to the lender in soft loan mechanisms. A long term contract is signed between the financial institution and the investor in leasing programs. The investor pays back the borrowed money through a series of payments during the contract period. The aim of the investment supporting schemes is to urge the investors to invest in renewable energy by enabling attractive financial solutions, hence creating a competitive market.

The Green certificate program is a type of energy generation supporting scheme mostly used in Europe. It represents the environmental value of the energy consumed or generated. The organizations holding green certificates are supported by national trading schemes such as having higher FiT. These certificates are issued for a predetermined period of time.

Historically, feed in tariffs are the most widespread support mechanism adopted all over the world, with a market share of approximately 65% in 2015. Direct subsidies and tax rebates are in second place, with a share of 20%, followed by self-consumption/net-metering, green certificates or renewable portfolio standard (RPS) based schemes and power purchasing agreements (PPA) with shares of 8%, 4% and 2% respectively. (IEA-PVPS, 2015). The support schemes developed for the PV market until the end of 2014 are illustrated in Figure 6.

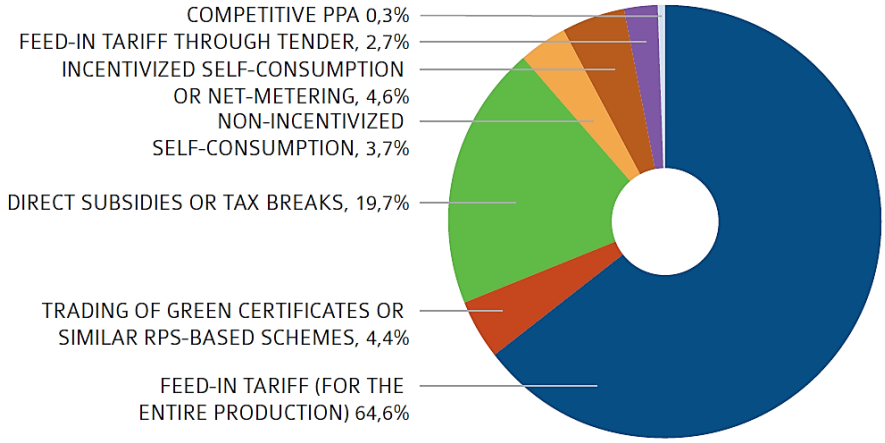

Figure 6: Historical support schemes in the PV market (IEA-PVPS, 2015).

Feed-in-Tariff (FiT) or Feed-in-Premium (FiP) mechanism is used in the markets where the grid parity has not yet been reached. Grid parity occurs when the cost of electricity generation from alternative sources falls below the price of power supplied by the grid operator. FiT is a typical support scheme applied in an immature market in order to initiate and develop the usage of PV energy. In the FiT mechanism, excess PV energy injected to the grid is valued at a price higher (if the market is immature) or lower (if the market is mature) than the retail price of electricity. The FiP is a kind of FiT approach where the value of the PV electricity exported to the grid is always higher than the retail price of electricity. Figure 7 shows a typical

connection of two metering units which are used in order to measure on-site generation and consumption distinctly in the FiT compensation model.

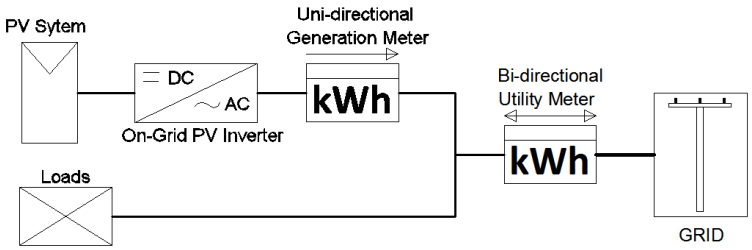

Figure 7: Connection of the metering units in FiT compensation model

Tendering procedure is a kind of FiT model. It is organized by regulatory bodies in such a way that a certain capacity of PV is put out to tender. Several bids are collected in the auction and a FiT-based contract is signed between the utility and the investor who wins the auction. A fixed FiT is paid for a predefined period of time. As it can be seen in Figure 6, tendering procedure is not a widely applied program in the world because inconsistencies may arise in the auctions held by different regulatory bodies. Therefore, this model may lose its attractiveness from the investor's point of view.

Power purchase agreement (PPA) is a contract commonly between a seller who generates PV electricity and a buyer (i.e. utility) who look to buy the electricity. If the local legislations permit, a third party can also own the generation asset through leasing structures. The buyers generally give purchasing priority to the renewable energy produced by the investors who are engaged in a PPA. According to IEA-PVPS, the market share of the competitive PPA schemes is only 0.3% as end of 2014. Figure 8 shows a typical connection of two metering units which are used in

order to measure on-site generation and consumption distinctly in the PPA compensation model.

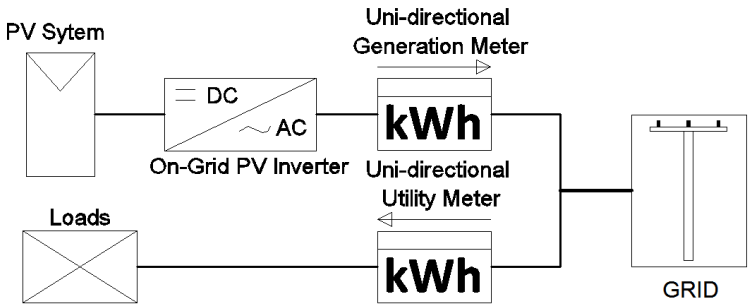

Figure 8: Connection of the metering units in PPA compensation model.

Self-consumption refers to the possibility of any kind of electricity consumer to connect a PV system, with a capacity corresponding to his/her consumption, to his/her own system or the grid, for his/her own or for on-site consumption, while receiving value for the non-consumed electricity which is fed into the grid (EPIA, 2013). Self-consumption can be analyzed in two main subcategories which are incentivized and non-incentivized models. PV production and consumption are compensated in real-time in the non-incentivized model. On the other hand, the compensation period is larger (i.e. monthly, yearly or even larger) in the incentivized model. If the compensation of production and consumption is based on energy flows, this is called a net-metering scheme. If the compensation is based on cash flows, it is called net-billing scheme. Figure 9 shows a typical connection of a single bi-directional metering unit which is capable of measuring the on-site generation and consumption simultaneously in the self-consumption compensation model.

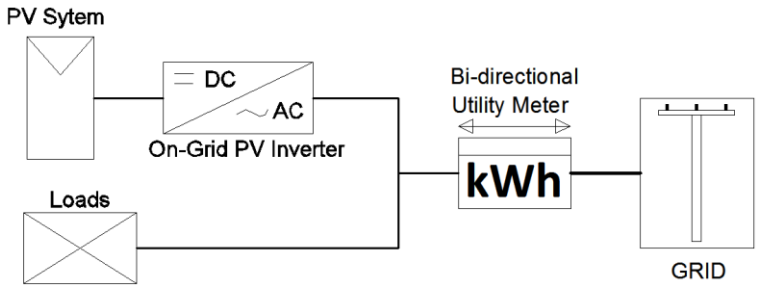

Figure 9: Connection of the metering units in self-consumption compensation model.

In 2015, the incentivized self-consumption mechanism such as net-billing and net metering was the second largest incentive with a share of 15% after feed-in-tariff (EPIA, 2016).

1.5 Thesis Objective

Previous studies have discussed the optimization of the layout of a large-scale PV plant (Kerekes et al., 2013), feasibility assessment of large-scale PV systems through sensitivity analysis of economic factors (Talavera et al., 2014), optimization of a large-scale PV plant for which FiT scheme is applied (Muneer et al., 2011) and impact of PV-battery systems on self-consumption on the basis of electricity cost (Merei et al., 2016). This research details the process flow of design and installation of a large scale PV power plant. The key objectives are to increase awareness of self-consumption mechanism in the design stage of large PV plants and also to make it available as a standard guide for technical staff and investors while selecting and installing large scale PV. This study also champions awareness of self-consumption in countries where there is no premium tariff or incentive for electricity fed into the grid. Northern Cyprus is considered as an example for such an approach mentioned above.

1.6 Organization of the Thesis

This thesis is organized as follows. Chapter 2 provides an extensive review of the self-consumption mechanism. Subcategories of self-consumption are analyzed and parameters which define self-consumption schemes are stated. In addition, the self-consumption compensation model in different countries around the world is presented. The key aspects in designing a large scale PV plant are stated in Chapter 3. Furthermore, the contribution of these key aspects to optimize the design of a large scale PV plant under the self-consumption mechanism is described. Chapter 4 presents the proposed methodology that guides the investors and technical staff in the design of such a system, with core emphasis on self-consumption policy. The optimum capacity of a large-scale PV power plant is determined by an iterative approach as stated in the flowchart, which considers the payback period as the decision criterion. Chapter 5 provides simulation and results based on the proposed methodology. Finally, conclusions are presented in Chapter 6.

Chapter 2

SELF-CONSUMPTION POLICIES

2.1 Characteristics of the Self-Consumption Policies

As described in section 1.4, the self-consumption mechanism mainly targets the local use of PV electricity generated by prosumers. Prosumer refers to an electricity consumer who compensates a part of his/her consumption by producing electricity. The amount of the self-consumption may change from a few percent of the consumption to 100%.

There is diversity of policies that permits PV self-consumption in different regulatory environments around the world. The main characteristics and parameters defining the self-consumption mechanism stated in (IEA-PVPS, 2016) are summarized in Table 3.

Various self-consumption business models have been developed so far depending on the maturity of the PV market. Each of these can be utilized in order to achieve high rates of self-consumption and increase PV competitiveness. The main driver of these business models is the levelized cost of electricity (LCOE) of PV and the grid parity. Depending on the regulatory environment, five main business models can be listed as follows (IEA-PVPS, 2016):

- Non-incentivized self-consumption
- Self-consumption with a feed-in-tariff scheme

- Net-billing
- Net-metering
- Self-consumption with feed-in-premium

Table 3: Main characteristics and definitions of PV self-consumption scheme (IEA-PVPS, 2016).

Characteristics		**Definition**
PV Self-Consumption	Right to self-consume	Subscribers are legally permitted to connect their PV systems to the power grid.
	Revenues from self-consumed PV	PV system owners can earn bonus/premium or green certificates for each kWh of self-consumed PV electricity. This becomes a direct income for the subscribers.
	Charges to finance T&D	Utility charges the PV system owners with additional costs or taxes.
Excess PV Electricity	Revenues from excess electricity	Excess PV electricity injected to the grid may find value depending on the applied policy. Energetic based compensation: Net-metering Monetary based compensation: Net-billing Traditional compensation: Feed-in-Tariffs No value for compensation: Non-incentivized
	Maximum timeframe for compensation	Consumed electricity is compensated in a predefined timeframe. Net-metering or Net-billing: Weekly, monthly, yearly or more Non-incentivized scheme: Real time
	Geographical Compensation	Consumption and production can be compensated in different locations. On-site generation is not necessary.
Other System Characteristics	Regulatory scheme duration	Duration of the compensation scheme.
	Third party ownership	A third-party can own the PV system through structures such as leasing or PPA.
	Grid codes and additional taxes/fees	The PV system has to comply with the grid codes. Some additional costs may arise due to the requests of the utility.
	Other enablers	Storage bonus, demand side management, time of use tariffs etc.
	PV size limitation	Utility can apply an upper limit for the PV systems under self-consumption scheme.
	Electricity system limitations	The governing body can set an upper limit for the maximum PV penetration.
	Additional features	All other parameters not considered above.

Self-consumption with premium can be preferred in immature PV markets where the cost of the PV electricity is higher than the price of the retail electricity. When the grid parity is achieved, either a FiT which is less than the retail electricity price or a non-incentivized self-consumption business model can be utilized. If the market is in

transition, that means LCOE of PV starts falling to the level of the retail electricity price, a net-metering or net-billing scheme can be applied. Figure 10 summarizes the business models in the self-consumption mechanism.

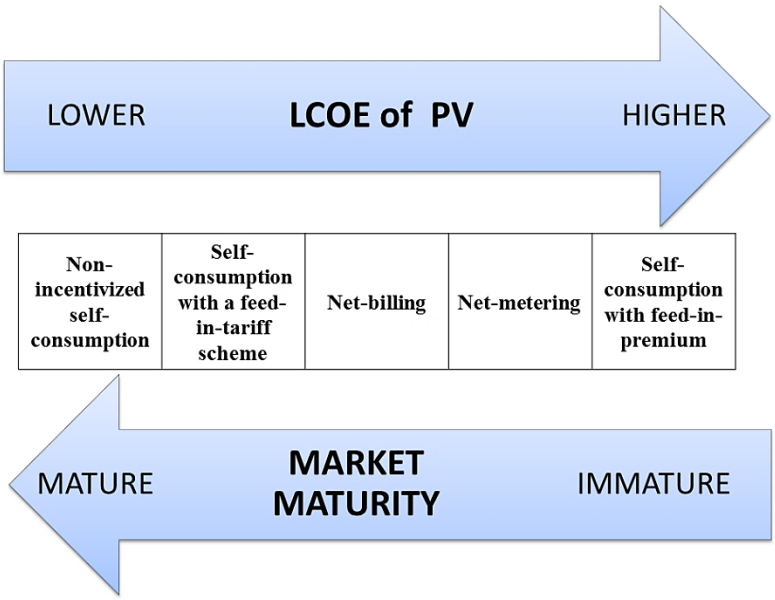

Figure 10: Main self-consumption business models.

Furthermore, the self-consumption business model is applied considering the type of the consumer. The consumption profile of commercial and industrial consumers aligns well with the PV generation. Therefore, high self-consumption ratios can be achieved. In places where the gird parity is already achieved, non-incentivized self-consumption model or FiT scheme is a viable solution. The demand pattern of a residential consumer often does not align with the PV generation. Net-metering or net-billing schemes overcome the difficulties of such consumers in achieving high self-consumption ratios and urge them to invest more in PV (European Commission, 2015).

In the light of self-consumption business models and consumers characteristics, the PV applications under the regulatory environment of Northern Cyprus can be

analyzed. Table 4 describes the current state of the PV applications in Northern Cyprus.

Table 4: Self-consumption mechanism applied in Northern Cyprus

Characteristics		**Residential**	**Non-Residential**
PV Self-Consumption	Right to self-consume	Yes	Yes
	Revenues from self-consumed PV	Savings on the electricity bills	Savings on the electricity bills
	Charges to finance T&D	None	Only for medium voltage applications
Excess PV Electricity	Revenues from excess electricity	Net-metering	None
	Maximum timeframe for compensation	One Month but no payment is proceeded until the subscription ends	Real time
	Geographical Compensation	On-site	On-site
Other System Characteristics	Regulatory scheme duration	20 years	Unlimited
	Third party ownership	None	None
	Grid codes and additional taxes/fees	Yes	Yes
	Other enablers	None	None
	PV size limitation	Up to 5 kWp for 1-phase Up to 8 kWp for 3-phase	Up to 500 kWp
	Electricity system limitations	10% of the total installed capacity	10% of the total installed capacity
	Additional features	None	None

Many European countries have already promoted the self-consumption mechanism. Spain, with no particular premium, authorized self-consumption in 2011 for systems up to 100kW. Germany removed the premium tariff in April 2012 as the FiT levels fell below the retail electricity prices. In order to force self-consumption, an upper limit was set for the produced electricity by the systems between 10 kW and 1 MW. According to this, the remuneration for self-consumed electricity sold to the grid was limited by 90% of the produced solar energy. A lower market price is paid instead of FiT, if the remaining 10% has to be injected into the grid. Furthermore, Germany funded 8300 battery storage systems in 2014 in order to urge self-consumption. The PV systems sized up to 500 kW in Italy can benefit from the self-consumption

premium tariff along with the FiT for the electricity injected into the grid (European Commission, 2015), (Dehler, et al., 2015).

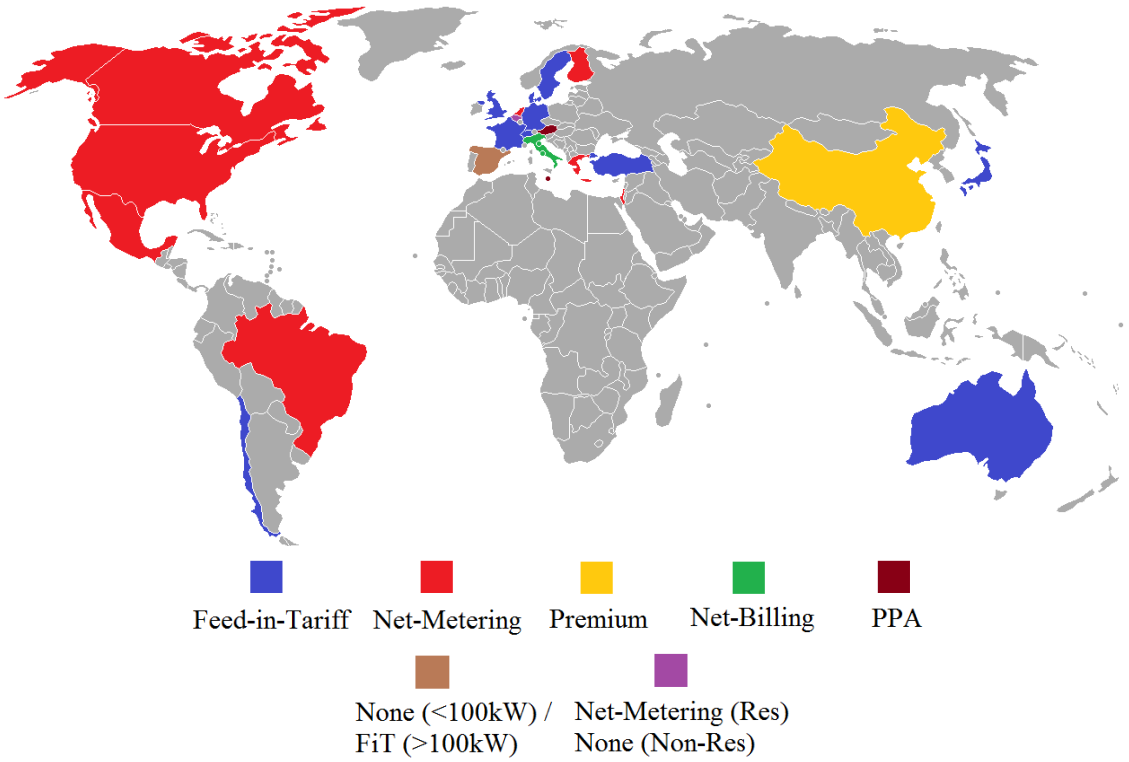

Figure 11: Self-consumption models in different regulatory environments.

2.2 Complementary Support Schemes

It is evident that self-consumption schemes are steadily being patronized in the EU; it should be promoted further as they have multiple benefits. Figure 11 illustrates the countries where consumers have the right to self-consume PV electricity. The locally produced and consumed PV electricity helps the prosumers to reduce their electricity bills. However, implementation of the self-consumption mechanism varies from country to country. Many European countries such as Germany, France, Denmark, Sweden, Switzerland, Turkey and the UK apply FiT based compensation. Additionally, Japan, Australia and Chile use FiT scheme as their primary

compensation policy. The FiT based self-consumption schemes are supported in different complementary ways in these countries. An overview of the complementary support schemes applied in Europe is shown Table 5.

Table 5: Major support schemes in Europe

Countries	Supporting measures	
France	FiT (20 years)	Capital subsidies
	Tender programs	Tax credits
	Reduced VAT rate	
Germany	FiT (20 years)	Self-consumption
	Market premium	Capital subsidies
	Low-interest loans	
Denmark	FiT (20 years)	Net-metering (1 hour only)
	Third party ownership	
Sweden	FiT (20 years)	Tax credits
	Green Certificates	
Switzerland	FiT (Unlimited)	Direct subsidies
	Multi-family housing compensation	
Turkey	FiT (10 years)	Local content bonus
	No license (<1 MW)	
United Kingdom	FiT (20 years)	Self-consumption
	Quota system with ROCs	Export tariff
	Tax breaks	Reduced VAT rate

On the other hand, Canada, USA, Mexico, Brazil, Finland, Greece, the Netherlands and Israel are prominent countries that utilize net-metering compensation model in the self-consumption mechanism. The net-metering schemes of the aforementioned countries vary by the revenues of the excess electricity exported to the grid, the timeframe for compensation and the netting period. In Brazil, the excess electricity can be fed into the grid. The difference between the energy consumed and fed into the grid is paid by the prosumers. Moreover, the excessive energy can be compensated during three years over retail electricity prices. In Canada, the implementation of the support scheme varies by jurisdictions in different provinces. A full net-metering scheme is applied in the countries stated above excluding Canada and Brazil. In this support mechanism, PV electricity surpluses are stored as energy

credits in order to offset the electricity consumption during the netting period. The compensation occurs in real-time. However, the energy meters read the consumed and produced electricity in every 15 minutes. An overview of the complementary support schemes for net-metering compensation model applied around the world is shown Table 6.

Table 6: Major support schemes in net-metering compensation model

Countries	Supporting measures	
Brazil	Net-metering up to 1 MW_p	Virtual net-metering is allowed
	Time-of-Use tariffs	Renting
Canada	Net-metering	Tendering & PPA
	Tax incentives	Time-of-Use tariffs
Greece	Net-metering	PV systems less than 20 kW_p are supported
	Netting period: Yearly	Non-incentivized
Finland	Net-metering	Up to 30% of investment subsidy
	Tax credits	On-site compensation
Israel	Full net-metering	Exchange for energy credits between users
Mexico	Full net-metering	Leasing is possible
	Virtual net-metering is allowed	Additional Financing options
The Netherlands	Full net-metering	Multi-family housing compensation
	PV system limit: 15 kW	
USA	Full net-metering	Simplified interconnection procedure
	On-site compensation	Accelerated interconnection timeline

Besides these predominant compensation models, a small number of countries utilize different compensation models. For instance, China applies a FiP scheme along with bonus for each kWh of saving on the electricity bill. On the other hand, Italy's "Scambio Sul Posto" offers a net-billing solution for the remuneration of PV electricity exported to the grid. This is achieved through various quotas based on grid service cost and electricity market prices. In Spain, two different types of regulations are in force depending on the system size. A non-incentivized self-consumption scheme is applied for the PV systems below 100 kW. The systems above 100 kW are

allowed to sell the excess PV electricity to the grid. The exported PV electricity gets a feed-in-tariff at the wholesale electricity price. Additionally, grid usage and energy production taxes have to be paid by the users. In Belgium, net-metering compensation model is applicable only for residential subscribers. Non-residential users are also allowed to self-consume but the excess PV electricity injected into the grid receives no compensation unless a PPA is signed.

2.3 Self-Consumption Scheme Variants and Challenges

To sum up, self-consumption mechanism for PV systems have so many benefits. When properly designed, it keeps grid costs under control through reduction of peaks. It ensures energy conservation to be driven at consumer level, thereby assisting in bridging the energy efficiency gap yet to be filled both at EU level and globally. When utilized together with demand side management policies and advanced energy storage systems, the types of self-consumption compensation models help the users to use energy efficiently by pushing them to adapt their load curve to the PV generation. Another benefit of self-consumption, which has the potentials of meeting climate protection, energy efficiency and renewable energy targets, is the leverage provided for private investors. Generally aggressive support schemes such as FiP are used in order to initiate and develop the renewable energy market. In such support mechanisms, the investors tend to inject as much energy into the grid as possible. This may introduce grid stability problems as discussed in Chapter 3.6. However, in self-consumption business models, the investors are encouraged to consume the energy generated by their renewable energy systems while keeping the injected energy into the grid at a minimum level. By this way, not only the possible congestion in the power distribution network is avoided, but also the share of renewables in the global consumption can be increased. The EU has high

targets on renewable energy for 2020; such targets can be achieved by the contribution of self-consumption.

The investment cost of PV systems is declining rapidly. Moreover, the markets which have already reached maturity due to the incentivized business models such as FiT or FiP, are shifting their solar PV policies towards self-consumption mechanism. The good match between the consumption and generation curve makes self-consumption scheme attractive for non-residential consumers such as SMEs. The positive impact of the mechanism on prosumers, electricity system actors and public authority has been anticipated by global PV markets. In many countries, duration of the regulatory scheme is unlimited. This urges the consumers to install PV systems because they can benefit from these systems until the end of their economic lifetime. Considering the benefits stated above, the self-consumption scheme has already started to be supported proactively all around the world. Figure 12 illustrates the regulatory scheme duration in Europe. The duration of the regulatory scheme is unlimited in the countries labeled as red color. Majority of these countries employs a net-metering business model of the self-consumption mechanism. The colors other than red indicate that the regulatory scheme is limited to 30 years, in those countries. A FiT support scheme is used in such regions.

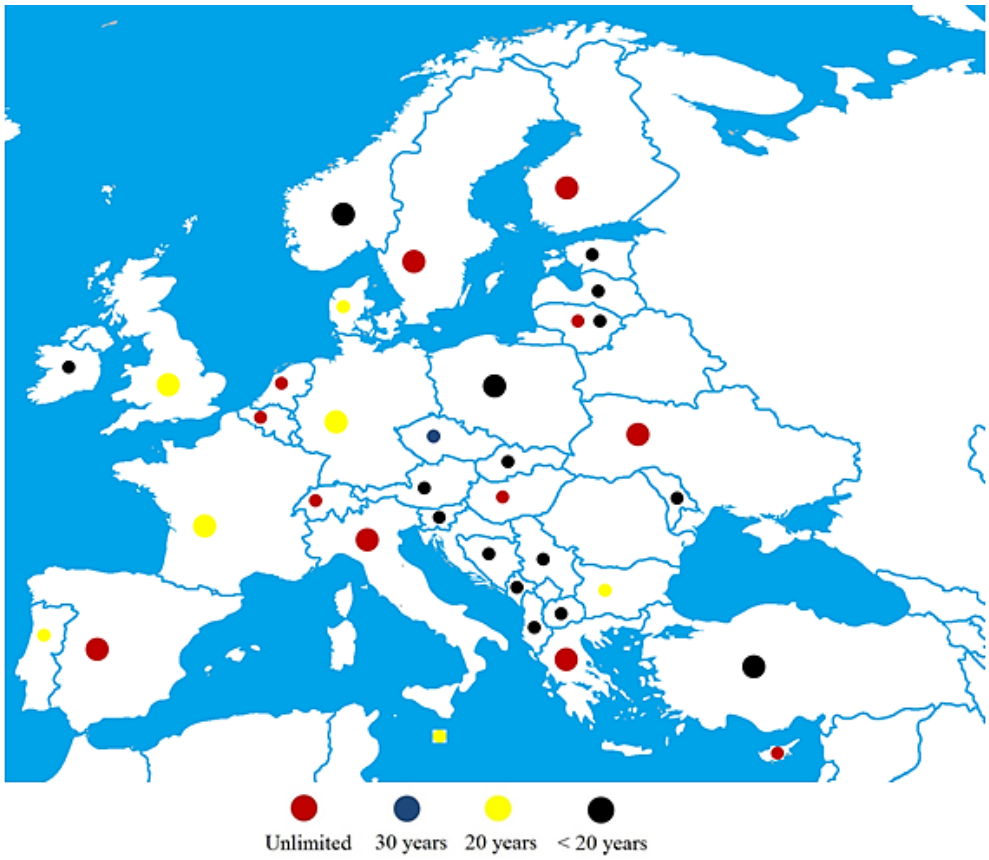

Figure 12: Regulatory scheme durations in Europe

Feed-in-tariff is a useful method in order to initiate and develop the PV market until the grid parity is reached. After the transition to competitiveness for PV is accomplished, the FiT scheme can be switched to the net-metering scheme. As a matter of fact, the grid parity has already been reached in the European countries where a net-metering support scheme is employed (Deutsche Bank AG, 2015).

Despite the huge benefits that can be derived from self-consumption, it faces several challenges such as under-development of smart meters, storage and financing. Another challenge is the issue of grid integration and system optimization. Extra charges taken for transmission and distribution systems plus additional grid taxes and fees stand as a barrier against the development of the PV market. This is one of the biggest reasons why the development speed of the PV market in countries such as

Australia, Belgium and Turkey is very slow. The biggest of all the challenges is lack of consumer awareness, regulatory frameworks, market size and understanding of consumers about the motivation to switch to existing alternatives. These drawbacks may affect the competitiveness of self-consumption business models and grid integration in a negative way.

Chapter 3

LARGE SCALE PV SYSTEM DESIGN ASPECTS

The following sections illustrate various aspects of designing a large-scale PV power plant for a big consumer. It serves as a guide for investors and concentrates on optimizing the installation capacity by implementing the methodology that is going to be discussed in Chapter 4.

3.1 Site Survey for PV Power Plant

Site selection for PV plants is very important and involves a wide range of information that can improve the performance and decrease the cost of the plant. Before determining the capacity of the PV plant, areas which are suitable for installation should be identified. In most of the large scale PV plant applications, direct grid feed-in without any internal consumption is allowed. In practice these are based on free standing open field installations. Land, maintenance and transportation costs, topography, distance to the grid, availability of the solar resource and the impact on the environment are essential factors in site selection. In addition to all of the factors listed above, the investor has to consider any removable of fixed obstacles that can cast partial shadow on PV modules. The cost of clearing the area from the obstacles should be taken into account.

This study focuses on the facilities which are subject to self-consumption mechanism. In other words, the facility must be a consumer and generate electricity from renewable energy resources for on-site consumption.

3.2 Electricity Consumption of the Facility

Electricity consumption mainly depends on the type of the building, regional climate and electricity prices (NREL, 2012). The load data based on these factors are important in determining the optimum PV plant capacity. Two different measurement methods can be used in order to determine accurate load profiles. The analysis can start with obtaining the monthly consumption data from the utility meter of the facility. Next, hourly consumption data should be measured. In a self-consumption mechanism, the aim is to maximize self-consumption, hence minimize the amount of the PV generation injected into the grid. Therefore, load matching is the key factor and important in determining the value of the on-site generation (Luthander et al., 2015). Due to this fact, hourly consumption profiles play more significant role in determining the capacity of the PV plant to be installed. Furthermore, the hourly profile data can be classified based on the working days, Saturdays, Sundays and public holidays (Talavera et al., 2014).

There is a couple of factors which should be taken into account in order to analyze the load curves in a PV self-consumption project. First of all, relative size of the on-site PV generation with respect to the electricity demand has to be taken into account. This is important in order to keep the injection of the excessive PV generation into the grid at minimum level. Second important factor is time resolution of the measurements. If the resolution of the collected data is low, then a misleading mismatch between the demand and PV generation curves can be realized. Therefore, it gives rise to an overestimation of the self-consumption (Talavera et al., 2014). Although, higher resolution data is always preferable, having the consumption and PV energy generation data with the same frequency provides a better match between

the curves. The measured data can be used in a PV simulation tool such as PV*SOL and the aggregated hourly profiles for the load can be obtained. Figure 13 illustrates a sample curve which combines the daily consumption and PV energy generation in an arbitrary day.

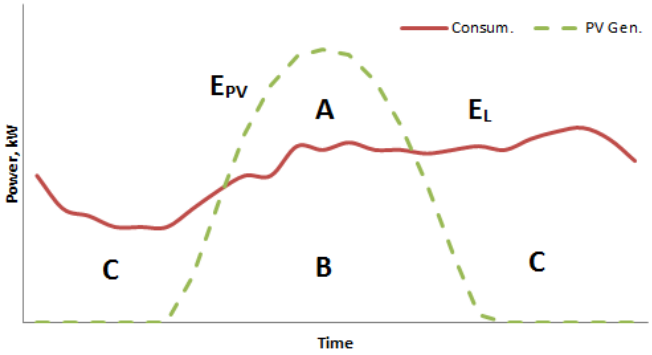

Figure 13: Daily consumption and PV energy generation profile

In Figure 13, the energy generated by the PV system and the energy consumed by the facility is shown as E_{PV} and E_L respectively. The rate of self-consumption can be calculated as follows:

$$Self - Consuption\ Rate = \frac{B}{A+B} \tag{1}$$

The aim of this study is designing a PV system by keeping the area, A, at the minimum level. Ideally this ratio should be as close as possible to 1. On the other hand, in the places where net-metering strategy is applied rather than self-consumption mechanism, the size of the PV system can be adjusted by taking the ratio of the PV energy generation to the energy consumption as shown below (Maranda & Piotrowicz, 2014):

$$Energy\ Ratio = \frac{A+B}{B+C} \tag{2}$$

In addition to the aforementioned criteria for having a better match between the consumption and PV generation curves, there are three different options used in self-consumption PV projects. These are; applying demand side management (DSM) for load shifting, using energy storage to shift a portion of the generated PV energy to evening hours (Luthander et al., 2015) and installing east - west oriented PV modules to broaden the generation plateau (Chobanov, 2014). These approaches can either be used separately or combined. Shifting loads from the periods without solar energy generation to the periods of excessive PV production involves the integration of an intelligent load management system. In residential buildings, DSM is typically applied by adjusting the operating time of the electrical appliances such as washing machines or heating ventilation and air conditioning systems. However, implementing DSM in industrial or commercial buildings is not as simple as mentioned above. The technical and economic processes in these sectors may be so sensitive that the DSM measures cannot be applied properly. For example, the energy demand due to educational and research facilities in a university may not be shifted to the periods of excessive PV production. Storage technologies, such as batteries or hot water storage tanks, can be used to cover a portion of the consumption in the absence of PV production. This can be achieved by combining PV system, batteries and an intelligent load management system as seen in Figure 14. Luthander et. al. have summarized different studies to measure improvements in different PV self-consumption mechanisms. According to their study, the self-consumption improvement for the PV system with battery varies between 10% and 30%. On the other hand, the DSM mechanism has improved the self-consumption by 2% to 15%. Best results have been achieved when the battery systems and DSM were used in combination (Luthander et al., 2015).

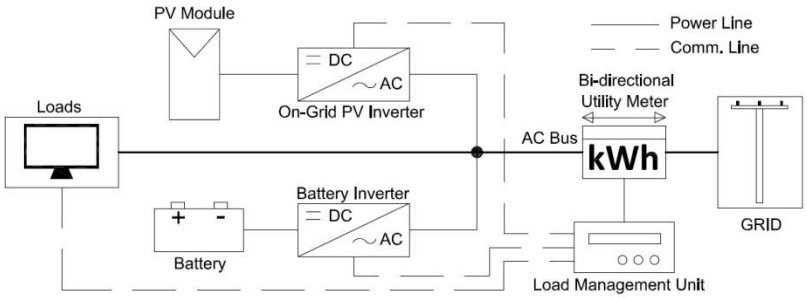

Figure 14: Typical implementation of battery combined DSM in PV applications

The orientation of the PV modules should be adjusted to minimize the PV energy injection into the grid, if the constant electricity pricing scheme takes place. However, different orientation options can be considered where time-of-use pricing scheme is applicable. The levelized cost of energy can be reduced with such an adjustment as the PV generation will mainly target the periods when the electricity price is higher (Sadineni et al., 2012). Region specific weather conditions (e.g. cloudy weather in the mornings or rain in the afternoons) also play a significant role in selecting the orientation of the PV modules (Rhodes et al., 2014). Moreover, the latitude of the site has an effect on the mounting strategy. For example, the simulation results have shown that a broader generation characteristic can be obtained with E-W oriented modules between April and October in Northern Cyprus. In the same time period, the daily generated PV energy from E-W oriented modules is more than that of South oriented systems.

3.3 Meteorological Data Collection

Collecting meteorological data is vital in estimating the amount of the PV energy generation. The meteorological data generally involves global radiation falling on horizontal and on the plane of array, wind speed and direction and ambient temperatures (Markides, et al., 2010). These data can either be collected by weather stations or obtained from online sources such as NASA, Meteonorm or PVGIS.

Nevertheless, the most consistent way of collecting meteorological data is installing a compact weather station at the site of installation. Most of the available commercial PV simulation software use monthly average irradiation and temperature data (NREL, 2014). Therefore, the data gathered by this method can be converted to average monthly values. Later, these values can be used in one of the commercially available PV simulation software to get the best simulation results.

The irradiation falling on the modules should be calculated as the input energy into the PV system. Unless measured beforehand, the irradiation incident on a tilted surface can be estimated by the following equation (Kalogirou, 2009):

$$\bar{R}_B = \frac{\sin(L-\beta)\cos\delta\sin h'_{ss} + (\pi/180)h'_{ss}\sin(L-\beta)\sin\delta}{\cos L\cos\delta\sin h_{ss} + (\pi/180)h_{ss}\sin L\sin\delta} \quad (3)$$

where $\bar{R}_B$ is the monthly beam radiation tilt factor, L is the latitude, β is the tilt angle, δ is the declination angle and h'_{ss} is the sunset hour angle on the tilted surface. h'_{ss} can be calculated as described in equation (4).

$$h'_{ss} = min\{h_{ss}, \cos^{-1}\}[-\tan(L-\beta)\tan\delta] \quad (4)$$

After calculating $\bar{R}_B$, daily total radiation on a tilted surface can be obtained by using equation (5).

$$\bar{H}_t = \bar{H}\bar{R}_B + \bar{H}_D\left(\frac{1+\cos\beta}{2}\right) + \bar{H}\rho_G\left(\frac{1-\cos\beta}{2}\right) \quad (5)$$

where $\bar{H}_D$ is the monthly average daily diffuse irradiation, $\bar{H}$ is the monthly average daily total irradiation and ρ_G is the ground reflectance (albedo).

After all, the climate data is entered into one of the solar energy simulation software in the market. These tools such as PV*SOL, PVsyst, TRNSYS etc. are capable of estimating the yearly yield of the PV system by taking the cable losses, module mismatch losses, system quality losses and inverter losses into account.

3.4 Component Selection for PV Power Plants

The grid-connected PV system is very common in countries where the policies support the excessive PV power generated to be injected into the grid. Figure 15 shows the components of a grid-connected PV system. This section focuses on the selection of the main components of such a system and the criteria to be taken into account by the investors in optimizing the performance of the system.

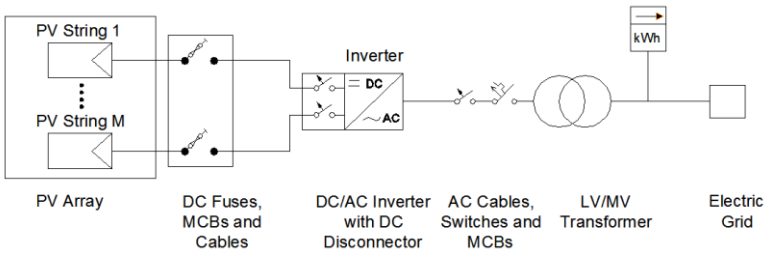

Figure 15: Single-line diagram of an on-grid PV system

3.4.1. PV Array

PV array is the heart of the system and is actually the interconnection of the PV modules that are responsible for supplying PV power. Therefore, the investors should have the data about performance, reliability, stability and degradation of the PV modules before the investment has been made. The performance of a PV system highly depends on the ambient and the cell temperatures. Here, the cell temperature is the most important parameter and has the greatest impact on the performance of a PV module. The heat exchange with the environment depends on ambient temperature, wind speed and direction, heat transfer coefficient between the module

and the environment and the thermal conductivity of the module (Skoplaki & Palyvos, 2009).

PV plant design heavily depends on the rated power of the PV modules as specified on their nameplates. It is important to know that the module can only work at its rated power under Standard Test Conditions (STC). STC stand for an irradiance of 1000 W/m^2, an atmospheric mass (AM) 1.5 solar spectrums and a temperature of 25℃. However, STC fails in estimating the real performance of the modules since there are only few days in a year that these conditions are observable. Solar irradiation is the parameter that has the strongest impact on the rise in cell temperature. Since the final operating temperature of a module is a result of the thermal equilibrium between the heat generated by the PV module and the heat lost to the surroundings due to conduction and convection, nominal operating cell temperature (NOCT) model better estimates the cell temperature. The NOCT conditions are; 800 W/m^2 of irradiance, 20℃ of ambient temperature and 1 m/s of wind speed. There are several studies in the literature and (Skoplaki & Palyvos, 2009) lists a number of equations, which are used to estimate the cell temperature.

After having the monthly average global irradiation data on a horizontal or on a tilted surface, the maximum power produced by each module in an array can be calculated.

$$P_{M,EST} = P_{M,STC} + \frac{dP_{M,STC}}{dT} \times (T_M - T_{STC}) \quad (6)$$

For the equation above, the required cell temperature can be calculated using NOCT approach in equation (7) which also is stated in the manufacturer's datasheet (Talavera et al., 2014).

$$T_M(℃) = T_A(℃) + G\left({}^{W}/_{m^2}\right) \times \frac{NOCT(℃) - 20℃}{800\,{}^{W}/_{m^2}} \quad (7)$$

The increase of the module temperature not only has an adverse effect on the module's output power but also has a negative impact on the open circuit and the maximum power point voltage of the module. Thermal performance of a module strongly depends on the cell technology. Thin film modules have superior thermal performance over crystalline modules. In other words; they have smaller temperature coefficients (Houshmand et al., 2015). Various studies in the literature have shown that the temperature coefficient of amorphous Silicon (a-Si) and Cadmium Telluride (CdTe) solar cells are around -0.2%/K and -0.25%/K respectively. In addition, Copper Indium Gallium Selenide (CIGS) solar cells tend to have temperature coefficients between -0.36%/K and -0.42%/K (IEA-PVPS, 2014). On the other hand, the temperature coefficient of multi-crystalline Silicon (mc-Si) solar cells varies between -0.38%/K and -0.49%/K. Commercially available single-crystalline (sc-Si) solar cells have a wider range of temperature coefficient. Based on the implementation concept, the temperature coefficient of sc-Si can be between -0.30%/K and -0.56%/K (Markides, et al., 2010). In addition to the temperature coefficient, long-term performance loss rate plays an important role in selecting the PV modules. In contrast to their lower temperature coefficients, thin film based PV modules suffer from higher performance losses in long-term operation. After five years of measurements, the study of Markides et al. has shown that the annual loss rate of thin-film PV modules is three times larger than that of wafer based technologies in Cyprus (Markides et al., 2014). As a result it should be noted that, modules having small temperature coefficients is a technical advantage especially for hot climates. However, long term performance of the modules must be considered

too, as it contributes highly to the levelized cost of electricity produced over its lifetime because module price accounts nearly 23% of the total system cost (NREL, 2015).

3.4.2. Inverters

PV systems are connected to the power grid over on-grid inverters which can be considered as the brain of the system. On-grid PV systems are designed to operate in parallel with the power grid. This type of inverters latches with the grid voltage and frequency. Its main task is to inject power to the grid. Basically it behaves like a current source (Rashid, 2007). In addition to its main task, a good quality inverter is expected to have some other characteristics, such as high efficiency, having a wide range built-in maximum power point tracker (MPPT), anti-islanding, operation under high temperature and humidity conditions and having low harmonic content. Moreover, modern inverters are expected to have services such as reactive power compensation, fault ride through, power quality improvement, grid voltage stability, islanding operations and black start capabilities (IEA-PVPS, 2014), (Shah et al., 2015). These services are required in order to maintain a stable operation of the power grid which is heavily dominated by distributed energy resources. Many local electrical wiring regulations make it mandatory for the inverters to have protective devices such as DC side disconnection device, residual current device, DC surge arrestor etc.

Depending on system size and partial shading conditions, implementation topology of the inverters can change. Central inverter is a better choice for larger PV systems where all of the PV modules are installed in the same area and have the same orientation and the angle. This topology allows easier system design and implementation and has the least cost per kW. On the other hand, the increase in the

DC cabling raises the initial cost of the system. Alternatively, string inverters can also be used in large scale PV installations as a flexible solution. Since each string is independently operated by its own MPP tracker, the system becomes more resilient to module mismatches and guarantees a higher yield under partial shading conditions (SMA Solar Technology AG, 2008). Despite, implementation of such a design is more complex and the cost per kW_p is higher than that of a central inverter. Besides the aforementioned implementation topologies, micro inverters can be considered as another alternative solution. However, the increased cost in large scale applications is the primary disadvantage of micro inverters.

Independent of the selected topology, the number of strings and the number of modules in these strings can be calculated by the following set of equations from (8) to (10). The operating point of the inverter must be between the MPP tracking limits. As the modules in a string are connected in series, the number of modules directly affects the string voltage. The string must be designed in such a way that the open circuit voltage of the string ($U_{oc\_max} \times n_{max}$) is less than the maximum DC voltage of the inverter (U_{inv_max}) in the coldest possible day and MPP voltage of the string ($U_{mpp\_min} \times n_{min}$) is not less than the minimum MPP tracking boundary of the inverter ($U_{inv\_mpp\_max}$) on a hot day (Gorji et al., 2011).

$$n_{max} \leq \frac{U_{inv\_max}}{U_{oc\_max}} \tag{8}$$

$$n_{min} \geq \frac{U_{inv\_mpp\_min}}{U_{mpp\_min}} \tag{9}$$

On the other hand, the maximum number of strings to be connected to the inverter is determined by the maximum current, namely the short circuit current, generated by the PV modules.

$$n_{String} = \frac{I_{inv\_max}}{I_{SC\_\max\_string}} \tag{10}$$

3.4.3. Other Components

Although, PV modules and inverters are the major components in a solar energy system, DC and AC cables, external lightning protection and grounding, protection devices, MV transformer and monitoring system are very important for a reliable PV power plant. These complementary system components and the strategies for optimizing the system performance are described in the following sub-sections.

i. DC and AC Cables:

Wiring and cabling in electrical systems are essential. It becomes more important in PV systems because the cables must withstand harsh environmental and electrical conditions for the entire lifetime of the plant. Ultraviolet radiation, precipitation, high operating temperatures and other environmental conditions must be taken into account while selecting the conductors in PV projects. The cables used on the DC side of the PV systems can be separated further into two categories; string or module cables and dc main cable. String or module cables are used to connect the modules one to another and to the combiner box or inverter. String cables are single core double insulated cables. These cables are generally laid across the mounting system without conduits. Therefore, they must be resistant to external influences such as ozone, petroleum, UV, acid and base. Moreover, these cables must be flame redundant, fire resistant and halogen free because, hazardous gasses are emitted if the

cable burns. Figure 16 illustrates the sting and main dc cables in a PV array with M modules connected in series and N strings connected in parallel.

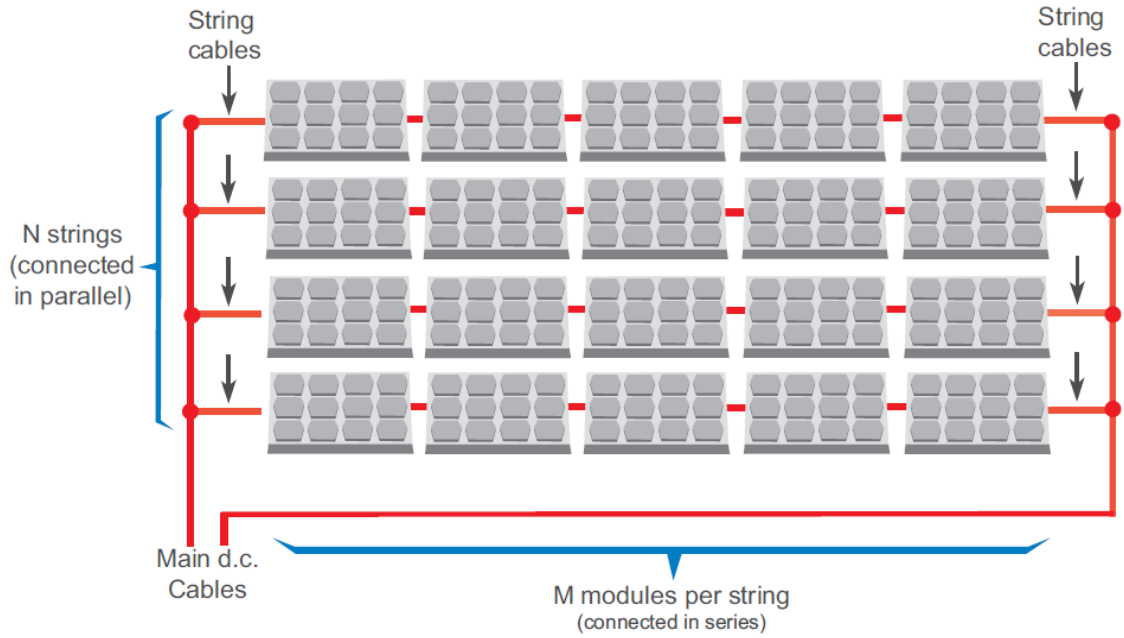

Figure 16: String and main DC cables in a PV array (MCS, 2012).

It is important to size the cables properly in a PV plant. Although, using oversized cables are often beneficial in terms of energy distribution, it may increase the first cost of the system without a proper engineering design. Under these circumstances, the designer must pay attention to the method of lying of cables, number of cores in each cable, location of the cables, ambient and operating temperatures of the cables (DGS LV Berlin BRB, 2008). Each one of these factors plays a significate role on the current carrying capacity of the cables which is often referred as I_z. The current carrying capacity shall not be less than the design current of the string which is I_b and the nominal current of the protection device which is I_n. The short-circuit current, I_{sc}, of the modules under standard test conditions should be considered while calculating I_b. I_{sc} may rise 25% from its value at STC if the solar irradiance exceeds 1000 W/m^2 (ABB, 2010).

In addition to the current carrying capacity, voltage drop across the cables is also important in conductor sizing. It is directly proportional to the cross-sectional area but inversely proportional to the length of the conductor. It is advised that the percent voltage drop on the DC side shall not exceed 1.5% of the nominal voltage of the system (Talavera et al., 2014).

The use of DC main cable completely depends on the design approach. It is used to connect the DC combiner box and the inverter. The design strategies stated for string cables are also valid for DC main cable. However, UV resistance and ability to withstand high operating temperatures may not necessary for this cable because it is generally installed in a conduit away from PV panels. The voltage rating of both the string and DC main cable should be at least 15% more than the open circuit voltage of the string (International Finance Corporation, 2012).

Cabling on AC side is more conventional than that of DC side hence the national codes and regulations which is readily used for electrical wiring applications can be used. There are two critical concerns about AC cabling. These are; the impedance of the AC line between the inverter and the point of common coupling and the voltage drop rate across this line. These parameters are important because they directly affect the operation and the feed-in capability of the inverter. Therefore, the instructions specified by the inverter manufacturer should be taken into account.

To sum up, optimal cable sizing in PV plants does not only have positive impact on profitability of the system but also it also improves the performance ratio, shows better response to potential short circuits and improves the lifespan of the cables.

Table 9 summarizes the components of a PV plant and the corresponding international standards.

ii. Over-Current Protection Devices:

Over currents may occur in PV systems both on supply (DC) and load (AC) side of the inverters. Therefore different methods shall be employed in order to protect the PV systems against any damage from short circuit and fault currents. The most commonly observed reasons for short circuit in PV systems are listed below (ABB, 2010).

- Insulation failure of the cables (e.g. fault between polarity of the PV system on the DC side)
- Fault to earth and double fault to earth in grounded systems (e.g. in case the conductor contacts with earth)
- Ground faults within PV panels (e.g. in case the cells are contacting with the panel frame due to the damage of the encapsulation)
- Grid voltage dips (inverters may generate higher currents in normal operation conditions)

The over-current protection on the AC side is a more familiar method of protection and can be achieved suitable miniature circuit breakers (MCBs) and molded case circuit breakers (MCCBs). On the other hand, protection against over-current on the DC side is slightly different and care must be taken while sizing and selecting the protection devices.

String fuses or DC MCBs can be used for over-current protection on the DC side after consulting the national codes and regulations. The devices employed in string and array protection must be DC compatible and double pole. Since the short circuit

current (I_{sc}) of a module is only slightly higher than its current at maximum power point (I_{mpp}), short circuit protection is not necessary when I_z of the string cable is at least 1.25 times of I_{sc}. This statement is valid only for the systems having at most two string connected to an inverter (IEC 60634-7-712:2002, 2002). Additionally the rated voltage of string fuses can be calculated by utilizing the following equation.

$$U_{rated} = U_{oc\_STC} \times M \times 1.15 \quad (11)$$

where M is the number of modules in a string.

If two or more strings are connected in parallel, a reverse current may occur in case of a fault across the string. A short-circuit in one or more modules in the string or in the string cable causes the open circuit voltage across the string to fall below the open circuit voltage of other healthy strings. Therefore, a reverse current starts to flow downstream from the healthy strings to the faulty string. According to IEC 61730-2 standard, a PV module has to withstand a certain amount of reverse current (IEC 61730-2:2016, 2016) and this value has to be declared on its datasheet by the manufacturer (EN 50380, 2003). However, if more than two parallel strings are used in an array, the fault current exceeds the capability of the module to withstand reverse currents. In this case, the string has to be protected against over-current by an extra protection device such as a gPV fuse or a DC MCB (IEC 60269-6:2010, 2010). Reverse current is dangerous because it may lead to excessive heating of the modules, hence destructing them and causing fire in the string. Equation (12) can be used to check whether an external protection against reverse current is required (Schneider Electric, 2015).

$$1.35 \times I_{R\_max} < (N-1) \times I_{sc\_max} \quad (12)$$

where I_{R_max} is the maximum reverse current characteristic of PV modules declared by the manufacturer and *N* is the total number of parallel strings.

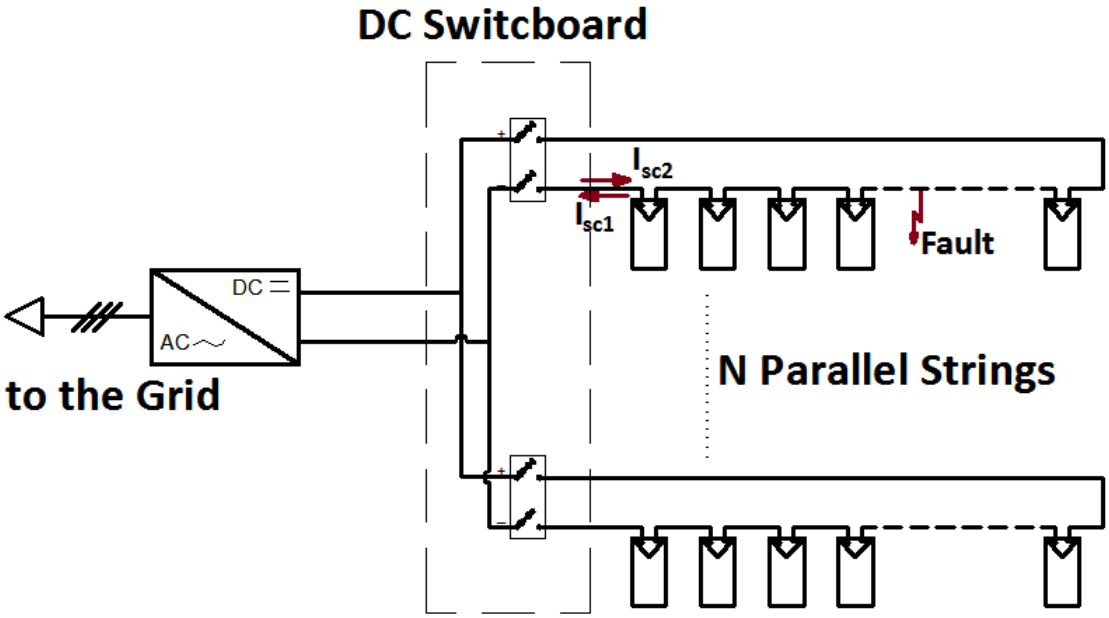

Figure 17: Upstream and downstream short-circuit currents in a string

The size and direction of I_{sc} varies depending on the location of the fault in the PV array. **Figure 17** shows a PV array with *N* parallel strings and *M* panels connected in series in each string. In such an array design, if a fault occurs in a string cable or a module in a string, an upstream (I_{sc1}) and downstream (I_{sc2}) short circuit currents at the same time (ABB, 2010). The magnitudes of these fault currents can be calculated using equation (13).

$$I_{sc1} = 1.25 \times I_{sc\_STC}$$
$$I_{sc2} = 1.25 \times N \times I_{sc\_STC} \quad (13)$$

Combiner boxes can be employed as subfield switchboards in large scale PV power plants especially when the system is designed by using central inverters. In this case, a fault may occur on the cable between the subfield switchboard and the inverter switchboard. Figure 18 illustrates a PV system designed with DC combiner boxes.

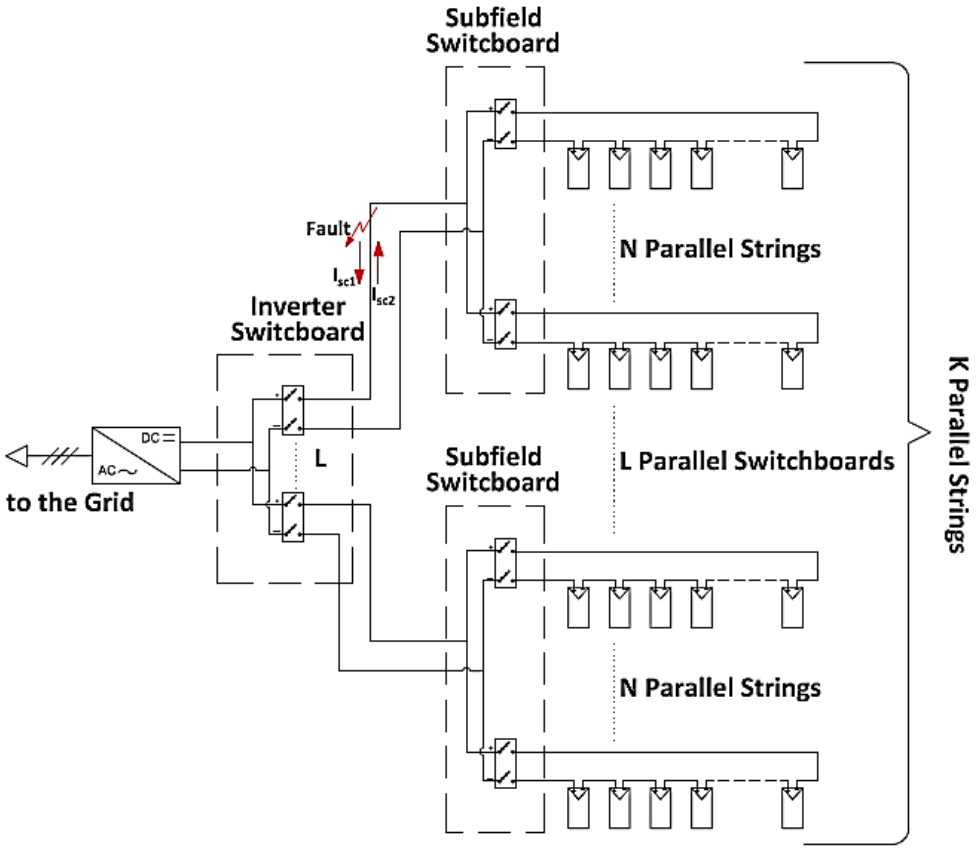

Figure 18: Upstream and downstream short-circuit currents in between strings

In case of the aforementioned fault, upstream (I_{sc3}) and downstream (I_{sc4}) short circuit currents flow at the same time (ABB, 2010). The magnitudes of these fault currents can be calculated using equation (14).

$$I_{sc3} = N \times 1.25 \times I_{sc\_STC}$$
$$I_{sc4} = (K - N) \times 1.25 \times I_{sc\_STC} \quad (14)$$

Equations (13) and (14) should be considered while choosing the protection devices. Furthermore, other factors influencing the size of the protection device are listed below (SMA Solar Technology AG, 2008):

- Loop impedance of the cable
- Mutual heating of protection devices
- Ambient temperature

- Type of the protection device
- Selectivity

Type of the protection device refers to the disconnection capability of the device under load conditions and. MCBs can disconnect the circuit under load. On the other hand, gPV and HRC fuses do not have load-break capability. Therefore, they can only be used with an isolator having load-break capability. The response time of the protection device is important too. If the fault current is less than the trigger current of the fuse, it would not blow (International Finance Corporation, 2012). This means that the over-current protection device may not protect the system because, it will be unable to detect the fault current.

The ambient temperature inside of the switchboard can reach high temperatures as these switchboards are generally installed outdoor. Fluctuating PV currents and the thermal stress on the over-current protection device may lead to undesired tripping. In order to avoid that manufacturer's declaration should be consulted. Typical screening factors for gPV fuses are given in equation (15) (SMA Solar Technology AG, 2008).

$$SF = \frac{I_{mpp\_max}}{I_{fuse\_nom}} < \begin{cases} 0.60, up\ to\ 40℃\ of\ ambient\ temperature \\ 0.55, up\ to\ 55℃\ of\ ambient\ temperature \end{cases} \quad (15)$$

Selectivity protects the system against involuntary tripping of upstream protection devices when they are installed consecutively. For instance, if a short circuit occurs in a string, the closest protection device opens the circuit earlier than the ones farther away. Operating characteristics of MCBs or gPV fuses should be taken into account.

Over-current protection on the AC side can be achieved by using proper MCBs, MCCBs and Residual current devices (RCDs). Inverter manufacturer's declaration is important when dimensioning the protection devices on the AC side. Loop impedance of the cable connecting the inverter and the sub-distribution switchboard plays a significant role in AC side protection. If the loop impedance is too high in such a way that it limits I_{sc}, the triggering current will not be so high to disconnect the protection device within the time value specified in the standards. In this case an RCD must be used to disconnect the circuit in case of a fault (IEC 60364-4-41:2005, 2005). Local rules, regulations and the type of the grounding system must be considered for the use of RCD as an extra precaution. Inverter manufacturer's declaration should be taken into account when selecting the rated residual current characteristic of the RCD. Moreover, the type of RCD regarding to its ability to sense, trip and withstand different current types is important for detecting the residual current flowing upstream. If an inverter does not galvanically isolate DC and AC circuits (i.e. transformerless inverter), a ground fault in the DC side may cause a residual current to flow to the AC side (Kumar & Eichner, 2013). According to the IEC 60755 standard, Type A or Type B RCDs has to be employed as they can sense AC/pulsed DC and AC/pulsed DC/smooth DC respectively (IEC 60755, 2008). It must be noted that some transformerless inverters limits or clears the DC components of upstream residual currents. Therefore, the inverter manufacturer's declaration must always be taken into account.

All in all, the relationship between cable sizing and the over-current protection cannot be considered separately. A protective device operates properly if (BS 7671:2008, Amendment 3: 2015, 2015), (IEC 60364-4-41:2005, 2005):

- Its nominal current (I_n) is greater than the maximum load current (I_b), but less than the current carrying capacity of the cable for continuous service (I_z).
- Its fusing/tripping current under conventional operation is less than $1.45 \times I_z$.
- Its 3-phase short-circuit current (I_{SC}) is less than the 3-phase short circuit breaking rating (I_{SCB}) at the point of installation.

Figure 19 illustrates the statements written above. Protection against over-current in association with the corresponding international standards is also summarized in **Table 9.**

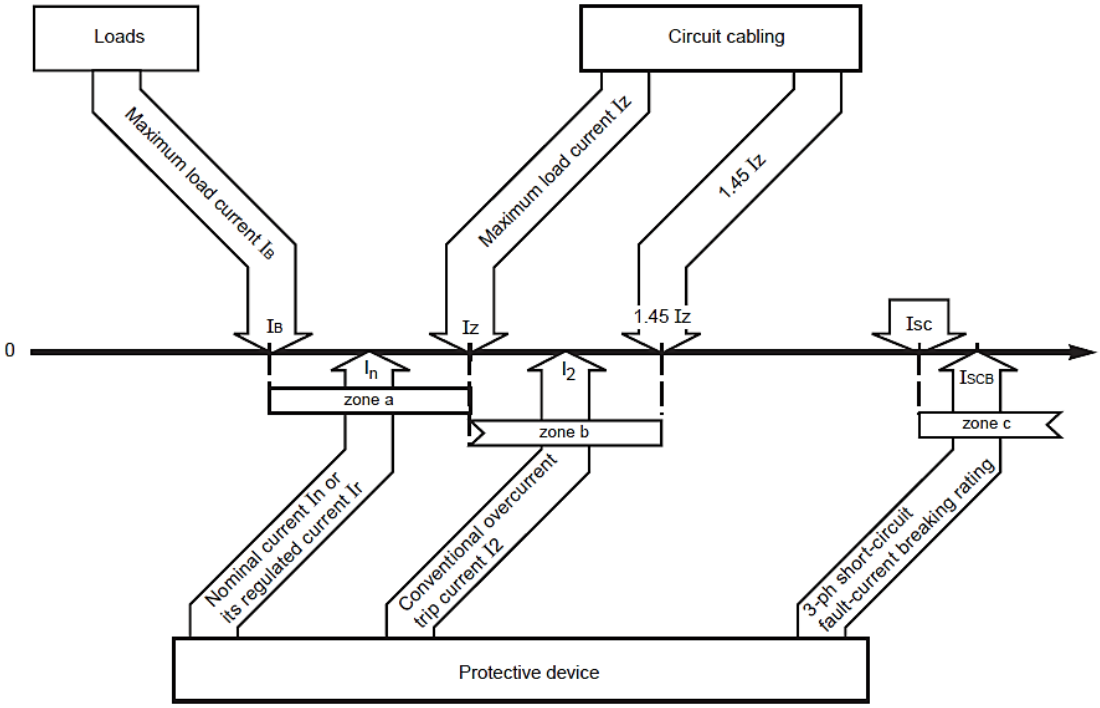

Figure 19: Current levels for determining circuit breaker or fuse characteristics (Schneider Electric, 2015)

iii. <u>Over-Voltage Protection Devices:</u>

Protection of a PV system against over-voltages is necessary either in ground-mount or roof top systems. There are several sources of over-voltages; sudden reduction of

large loads, switching of transient loads, harmonics from power network, electrostatic discharge and direct or indirect lightning. A PV system is vulnerable to these influences, especially lightning, unless it is protected by proper surge protection devices (SPD).

The knowledge of application of over-voltage protection in PV plants is still premature and thus ignored especially in small-scale plants. There is only few international standard dedicated to the protection of PV systems against voltage surges. CLC/TS 50539-12:2013 standard published by CENELEC is one of them. However, it only describes the selection and application principles of low voltage SPDs in PV systems (CLC/TS 50539-12:2013, 2013). On the other hand, the IEC 62305 standard series provides a comprehensive guide for protecting against lightning and voltage surges. The IEC 62305 standard involves four parts; general principles, risk management, physical damage to structures and life hazard and electrical and electronic systems within structures (IEC 62305:2013, 2013).

According to the IEC 62305 standard, a complete lighting protection system (LPS) includes external and internal lightning protection systems along with the equipotential bonding and an effective grounding system. PV systems have exposed surfaces and extensive layouts. Additionally, they are often installed in remote areas or on the rooftops. These factors increase risk of damage of equipment caused by direct and indirect lightning. The necessity of LPS in PV systems should be identified by a risk management. Risk management involves a risk analysis that identifies the objects to be protected, damages as a result of lightning strikes and all types of losses, such as loss of human life and loss of economic value. Moreover, it evaluates the risk for those losses and the need of protection regarding to the risks

(IEC 62305:2013, 2013). Regional lightning frequency, the location and physical size of the PV power plant must be known before starting the risk management. The common risks associated with the PV power plants are listed below (Pons & Tommasini, 2013):

- Component related failure of internal systems caused by over-voltages induced on incoming lines and transmitted to the structure when lightning strikes directly to or near a service connected to the structure.
- Component related failure caused by lightning electromagnetic impulses when lightning strikes directly to or near the structure.
- Component related physical damage caused by sparking inside the structure triggering fire or explosion when lightning strikes directly to the structure.

After the risk for an unprotected system is defined, risk management aims to reduce it until a tolerable risk level is achieved. While doing so, a technically and economically optimum protection method is defined and the protection class of LPS can be determined.

There are several measures for lightning and over-voltage protection for PV systems. These measures vary whether the PV system is mounted on a rooftop or ground and whether the building has an existing LPS. The flowchart in Figure 20 represents a quick guide in selection of measures for LPS in PV systems. Table 9 lists the international regulations for the use of LPS. Additional measures can be taken in order to reduce the inductive effects of indirect lightning. A lightning that strikes near a PV power plant causes very large current flow. This current induces a voltage in the conducting loop of module cables. It means that, the voltage induced on the DC circuit gets larger as large conductive loops are created. Therefore, positive and

negative conductors have to be lied as much as close to each other as shown in Figure 21 (DGS LV Berlin BRB, 2008), (Schletter Solar-Montagesysteme, 2014).

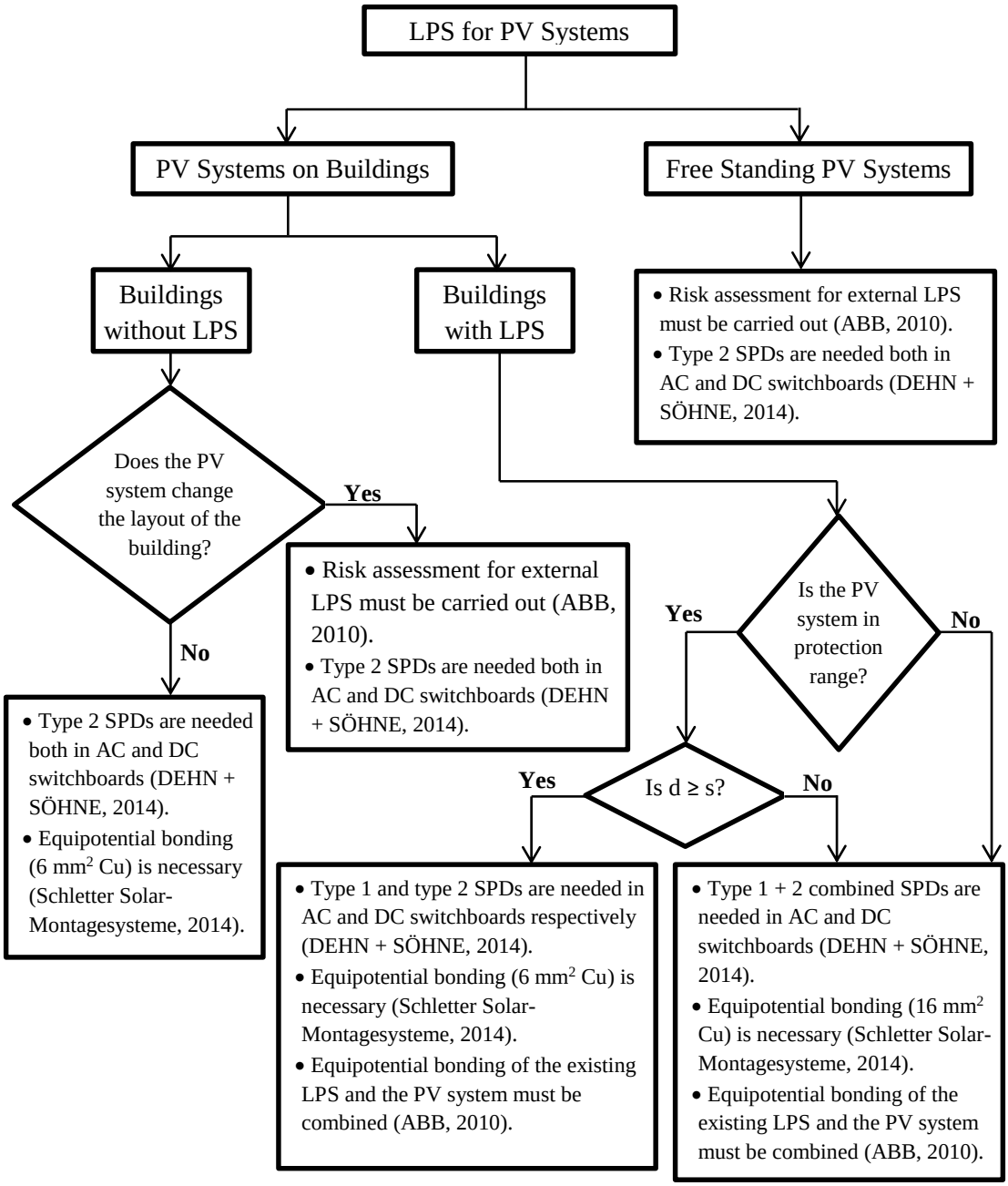

Figure 20: Steps for selecting LPS in PV systems

Internal lightning protection with SPDs becomes more important when the inductive effect of lightning is concerned. The SPDs can be separated into three main technology categories; spark gaps, varistors and diodes. Spark gaps are widely used

as SPDs due to their high discharge capacities, compact sizes and the capability of dissipating little energy across themselves. Varistors are widely employed as SPDs due to their economical cost and voltage limiting ability. Lastly, diodes have fast response time but low discharge capacity. In order to deal with inductive effects of indirect lightning, it is recommended to use Type 2 SPDs on DC side and Type 1 + 2 SPDs on AC side. Other characteristics that a SPD should have are given in equation (16) (ABB, 2010), (DEHN + SÖHNE, 2014), (Hernandez et al., 2014). The discharge capacity in kA must be calculated according to the IEC 62305 standards

$$\left.\begin{matrix} U_e = 1.25 \times U_{oc} \\ U_p < U_{inv} \end{matrix}\right\} for\ DC\ side \qquad \left.\begin{matrix} U_e = 1.1 \times U_o \\ U_p < U_{inv} \end{matrix}\right\} for\ AC\ side \tag{16}$$

where U_e is the rated service voltage, U_{oc} is the open circuit voltage of the PV string, U_o is the line to earth voltage, U_p is the voltage protection level and U_{inv} is the impulse withstand of the inverter on the DC and AC side respectively. The types of SPDs are referred to different names in different international standards. In order to avoid the confusion, it should be noted that the SPD operating with 10/350 μs surge current waveform is referred to Type 1/Class I/Class B in IEC/EN/VDE standards. Similarly, the SPD operating with 8/20 μs surge current waveform is referred to Type 2/Class II/Class C in IEC/EN/VDE standards. 10/350 μs surge current waveform is used to simulate the direct lightning strike and 8/20 μs surge current waveform is used to simulate the remote lightning strikes and surges from switching operations (OBO Betermann, 2015).

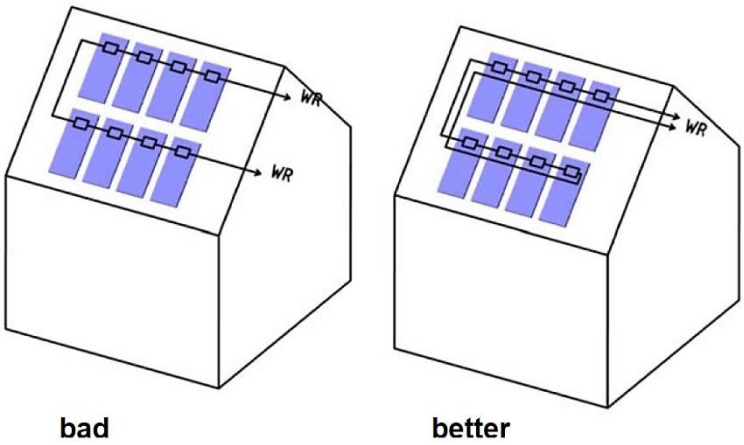

Figure 21: Recommended PV panel cabling method (Schletter Solar-Montagesysteme, 2014)

External lightning systems consist of three major components; air termination rod, down conductor and earth termination system. There are two LPS design methods in PV power plant from the air termination rod viewpoint. These are protection angle method and rolling sphere method. The former includes a number of air termination rods installed along the PV mounting system. The latter includes a number of air termination rods installed in such a way that the penetration depth of the sphere would not with the PV system (Charalambous et al., 2013), (OBO Betermann, 2015). These two different approaches are illustrated in Figure 22. The height, distance and the number of the air termination rods depend on the lightning protection class (I - IV) of the PV system (DGS LV Berlin BRB, 2008).

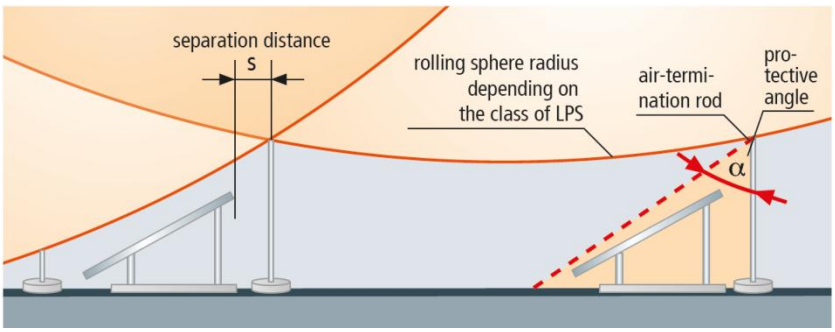

Figure 22: Rolling sphere method versus protective angle method (DEHN + SÖHNE, 2014)

According to the design principle of LPS, the air termination rod can be either isolated or non-isolated from the metal supporting structure of the PV system. For an isolated system, the separation distance (s) that stands for the minimum safety distance between the LPS and the metal framework of the PV system must be maintained as shown in Figure 22. The isolated LPS includes a mast type air termination rod having a concreter base, whereas the non-isolated system has an angled air termination rod mounted directly on the metallic infrastructure. This difference is illustrated in Figure 23.

Figure 23: Isolated (left) and non-isolated (right) LPS (Charalambous et al., 2013)

PV plants need an effective grounding in order to discharge the lightning current to the earth. To this end, a trip conductor circulates the entire PV area and forms meshes to ensure equipotential bonding of all PV metal frameworks. If the required grounding level is not achieved by this way, additional earth rods can be replaced vertically into the soil. An example for earth termination system is illustrated in Figure 24.

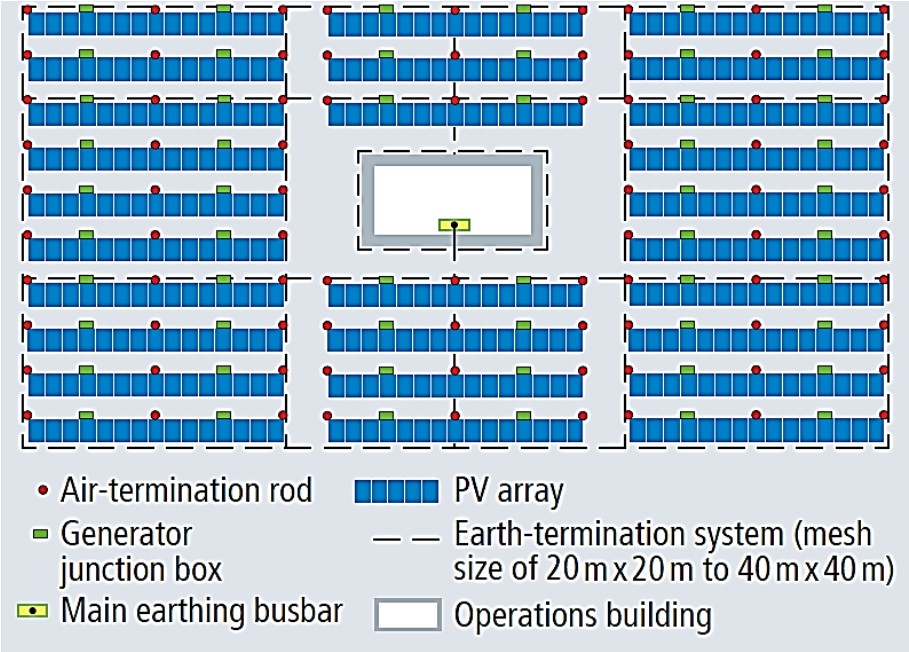

Figure 24: Earth termination system (DEHN + SÖHNE, 2014)

In conclusion, a PV system must be protected against lightning and other surges after conducting a risk assessment as states in IEC 62305 standards. It should be noted that, the dissipated energy of the lightning depends on location where the lightning strikes, lightning protection class, the design of the earth termination system and the electrical resistivity of the soil (Charalambous et al., 2013). In order to minimize the adverse effects of the lightning, a proper LPS has to be designed with suitable SPDs, air and earth termination systems. The LPS increases the investment cost of the PV system by less than 4% (Hernandez et al., 2014). This additional cost is insignificant when compared to loss of revenue regarding the damages from lightning strike. Furthermore, many insurance companies seek for a proper LPS installed in the PV plant before they insure the system. Protection against over-voltage in association with the corresponding international standards is also summarized in Table 9.

iv. Monitoring System:

Large-scale PV power plants are cost a lot of money and are expected to operate for 25 years. It is very possible that a PV system generates less energy than expected or

completely shuts down due to various failures and damages. A monitoring system ensures to detect the unusual events in the system, so the problems can be solved quickly. Therefore, the loss of revenue is minimized. Furthermore, a monitoring system allows the grid operator to adjust the plant according to the local directives, supports the grid, manages the electrical appliances via a smart home interface and send report in case of events. A complete monitoring system is supposed to collect data regarding the operation of the PV system and provide information regarding to the weather conditions.

The IEC 61724 standard defines the procedures for the monitoring of energy related PV system characteristics. Other IEC standards such as IEC 60904-1 and IEC 61829 are frequently referred in IEC 61724. These standards set the basic requirements for I-V characteristics of PV modules and define the uncertainty limits for the measurements. In order to analyze the electrical performance of PV systems, general guidelines stated in IEC 61724 should be followed. The parameters to be measured are stated in Table 7 (IEC 61724:1998, 1998).

On-site data acquisition is carried out in real-time. On the other hand recording and reporting intervals are much larger. These intervals in an on-site monitoring can be summarized as; $sampling\ interval < recording\ interval < reporting\ interval$. The monitoring systems can be classified according to the precision of the measurements as Class A, Class B and Class C. Class C monitoring systems provide basic precision and are generally used in residential or small-scale commercial applications. The precision of Class B systems are better. They are mainly used in commercial applications. Lastly, Class C monitoring systems have the greatest

precision level and are recommended for utility-scale applications (IEC 61724:1998, 1998).

Table 7: Parameters to be measured in a PV system

Field	Parameter	Reason
Meteorology	Global irradiance in the plane of array Ambient temperature Wind speed	Required for calculating the performance ratio of the PV power plant.
PV Array	Output Voltage/Current/Power Module temperature Mounting system characteristics	Required for analyzing the electrical performance of the PV system.
Energy Storage	Operating voltage Current/Power to/from storage	Required for following up the energy delivered to or from the storage device
Load	Load Voltage/Current/ Power	Required for determining the hourly, daily and monthly load profiles
Utility Grid	Utility voltage Current/Power to/from utility	Required for following up the energy delivered to or from the utility grid
Back-up Sources	Output Voltage/Current/ Power	Required for following up the energy delivered to or from the back-up sources

The specifications of the monitoring system should be well understood. One must pay attention to the following specifications of the device before selecting the monitoring system (SMA Solar Technology AG, 2008):

- The maximum number of inverters that can be connected to the device: A monitoring system which is capable of connecting the required number of inverters should be selected especially in decentralized PV systems.
- Supported communication protocols (Bluetooth, RS 485, Ethernet…): The inverters and the monitoring device must support the same communication protocols. Wireless or wired variants of communication protocols can be selected according to the size of the PV system. Further encryption may be

required for wireless communication protocols in order to increase the security.

- Maximum communication range: Each communication protocol has a different communication range. The voltage drop across communication cables should be considered in wired protocols.
- Ambient conditions for operation: The device should operate under high temperature and humidity conditions.
- Internal and external memory capacity: As the number of inverters connected to the monitoring device increases, more memory area is required to store the data for long period of time.
- Number of digital and analog I/O ports: The number and specifications of the sensors that can be connected to the monitoring system are important. It should be noted that many meteorological sensors are analog.

Furthermore, a monitoring system in a large-scale PV plant must perform the following functions for plant management:

- Static grid support: Supports the grid via adjusting the power factor of the plant, injecting reactive power and limiting active power injection if required.
- Dynamic grid support: Supports the grid via contributing the short-circuit ability of the grid and staying connected in case of major grid failure (fault ride through).
- Grid safety management: Supports the grid via limiting the overall power injection.

A complete monitoring system should collect meteorological data from the field as well as the energy related data. Global horizontal irradiance (GHI), direct normal irradiance (DNI), diffused global irradiance (DHI), global irradiance in the plane of array, wind speed and direction, relative humidity and the ambient module temperatures are the parameters which can be collected from the field. Among all, solar irradiance is the most important one. Pyranometers are used to collect the solar irradiance. There are two different kinds of pyranometers; thermopile pyranometers and reference cell. Thermopile pyranometers are superior in terms of long term reliable operation, limited uncertainty and little drift. According to ISO 9060 standard, pyranometers are classified as secondary class, first class and second class regarding to their measurement precision. Second class devices are the most economical solution for routine measurements. First class devices have better quality and are used in research grade applications. Secondary class devices have the highest level of accuracy and reliability, hence the most expensive (ISO 9060:1990, 1990) .

As a result, collecting and analyzing the meteorological and energy data from the field is extremely important to guarantee a reliable long term operation of PV systems. The following statements are significant for a successful monitoring system (Emery & Smith, 2011):

- Although they are expensive, select highly reliable hardware
- Decrease the external noise by using metal plugs. By this way, the communication cable will be grounded automatically as it is connected to the grounded body of the inverter.
- Select sensors with low uncertainty, low drift and high accuracy.

- Design a simple system to avoid unnecessary signal conditioning and provide more understandable data for the end users.
- Calibrate the sensors in every two years to avoid degradation.

Main factors influencing the performance of the PV system monitoring in association with the corresponding international standards is also summarized in Table 9.

v. *Medium-Voltage Transformer for grid conection:*

The key principle of power distribution is to increase the voltage to a higher level in order to minimize the I^2R losses across the power line. Step-up distribution transformers are used in large-scaled PV power plants in order to transmit the generated PV energy to the utility grid. A transformer plays a critical role in PV plant as it distributes the entire PV energy. Therefore, selecting according to the local electricity codes, sizing and protecting of it are significant.

Typically, distribution transformers are used to increase the PV output voltage to a voltage ranging 11 – 34.5 kV. If the PV plant is required to connect at the transmission network, an additional substation transformer is used to increase the voltage over medium voltage level. Sizing and selecting the transformer for a PV plant is rather different than that of in conventional power systems. It is a common practice to choose the transformer at the peak capacity of the PV system. However, this may lead to create unused capacity at the transformer due to the power generation pattern of the PV plant. A transformer having a higher rating than the peak capacity of PV plant, may cause instability during transients, increase losses and reduce efficiency. On the other hand, lower rated transformers may struggle to distribute all of the power generated to the grid in the peak hours. Moreover, temperature at the windings may rise due to overloading of the transformer (Rajender

et al., 2014). Here, the overloading capability and consequently the life loss factor obtained from the transformer's manufacturer are decisive while sizing the transformer.

There are several important transformer ratings to be considered before having a transformer. These are summarized in Table 8 (Kondrashov & Booth, 2015).

Table 8: Distribution transformer ratings

Ratings	**Explanation**
Voltage	Inverter manufacturer and the grid operator should be consulted to determine the voltages on LV and MV sides respectively.
Winding Connections	Typically Δ-Y (with Dyn11 vector group) connection is used. LV winding connections must comply with the inverter manufacturer's requirements.
Basic Impulse Level	It is the level of the momentary over-voltage that the insulation of the transformer can withstand
Impedance	%Z determines the amount of voltage drop across the transformer at full load. Lower %Z means less copper losses an enhanced efficiency.
Efficiency	It is the ratio of output power to input power.
Winding Material	Copper or Aluminum is used. Copper is a better conductor, so it accounts less loss. However, it is more expensive.
Temperature Rise	It is the average temperature rise of the transformer windings compared to the ambient temperature The operation temperature and the efficiency are closely related. Transformers having lower temperature rise are more efficient because they are capable of generating less waste heat.
Insulation Class	It depends on the temperature rise value. Cotton, silk, synthetic fibers, mica, glass fiber…
Cooling	Liquid-filled transformers employ a fluid (e.g. oil) that can circulate through the transformer via forced or natural convection. They are mostly preferred in PV applications. Less expensive. Dry-type transformers passive methods, so they are self-cooled. More expensive.
Seismic Resistance	It can be taken into account when the transformer is installed in certain facilities.
Altitude Deratings	Transformer's capacity decreases by 0.3% for every 100 m in elevations above 1000 m.

Large-scaled PV plants operate in parallel with the MV network. In order to accomplish this, MV switchgears employing suitable protection and disconnection mechanisms are utilized. Although it depends on country specific MV directives, a disconnector and a protection relay driven circuit breaker are used in such plants. The relay should perform the disconnection functions including, under/over voltage protection, over-current protection and under/over frequency protection. In many cases, an auxiliary power supply is required in order to reclose the circuit breaker after the fault is cleared. Main factors related with the MV transformer in association with the corresponding international standards are also summarized in Table 9.

Table 9: Overview of the main factors affecting the performance of the PV system and the referred international standards for optimizing the energy production

Component	**Main factors affecting the performance**	**Proposed Optimization Strategies**	**Related Standards**
PV Modules	Module Temperature Coefficient	Modules having low temperature coefficients should be chosen	IEC 61215, IEC 61730, EN 50380, IEC 62716, IEC 61701.
	Efficiency	Modules with higher efficiency are preferable. However, the efficiency of the module does not represent its quality.	
	Degradation	Modules with a lower degradation rate will yield more PV energy during the lifetime of the plant.	
	Module Mismatch	All modules in an array should be identical and operate under same environmental conditions.	
	Soiling	It is advised to clean the modules twice in a month. However, the frequency of rainfall, amount of the dust accumulation and economic parameters determine the cleaning strategy.	
Inverters	Efficiency and Performance	High efficiency inverters should be chosen. Besides, it should be noted that the efficiency of the inverter depends on the input side voltage and the load.	IEC 61727, IEC 62109, VDE-AR-N-4105, IEC 61000-3, VDE 0126-1-1, IEC 60529, IEC 60721-3-4, IEC 62103
	MPP Tracker	A fast responding and wide MPP range is preferable	
	Harmonic Content	Harmonic current must be low.	
	Grid Code	Inverters must operate in such a way that they fulfil the requirements of the grid. Cut-in and cut-out voltage levels and frequencies are among these requirements.	
	Environmental Conditions	Inverters should be able to operate in harsh environmental conditions.	
Cabling	Conductor Sizing	Correctly dimensioned DC and AC lines reduces amount of cabling, reduces the impedance hence voltage drop and power loss across them (ABB, 2010), (International Finance Corporation, 2012), (MCS, 2012) and (DGS LV Berlin BRB, 2008).	IEC 60228, IEC 60287, IEC 60364 or BS 7671 (UK)

	Voltage Drop	DC cabling losses should not be more than 1.5% (Talavera et al., 2014).	
	Operating Temperature	DC cables must have a wide range of operation temperature from -40˚C to +120˚C (International Finance Corporation, 2012) and (DGS LV Berlin BRB, 2008).	
Protection against over-current	Code Compliance	String and array protection can be achieved by miniature circuit breakers (MCB) or gPV fuses on the DC side. They should be sized and placed in such a way that they protect the strings against reverse current and the cables against over-current. The over-current protection equipment rating should be at least 1.25 times greater than the short circuit current of the string or array (Schneider Electric, 2015).	IEC 60898-1, IEC 60947-2, IEC 60364 or BS 7671 (UK)
Protection against over-voltage	Direct and Indirect Lighting	A complete lighting protection system includes external and internal lightning protection systems along with the equipotential and grounding systems (IEC 62305:2013, 2013).	IEC 62305, EN 50164, VDE-0100-712 TS 50539-12
	External LPS	The distance between the external LPS and the PV panel is important. Air termination rod is replaced in such a way that they do not cast core shadow on the panel.	
	Earth Termination System	Dissimilar metals should not be connected together in order to avoid galvanic corrosion. If the earth electrode is made of different material than the mounting system, suitable clamps should be used to connect them together.	
Monitoring	Weather Station	An on-site weather station having the capability of collecting direct, diffuse and global irradiance, wind speed and direction, ambient and module temperatures and the relative humidity has an important role in evaluating the performance of the PV plant.	IEC 61724, ISO 9060
	Power Measurement	The AC & DC current, voltage, power and energy data obtained from the inverters should be synchronized with the weather data. So an availability analysis can be performed.	
	Reporting	The periodical detailed yield reports and the fault reports must be sent to the devices determined by the investor. By this way, immediate action can be performed right after the fault occurs.	
MV Transformer	Grid Code	Type, voltage rating, winding connections, efficiency, cooling medium are important parameters which must be considered in selecting a distribution transformer	IEC 60076 IEC 61936
	Sizing	A transformer having a higher rating than the peak capacity of PV plant, may cause instability during transients, increase losses and reduce efficiency. On the other hand, lower rated transformers may struggle to distribute all of the power generated to the grid in the peak hours. Moreover, temperature at the windings may rise due to overloading of the transformer (Rajender et al., 2014).	
	Protection	Over-current and over-voltage protection must be done according to the regulations set by DSOs.	

3.5 Mounting System

PV systems need robust and reliable mounting systems which can withstand harsh environmental conditions while holding the PV array. The tilt angle and the orientation are two important factors affecting the PV energy generation. However, they are application dependent. The optimum tilt angle for a fixed angle PV system can be taken as the latitude of the site of construction (Kalogirou, 2009). The injected PV energy into the grid gains no value in non-residential PV applications, where the self-consumption mechanism is applied, in Northern Cyprus. Therefore, matching the PV generation and the consumption profiles is very important in reducing the first cost, thus the payback period of the investment. For example, if a facility consumes more electricity during daytime in summer, then reducing the tilt angle of the PV system will generate more energy and the generation curve will better match with the consumption curve. That means the tilt angle is important in capturing a better seasonal irradiation distribution. The variation of the tilt angle also has an impact on the soiling of the modules. It should be noted that, the type of the module (with or without frame) affects the long term dust accumulation. The recommendations of the manufacturer on the minimum tilt angle must be taken into account for proper self-cleaning of the modules from normal rain showers. Otherwise, dirt may accumulate at the bottom edges of the framed modules which are not subjected to cleaning periodically. Additionally, it affects the inter-row spacing due to the fact that the front row always casts shadow on to the row behind it (International Finance Corporation, 2012).

In recent years, single or dual axis tracking PV systems has gained a well-deserved popularity. Their higher energy yield makes them attractive for the investors. The

yearly energy yield can be increased by 25-35% for single axis trackers and 35-45% for dual axis trackers (IEA-PVPS, 2015), (Vokas et al., 2015) and (Eke & Senturk, 2012). However, the increased cost and land requirement of tracking systems have to be considered too. On average, tracking systems are 15% more expensive than fixed angle systems in terms of installation cost (Barbose & Darghouth, 2015). The land requirement for single and dual axis tracking systems is 15% and 71% respectively higher than that of fixed angle systems (NREL, 2013). Tracking the sun increases the amount of irradiation incidence on the PV array surface. On the other hand, the module temperature increases with the irradiation level. Therefore, the rise in the energy yield of solar tracking systems in the regions having high irradiation levels and hot climate may not be as high as the energy yield increase in colder regions (Sharaf Eldin et al., 2016).

The mounting topology always contributes to the increase in the temperature of the PV array, whether it is designed for a sloping roof, flat roof, façade or open space. As stated in (DGS LV Berlin BRB, 2008) building integrated systems without ventilation see more increase in the module temperature than free standing installations. This is due to convective heat transfer of the wind across the module. The integrated PV systems with an air gap of 10 to 15 cm ensure proper ventilation between the modules and the building façade (Agathokleous & Kalogirou, 2016). The study in (Kurtz, et al., 2009) shows that rack mounted module temperatures barely exceed 70℃ in the Middle East region. On the other hand, it is calculated that the roof mounted module temperatures can easily exceed 90℃ in the same region.

3.6 Grid Connection and Permit Process

Grid connection application is one of the most important administrative procedures which can take a long time depending on the size and the complexity of the PV system. The inverters and the other protection devices (either for low or medium voltage network) used at the point of common coupling must comply with the grid codes. The distribution system operator (DSO), which is in charge of defining the connection requirements of the power generating units to the LV and MV networks, is one of the key actors in the design, installation and commissioning stages.

All generation sources can cause instability if not operated properly. However, distributed energy resource systems such as photovoltaics are more likely to cause grid instability in case of high penetration (Liserre et al., 2010). A power grid has to be well planned to avoid falling into instability, if it is heavily dominated by distributed generation systems. The operation of the power system can be affected by the high penetration of such systems due to their intermittent power generation characteristics which depend heavily on dynamic weather conditions. Aspects influenced by the connection of distributed generation units can be listed as follows (Coster et al., 2011):

- voltage control,
- power quality,
- protection system,
- fault level,
- grid losses.

A well designed distributed generation system can have positive impact on the aspects listed above. The grid code not only serves DSO for operating a reliable and a stable network but also guides the designers and the investors in planning the system and selecting the components. Therefore, the inverters should have the functions such as active power and frequency dependent active power limitation, reactive power provision and dynamic grid support.

3.7 Plant Layout Design

Plant design is very important to achieve a high performance in the long term operation of the PV plant. The performance of a PV plant can be optimized by combining several factors which are related with the electrical and general layouts of the plant. The latter focuses on the physical factors such as, reducing the inter-row spacing without suffering from associated shading losses, choosing tilt and azimuth angles. Thus the yield is optimized while using minimum area for the system and creating access routes between the arrays for maintenance. Modules mounted in different orientations can be a solution of providing a more broad generation profile of the PV plant. Rhodes et al. (2014) has shown that the selection of the orientation and tilt angle other than the generally accepted values (due south for orientation & latitude for tilt angle) has positive effect in terms of energy generation (Rhodes et al., 2014). East-West oriented PV modules are used in large scale applications in order to increase the installed capacity of the PV plant because they require less area than the conventional south oriented PV plants (Sankar & Kalathil, 2014). In addition, the East-West orientation helps to eliminate the shading distances between the rows.

On the other hand, electrical design is important too. The target of a large-scale PV plant is to reduce the levelized cost of electricity generated while keeping the

component quality at a high level. Therefore, it is important to find a satisfactory compromise between the cost and the quality.

Another important parameter in optimizing the efficiency of PV power plants is the performance ratio. Performance ratio is the ratio of the actual yield of the plant to the theoretical possible energy to be generated. This parameter is used worldwide to evaluate the efficiency of the PV plants and it is largely independent of the irradiation incident on the modules.

$$PR = \frac{Actual\ Reading\ of\ Plant\ Output\ p.a.}{Calculated\ Nominal\ Plant\ Output\ p.a.} \tag{17}$$

Environmental factors such as variable solar irradiation, module temperature, shading and soiling, and electrical factors such cabling, inverter and transformer losses have impact on the performance ratio. As stated in (Fraunhofer ISE, 2014) a carefully planned PV plant has a performance ratio between 80 and 90 percent.

Another method of increasing the yield of the PV plant is adjusting the ratio of the PV array power at standard test conditions to the rated power of the inverter. This ratio is known as the sizing factor (SF) and is shown in equation (18) (Velasco et al., 2010).

$$SF = \frac{P_{PV}}{P_{INV}} \tag{18}$$

where P_{PV} is the PV array output power and P_{INV} is the rated DC input power of the inverter.

The solar array and the inverter(s) have to be optimally matched to each other's output values. As a guide 1:1 ratio between the PV array power and the rated DC power of the inverter is used. However depending on the available area, this ratio is not always applicable. Instead, the nominal power of the inverters tends to be ± 20% of the PV array output (DGS LV Berlin BRB, 2008). Finding an optimal sizing factor directly affects the yearly yield of the PV plant. Therefore the following factors should be considered before designing PV array (Velasco et al., 2010):

- Irradiance and temperature evolution at the PV installation site
- Characteristics of the PV cells
- DC wiring losses
- Inverter electrical characteristic: Maximum power, efficiency curve etc.
- Available surface area at the PV site
- Location with no shadowing patterns (if possible)
- Cost of the investment

In Mondol et al. (2006) the sizing factor is determined by the total system output, system output per specific cost of a system, PV surface orientation and inclination, tracking system, inverter characteristics, insolation and PV/Inverter cost ratio (Mondol et al., 2006). The influence of inclination and of the inverter type, the influence of PV technology and the site influence is tested in Notton et al. (2009). Bakas et al. (2011) shows that the modules per string and the sizing factor have to be determined by considering environmental conditions of the system location especially the ambient temperature (Notton et al., 2009), (Bakas et al., 2011).

3.8 Costs Associated with PV Plants

Detailed investment cost analysis has to be done by the investors before constructing a large-scale PV plant. The target of such an investment is to maximize the net present value (NPV) and internal rate of return (IRR) and also minimize the payback period (PBP) of the system. Therefore, the cost has to be identified well before the investment is done. As defined in equation (19), the initial cost includes the equipment cost, land cost, transportation cost, labor cost and grid connection cost, respectively (Muneer et al., 2011).

$$C_{initial} = C_{EQ} + C_L + C_{TP} + C_{Lb} + C_{per} \tag{19}$$

The equipment cost, $C_{EQ}(€)$ consists of various components as written in equation (20) and the abbreviation expansions are listed in Table 10.

$$\begin{aligned} C_{EQ} = \left(N_{PV} \times C_{PV} \times \frac{P_M}{1000}\right) + (N_i \times P_i \times C_i) + C_{MS\_t} + (L_{dc} \times C_{dc}) \\ + (L_{ac} \times C_{ac}) + C_{PD\_t} + C_{LPS\_t} + (L_{MV} \times C_{MV}) + C_{Tr} \end{aligned} \tag{20}$$

As stated in (NREL, 2015) equipment cost is almost 60% of the capital cost in utility scale systems. However, considering the price trend in recent years, the module and inverter costs are expected to decrease in the near future (Fraunhofer ISE, 2015). The land cost can be determined by using the market prices in the associated region. Labor cost is generally determined by local conditions. The transportation cost depends on the type of transportation and can be separated into two sub-categories; transportation up to the customs of the country and the transportation from the customs to the site of construction. The grid connection cost involves all the administrative and permitting costs which have to be paid to the local or national electricity authority. Legal fees and taxes can be considered in this category.

Table 10: Nomenclature for equation (20)

N_{PV}	Number of PV Modules
C_{PV}	Unit Cost of a PV Module (€/kWp)
P_M	Size of a PV Module at STC (kWp)
N_i	Number of Inverters
P_i	Size of an Inverter (kW)
C_i	Unit Cost of an Inverter (€/kW)
C_{MS_t}	Cost of the Mounting System (€)
L_{dc}	Total Length of the DC Cables (m)
C_{dc}	Unit Cost of DC Cables (€/m)
L_{ac}	Total Length of the AC Cables (m)
C_{ac}	Unit Cost of AC Cables (€/m)
C_{PD_t}	Total Cost of the Over-Current Protection Devices and the Electric Distribution Boards (€)
C_{LPS_t}	Total Cost of the Lightning Protection (€)
L_{MV}	Total Length of the MV Cables (m)
C_{MV}	Unit Cost of MV Cables (€/m)
C_{Tr}	Total Cost of MV Transformers (€)

Financing cost should be considered as well if the investor uses bank loan. Financing cost is a significant parameter in PV projects. It is based on many factors such as interest rate, length of payments, risk of the investment and the simplicity of the payment plan. Depending on the structure of the financing, return on investment and the size of the PV system, it may contribute up to 45% of the electricity generation cost (JRC, 2014) and (NREL, 2012). In case of a financing cost, the loan payment can be calculated as:

$$A_{loan} = C_{loan}\left[\frac{i(1+i)^n}{(1+i)^n - 1}\right] \tag{21}$$

where n is the lifetime of the investment, i is the interest rate, A_{loan} is the loan payment and C_{loan} is the loan amount. The down payment and initial rebates (if any)

should be subtracted form initial cost of the project while calculating amount of the loan.

The operating and maintenance (O&M) cost becomes an important factor of the investment, as a PV plant has 25 years of lifetime on average. The total cost can be expressed as the combination of the initial cost and the O&M cost.

$$C_{TOT} = C_{initial} + C_{OM}\left[\frac{\left(1+i_f\right)^n - 1}{i\left(1+i_f\right)^n}\right] \tag{22}$$

where i_f is the inflation adjusted interest rate which is defined in equation (23).

$$i_f = i + f + if \tag{23}$$

where i and f are the interest and inflation rates respectively. The i_f rate, also known as return on investment (ROI) from the investor's vantage point, is essential to measure the economic worth of a project. The (ROI) directly affects the levelized cost of electricity (LCOE). Private investors tend to a higher ROI than societies because they want to maximize the profitability of their investments. Although, higher ROI is desired, it increases LCOE, cost of financing and hence the risk of the investment (JRC, 2014). It can be an indicator of price competitiveness which is the comparison of PV LCOE and the retail electricity price (JRC, 2014). Moreover, ROI can be used to compare the PV investment with other kind of investments through an incremental cash flow analysis.

Once the costs associated with the PV plant has been identified, the investment can be evaluated based on PBP and NPV. Normally, PBP, on its own, is not enough to measure the worth of an investment because it suffers comparing the alternatives

having different economical lives. The risk of making incorrect decision can be overcome by using PBP in conjunction with NPV. PBP is the time required to recover the initial investment with the estimated revenues (Blank & Tarquin, 2005). It is the period *n* that makes the following equation true.

$$0 = -C_{initial} + \sum_{t=1}^{t=n} NCF_t \left[\frac{1}{(1+i)^n}\right] \tag{24}$$

where NCF_t is the net cash flow in year t.

Chapter 4

METHODOLOGY

4.1 Structure of the Methodology

This section discusses and generalizes the methodology applied through the design and installation processes of a large-scale PV plant which is subjected to a self-consumption mechanism.

PV system sizing is very important in places where a self-consumption mechanism is applied. The proposed method targets large consumers who intend to install large scale PV power plants in order to meet a part of their electricity consumption while keeping the power injected to the grid at the minimum level. In accordance with this target, the proposed method involves assessing the factors such as electricity consumption and PV energy generation characteristics, performing a site survey and determining the type of mounting system, selecting the PV technology and considering the costs involved in the design process. Figure 25 depicts the proposed method that aims to achieve the most suitable PV system design technically and economically. This is carried out by finding the minimum payback period of a large scale PV plant investment (Şenol et al., 2016).

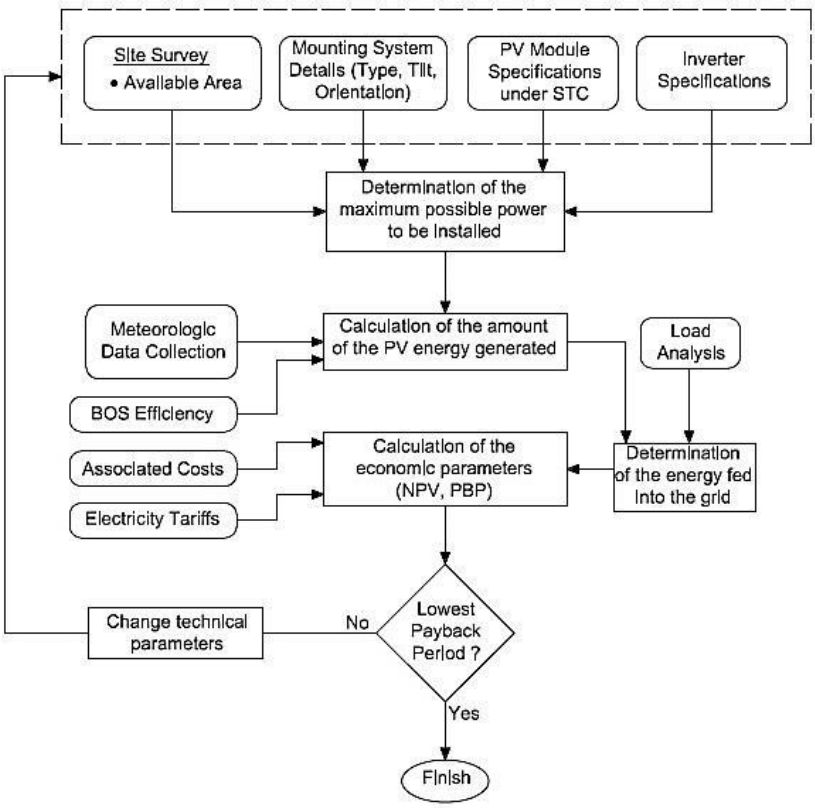

Figure 25: Flowchart of the proposed process to determine the optimal PV plant size

The stages of the proposed method, which are emphasized in Figure 25, are described below.

1. PV module and inverter specifications are used along with the mounting system details such as tilt angle, orientation and type (fixed angle or tracking system) of the mounting system, as primary input parameters. The available area data is obtained from the site survey.

2. The available area data are used to determine the maximum possible PV power to be installed. Therefore, it is considered as the main constraint in the proposed method. The initial design of the power plant is done for the maximum available area. If there is no limitation for area, another parameter (such as budget) could be used as the main constraint.

3. The amount of the generated PV energy per year is calculated by using the meteorological data and the balance of system (BOS) efficiency. The parameters in step 1 are also used in this stage, since the system size is an important factor in energy calculations. The optimum system design should be done to obtain highest energy output from the installed capacity.

4. PV energy generation profile and the electricity consumption profile of the facility are compared and the amount of the PV energy injected to the grid is determined.

5. Economic parameters such as Net Present Value (NPV) and Payback Period (PBP) are calculated. The information obtained from step 4, electricity tariffs and the associated costs such as land cost, equipment cost, labor cost and transportation cost are taken into account in this stage.

6. The proposed method separates the problem into two categories and is implemented by using the Global Optimization Toolbox in MATLAB platform on each category. The algorithm starts with the preassigned values for the decision variables such as number of PV modules connected in series across each string, number of PV strings connected to an inverter, the number of inverters and the tilt angle of the PV modules. By this approach, an initial size for the PV power plant is determined in such a way that the self-consumption rate is maximized; hence the energy injected into the grid is minimized. The second stage uses the results of the decision variables from the first phase. Here, the number of PV module rows and columns in a PV block are adjusted within the limits of the initial PV plant area. Then, the installation capacity is increased

until it is equal to the available area obtained from the site survey. On the other hand, the unit cost of the installation is reduced while the capacity of the PV plant increases.

7. This method seeks for the lowest payback period by an iterative approach. The installation capacity is increased by the steps of the selected inverter size and the PBP is calculated after each step.

8. This approach could be re-applied for different types of PV technologies, different products (brands) and different design principles.

9. Once the lowest PBP is found, the algorithm stops and the PV plant capacity corresponding to the lowest PBP are taken as the result.

4.2 The Objective Function

The optimal values of the decision variables are calculated by the optimization algorithm which is implemented by using the Global Optimization Toolbox in MATLAB platform. The decision variables are listed in Table 11.

The objective function that is considered in the proposed optimization method is based on the payback analysis which consists of two phases. Payback period is used to determine the time required to recover the initial investment cost with a rate of return that is defined as an input parameter. The first phase includes the calculation of the highest self-consumption rate. In other words, the ratio of the energy injected into the grid to the PV energy generated is kept at minimum (ideally at zero percent). Equation (25) describes the objective function.

$$\min_{\mathbf{X}}\{\%E_{lost}(\mathbf{X})\} = \min_{\mathbf{X}}\left\{\frac{EF_y(\mathbf{X})}{E_{pl\_y}(\mathbf{X})}\right\} \quad (25)$$

subject to: the design constraints

where $\mathbf{X} = \{\beta, N_p, N_s, N_i\}$ is the decision variables vector, $EF_y(\mathbf{X})$ is amount of annual energy injected into the grid for free of charge and $E_{pl\_y}(\mathbf{X})$ represent amount of the energy generated by the PV plant in each year. Equations from (89) to (91), which are shown in Section 4.4, are used to calculate the design parameters mentioned above.

Table 11: Decision variables

Variable	Explanation	Reference Point
N_s	Number of PV modules connected in series across each string	Mainly based on the voltage operating range of the inverter
N_p	Number of PV strings connected to an inverter	Mainly based on the DC input current of the inverter
N_i	Number of Inverters	Mainly based on the annual self-consumption rate
N_r	Number of rows in a PV block	Mainly based on the available PV area dimensions
N_c	Number of columns in a PV block	Mainly based on the available PV area dimensions
β	PV module tilt angle (^{0})	Manly based on the seasonal optimum tilt angle

The second phase of the optimization algorithm is used to determine the number of rows and the columns in a PV block for the maximum area occupied by the PV plant. The decision variables obtained from the first phase are used here to determine the area of the PV plant.

$$\max_{\mathbf{Z}}\{A_{tot}(\mathbf{Z})\} = \max_{\mathbf{Z}}\{N_{bl}(\mathbf{Z})A_{bl}(\mathbf{Z})\} \quad (26)$$

where $\mathbf{Z} = \{N_r, N_c\}$ is the decision variables vector, $N_{bl}(\mathbf{Z})$ is the number of PV blocks and $A_{bl}(\mathbf{Z})$ is the area occupied by each PV block. Further information on the calculation of these parameters can be found in equations (79) and (77) respectively in Section 4.4.

The algorithm searches for the minimum payback period of the project which is subjected to the decision variables obtained in the first two phases and returns the corresponding PV plant size. If there are multiple system sizes which have the lowest payback period, then NPV of those projects is calculated as well. All in all, the system having the lowest PBP with the highest NPV is chosen. Although, the algorithm compares the alternatives of various PV plant sizes having the same design criteria and the economic lifetime, there is always risk of making incorrect decisions if the PBP analysis is applied solely. This risk is induced because the PBP analysis neglects the cash flows after the payback time. Therefore, the overall profitability of the investment is ignored. In order to overcome this problem, the proposed algorithm evaluates the NPV of the alternatives having the lowest PBP. Thus, a quick and reliable judgment can be made by the investors by using the proposed method which is the combination of PBP and NPV analysis.

The algorithm returns a vector that involves the accrued cash flows for each year throughout the lifetime of the project. Accrued cash flow vector has two components; the initial cost of the project at year 0 and the net cash flows from year 1 to year n. Figure 26 shows a typical accrued cash flow diagram with the year of the investment and the payback year.

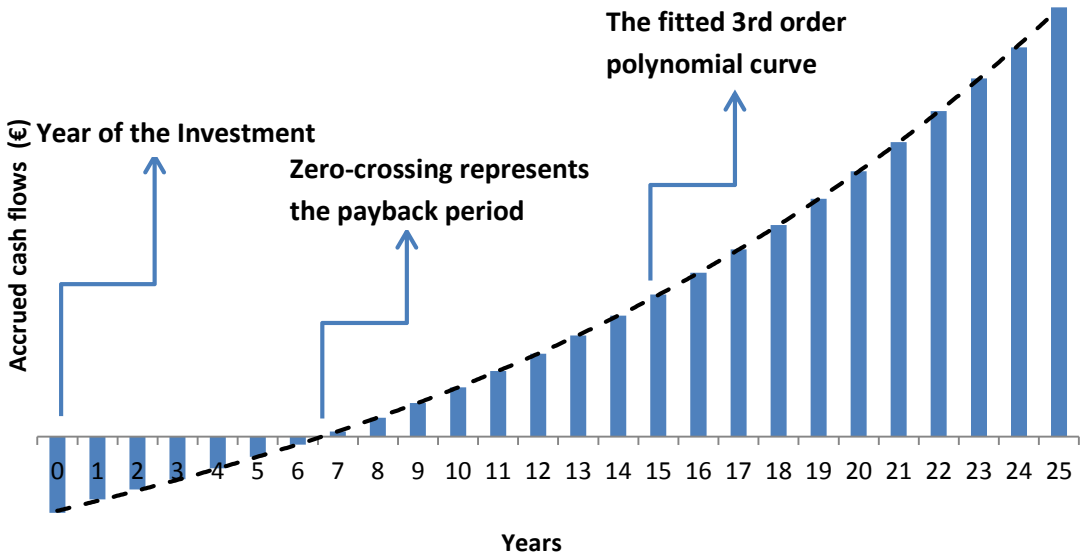

Figure 26: A typical accrued cash flow diagram of a PV power plant

Each element of the accrued cash flow vector is used as an input of a third order polynomial fit function. Thus, the accrued cash flow data can be represented as a nonlinear function such as $f(n) = an^3 + bn^2 + cn + d$ where n is the payback period. The function is solved and three roots are obtained for each iteration. The algorithm extracts the root closest to zero. The number of inverters is increased in each repetition until the PV plant size exceeds the available area. The relationship between the number of inverters and the area is stated in equations (27) and (31). The principle relies on calculating the amount of land area required (m^2) to install 1 kW_p PV system.

$$sp_{size} = \frac{A_{tot\_ini}}{\boldsymbol{N_{i\_ini} N_s N_p} P_{M\_STC}} \tag{27}$$

where N_{i_ini} and A_{tot_ini} are the initial values of the inverter number and area occupied by the PV plant calculated in the first and the second phases of the

optimization algorithm respectively. After the specific size is determined, the maximum possible number of the inverters is calculated.

$$\boldsymbol{N_{i\_max}} = floor\left(\frac{A_{max}}{sp_{size}\boldsymbol{N_s N_p} P_{M\_STC}}\right) \tag{28}$$

where A_{max} is the maximum available area and P_{i_out} is the rated AC output power of an inverter. Then the number of the inverters is incremented from a value which is three inverters less than $\boldsymbol{N_{i\_ini}}$ up to $\boldsymbol{N_{i\_max}}$. The iteration starts from $\boldsymbol{N_{i\_ini} - 3}$ in order to cover the smaller systems and to remain on the safe side. Although, $\%E_{lost}$ of the smaller PV plants are further less than the initial plant size (which is calculated in the first phase of the algorithm), the unit price of the initial investment cost is higher. Therefore, the systems smaller than the initial plant have longer payback periods.

4.3 Design Constraints

The design constraints are primarily based on the electrical characteristics of the selected PV modules and inverters. Secondly, the physical parameters of the PV modules are used in order to determine the total area occupied by the PV plant. This area cannot be larger than the maximum available area that is determined in the site survey. The electrical parameters used to determine the design constraints are listed in Table 12.

The maximum (N_{s_max}) and minimum (N_{s_min}) number of PV modules which can be connected across each PV string and the maximum number of PV strings (N_{p_max}) to be connected to an inverter are calculated by using the corresponding electrical parameters in Table 12.

Table 12: PV module and inverter parameters

PV Module Specifications		Inverter Specifications	
$\boldsymbol{P_{M\_STC}}$	Nominal power of a PV module under STC (kW_p)	$\boldsymbol{P_{i\_max}}$	Maximum DC input power (kW)
$\boldsymbol{V_{M\_mpp}}$	Module voltage at MPP (V)	$\boldsymbol{V_{i\_max}}$	Maximum DC input voltage (V)
$\boldsymbol{I_{M\_mpp}}$	Module current at MPP (A)	$\boldsymbol{I_{i\_max}}$	Maximum DC input current (A)
$\boldsymbol{V_{M\_oc}}$	Open circuit voltage of a module (V)	$\boldsymbol{V_{i\_mpp\_max}}$	Maximum MPP voltage (V)
$\boldsymbol{I_{M\_sc}}$	Short circuit current of a module (A)	$\boldsymbol{V_{i\_mpp\_min}}$	Minimum MPP voltage (V)
$\boldsymbol{\gamma}$	temperature coefficient of $\boldsymbol{P_{M\_STC}}$ (%/℃)	$\boldsymbol{P_{i\_out}}$	Rated AC output power (kW)
$\boldsymbol{\beta_{oc}}$	temperature coefficient of $\boldsymbol{V_{M\_oc}}$ (%/℃)	$\boldsymbol{V_{i\_out}}$	Nominal AC output voltage (A)
$\boldsymbol{\alpha_{sc}}$	temperature coefficient of $\boldsymbol{I_{M\_sc}}$ (%/℃)	$\boldsymbol{I_{i\_out}}$	Nominal AC output current (A)
		$\boldsymbol{\eta_i}$	Efficiency of the inverter (%)
		$\boldsymbol{\eta_{mppt}}$	Efficiency of the MPP tracker (%)

In order to determine these parameters, the effect of the temperature on and the thermal characteristics of the PV modules must be taken into account. The maximum open circuit voltage of a PV module on the coldest day (T_c) can be calculated by using equation (29).

$$V_{M\_oc\_max} = V_{M\_oc} \times \left(1 - \frac{(25 - T_c) \times \beta_{oc}}{100}\right) \tag{29}$$

The maximum and the minimum MPP voltage of a PV module on the coldest (T_c) and the warmest (T_h) day can be calculated by using equations (30) and (31) respectively. The deviation of these extreme temperatures from 25℃, which is the

reference module temperature referred in standard test conditions, emphasizes the importance of the climatic conditions on the operating range of the PV array.

$$V_{M\_mpp\_max} = V_{M\_mpp} \times \left(1 - \frac{(25 - T_c) \times \beta_{oc}}{100}\right) \tag{30}$$

$$V_{M\_mpp\_min} = V_{M\_mpp} \times \left(1 - \frac{(25 - T_h) \times \beta_{oc}}{100}\right) \tag{31}$$

The maximum number of PV modules that can be connected across a PV string can be determined by considering both the maximum DC input and MPP voltages of the inverter. These values are declared by the inverter's manufacturer. Equation (32) and (33) show the maximum and minimum permissible number of PV modules to be connected across a PV string respectively.

$$N_{s\_max} = \min\left[floor\left(\frac{V_{i\_max}}{V_{M\_oc\_max}}\right), floor\left(\frac{V_{i\_mpp\_max}}{V_{M\_mpp\_max}}\right)\right] \tag{32}$$

$$N_{s\_min} = ceiling\left(\frac{V_{i\_mpp\_min}}{V_{M\_mpp\_min}}\right) \tag{33}$$

Maximum number of PV strings which can be connected to the DC terminal of an inverter is calculated in equation (34). Here, the short circuit current is amplified by 25% for the worst case scenarios (i.e. low cable operating temperature, the place of the short circuit in the string, disconnection characteristics of the fuses or disconnectors, number of simultaneous faults in an array…). This amplification factor is advised in many best practice applications.

$$I_{M\_sc\_max} = 1.25 \times I_{M\_sc} \tag{34}$$

The maximum number of strings that can be connected to an inverter depends on the maximum permissible DC input current of the inverter. As the strings are connected in parallel, the sum of the maximum currents supplied by each string must be less than this limit.

$$N_{P\_max} = floor\left(\frac{I_{i\_max}}{I_{M\_sc\_max}}\right) \tag{35}$$

Equations from (29) to (35) are used to define the two major design constraints. These are $\boldsymbol{N_s}$ and $\boldsymbol{N_p}$. N_{s_max} and N_{s_min} are the upper and lower boundaries of the decision variable $\boldsymbol{N_s}$. Similarly, N_{p_max} is the upper boundary of the decision variable $\boldsymbol{N_p}$. Equations show these constraints.

$$N_{s\_min} \leq \boldsymbol{N_s} \leq N_{s\_max} \tag{36}$$

$$1 \leq \boldsymbol{N_p} \leq N_{p\_max} \tag{37}$$

Choosing the maximum values of both N_s and N_p may not always give the correct number of PV modules connected to an inverter. Therefore, an extra constraint is required in order not to violate the maximum permissible DC power input of the inverter. Equation (38) is used to state an upper and a lower limit for the correlation of the PV array output power and the rated DC input power of the inverter. The ratio of these parameters is also known as the sizing factor.

$$0.9P_{i\_max} \leq \boldsymbol{N_s N_p} P_{M\_stc} \leq 1.1P_{i\_max} \tag{38}$$

The output power of the PV array is allowed to be 10% less or greater than the maximum DC input power of the inverter. The reason of using these boundaries is

the current rules and the regulations of the electricity authority, KIB-TEK, in Northern Cyprus. These boundaries can be selected by either referring to inverter manufacturer's declaration or local electrical wiring regulations.

The constraint regarding the number of inverters is based on the principle that is described in equations (27) and (28). In this stage, sp_{size} is taken as 22 which is the weighted average of the land requirement of the PV plants (NREL, 2013). $\boldsymbol{N_i}$ plays a significant role in PV plant size and area. There is a need to assign a constraint to $\boldsymbol{N_i}$ in order to make sure that the calculated PV plant size in the first phase does not exceed the maximum available area.

$$sp_{size} N_i P_{i\_out} \leq A_{max} \tag{39}$$

Furthermore, two physical constraints are used in the occupied area calculations of the PV plant. First of all, the total area of the PV plant (A_{tot}) cannot be larger than the maximum permissible area (A_{max}). Secondly, the length of the PV blocks (L_{bl}) is not allowed to exceed the maximum permissible length of the southern side of the available area (L_A). These constraints are given in equations (40) and (41).

$$A_{tot} \leq A_{max} \tag{40}$$

$$L_{bl} \leq L_A \tag{41}$$

The width of the available area is also indicated as a limitation for a homogeneous distribution of the PV blocks in the PV area. The width is determined in equation (42) According to equation (43) the multiplication of the total number of PV blocks (N_{bl}) and the distance between two successive PV blocks (D) must not be larger than the width of the available PV area.

$$W_A = \frac{sp_{size} N_i P_{i\_out}}{L_A} \tag{42}$$

$$N_{bl} D \leq W_A \tag{43}$$

The width of a PV block (W_{bl}) is limited to 4 meters due to practical reasons. It is difficult and hence requires more manpower to install or maintain PV modules on high mounting systems. After the commissioning, visual inspection becomes very important in a PV power plant. Detecting the hotspots, cell deformations, burned busbars, delamination, corrosion, soiling or other physical damage gets harder as the PV module height increases.

The PV area illustrated in Figure 27 shows the pre-assumed PV area with its length and width. Similarly, distance that separates the PV blocks, tilt angle and dimensions of the PV blocks can be seen in Figure 27.

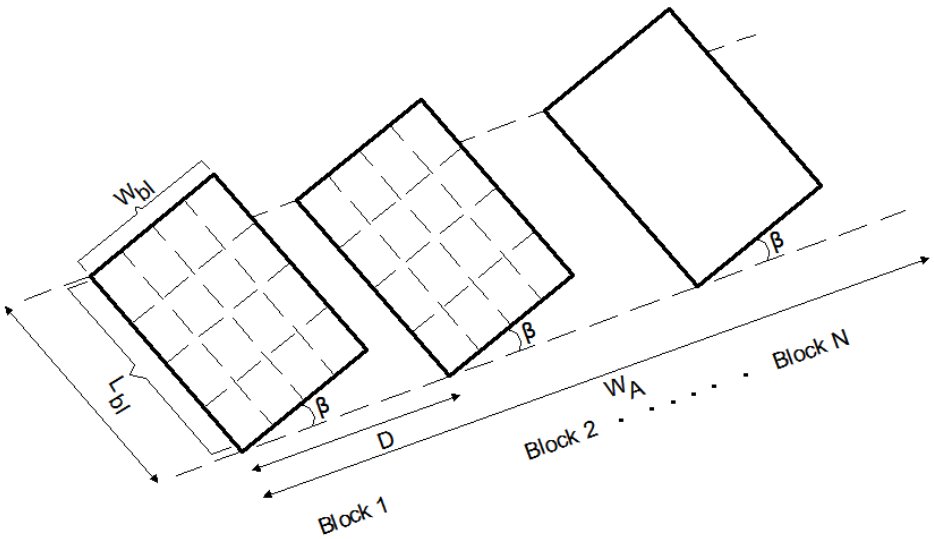

Figure 27: PV block and available PV area dimensions

The performance of a PV module is affected by the amount of the solar radiation incident on it. The optimum tilt angle depends mainly on the latitude. In order to harness the maximum amount of solar energy, solar systems are installed with a latitude dependent tilt angle. However, the solar energy generation characteristics of PV systems installed at the optimum tilt angle may not fit the electricity consumption curve of a facility. In order to provide better match between yearly consumption and the generation curves, seasonal optimum tilt angles are used in a weighted average equation of seasonal electricity consumption. Table 13 summarizes the relationship between the seasonal optimum tilt angle and the latitude for different locations.

Table 13: Seasonal optimum tilt angles for different locations

Study		Latitude	Winter	Spring	Summer	Autumn
(Adedeji et al., 2015)		35°N	L+22	L-15	L-32	L+12
(Yılmaz et al., 2016)		37°N	L+24	L-15	L-33	L+9
(Kacira et al., 2004)		37°N	L+20	L-8	L-20	L+9
(Mondol et al., 2007)		54°N	L+13	L-24	L-40	L-2
(Mehleri et al., 2010)		37°N	L+18	L-12	L-32	L+8
	(1)	37°N	L+18	L-17	L-33	L+8
	(2)	40°N	L+17	L-19	L-34	L+7
	(3)	37°N	L+20	L-16	L-32	L+10
(Bakirci, 2012)	(4)	40°N	L+21	L-18	L-34	L+8
	(5)	41°N	L+15	L-19	L-35	L+5
	(6)	38°N	L+19	L-17	L-33	L+9
	(7)	41°N	L+17	L-19	L-34	L+6
	(8)	41°N	L+16	L-21	L-35	L+3
(Hussein et al., 2004)		30°N	L+25	L-13	L-30	L+10
(Kaldellis & Zafirakis, 2012)		37°N	-	-	L-22	-
(Shu et al., 2006)		33°N	L+28	L-5	L-18	L+15
(Tiris & Tiris, 1998)		40°N	L+18	L-18	L-35	L+7
(Ghosh et al., 2010)		23°N	L+13	L-16	L-20	L+17
(Benghanem, 2011)		24°N	L+13	L-7	L-12	L+4
(Agarwal et al., 2012)		28°N	L+28	L-12	L-26	L+13
(Yakup & Malik, 2001)		5°N	L+22	L-12	L-25	L+9
Average		**-**	**L+20**	**L-15**	**L-29**	**L+8**

The optimum tilt angle is calculated in such a way that the seasonal consumption is met better with the solar energy generation. For instance, if the consumption of a

facility is significantly higher in winter, then the PV modules should be installed with a steeper angle. This approach helps to increase the self-consumption rate, Yearly electricity consumption is expressed as seasonal percentages as shown in Equation (46).

$$\begin{aligned} \%L_w &= \frac{L_w}{L_y} \\ \%L_{sp} &= \frac{L_{sp}}{L_y} \\ \%L_{su} &= \frac{L_{su}}{L_y} \\ \%L_{au} &= \frac{L_{au}}{L_y} \end{aligned} \tag{44}$$

After the seasonal consumption percentages are calculated, the average values of the optimum seasonal tilt angles can be utilized accordingly to calculate the yearly optimal tilt angle that maximizes the self-consumption rate.

$$\begin{aligned} \beta = (L + 20) \times (\%L_w) + (L - 15) \times \left(\%L_{sp}\right) + (L - 29) \times (\%L_{su}) \\ + (L + 8) \times (\%L_{au}) \end{aligned} \tag{45}$$

The rest of the constraints are related with the decision variables. $\boldsymbol{N_s}$, $\boldsymbol{N_p}$, $\boldsymbol{N_i}$, $\boldsymbol{N_r}$ and $\boldsymbol{N_c}$ must be positive integers. $\boldsymbol{\beta}$ and $\boldsymbol{n}$ must be positive but not necessarily integer. Additionally $\boldsymbol{\beta}$ is restricted to have values up to 20° above or 20^{0} below the latitude. However, if the location of the PV plant is close to equator (0°) or to the poles (90°), $\boldsymbol{\beta}$ has the risk of getting inconsistent values. This can be prevented by further limiting it. Therefore, the minimum and maximum values of $\boldsymbol{\beta}$ can be 0° and 90° respectively.

4.4 Design Parameters

The tree of equations for the objective function stated in equation (25) involves two sub-branches. The first sub-branch involves the net cash flow analysis which is based on the PV energy generation and the electricity consumption. Meteorological data is utilized to determine the solar irradiance incident on the PV modules. This data is then used in the PV energy generation equation. The second sub-branch includes costs associated with a large-scale PV power plant and the layout of the PV modules in the available PV area. Equations comprising the objective function are written in a nested approach. The overall flow of the equations can be seen in Figure 28.

The simplest equation in the first sub-branch starts with the declination angle calculation. This quantity is based on the Earth's axis which is always inclined at 23.45° from its elliptic axis. It also changes throughout a year as the Earth is moving around the Sun. It is equal to 0° at the equinoxes (March, 21 and September, 23), 23.45° at the summer solstice (June, 21) and -23.45° at the winter solstice (December, 21). The computation of the declination angle is shown in equation (46).

$$\delta = 23.45\left(\frac{360}{365}(284 + d)\right) \tag{46}$$

where d is the number of days in a year. Declination angle is used as an input variable in the incidence and zenith angle calculations. The angle of incidence (θ) is the angle between the sun's beams falling on a surface and the normal to the same surface. The cosine of the incidence angle is significant in order to determine the amount of the solar irradiance falling on a tilted surface and shown in equation (47).

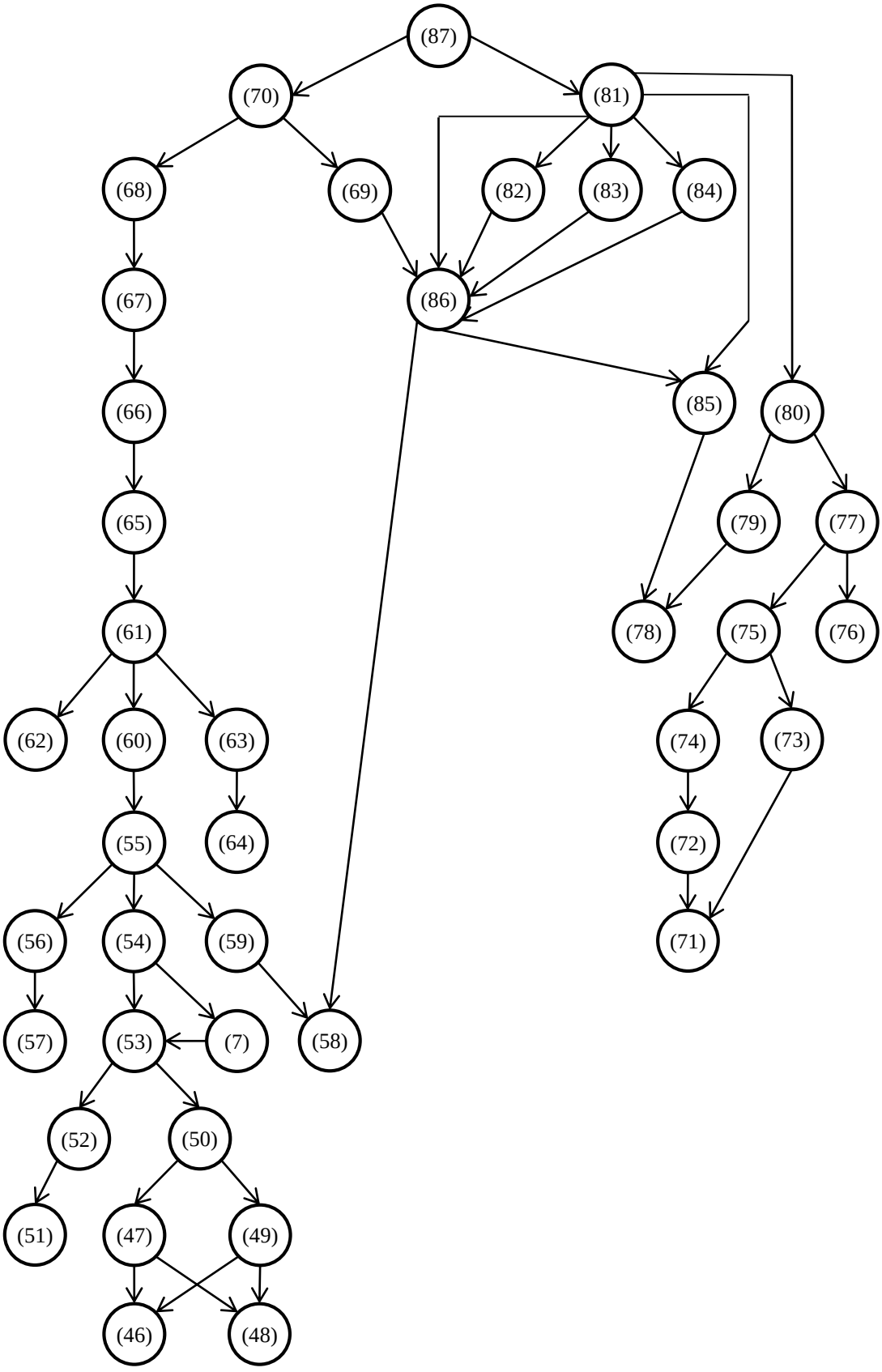

Figure 28: Equation tree of the optimization algorithm

$$\begin{aligned}\cos\theta = {} & \sin L \sin\delta \cos\beta - \cos L \sin\delta \sin\beta \cos Z_s \\ & + \cos L \cos\delta \cos h \cos\beta \\ & + \sin L \cos\delta \cos h \sin\beta \cos Z_s \\ & + \cos\delta \sin h \sin\beta \sin Z_s\end{aligned} \tag{47}$$

where L is the latitude angle, β is the tilt angle of the PV modules, h is the hour angle and Z_s is the azimuth angle of the PV modules. L and Z_s are the constant parameters and defined by the user in the beginning of the algorithm. The hour angle is the angle which the Earth would turn to bring the local meridian directly under the sun. It is used as a vector that represents the average hour angle at each hour (from 00:00 to 23:00) in a day. It is expressed in equation (48).

$$h = \mp 0.25(number\ of\ minutes\ from\ local\ solar\ noon) \tag{48}$$

where (+) is used for afternoon hours and (-) is used for morning hours. The hour angle, latitude and declination angle are illustrated in Figure 29 and Figure 30.

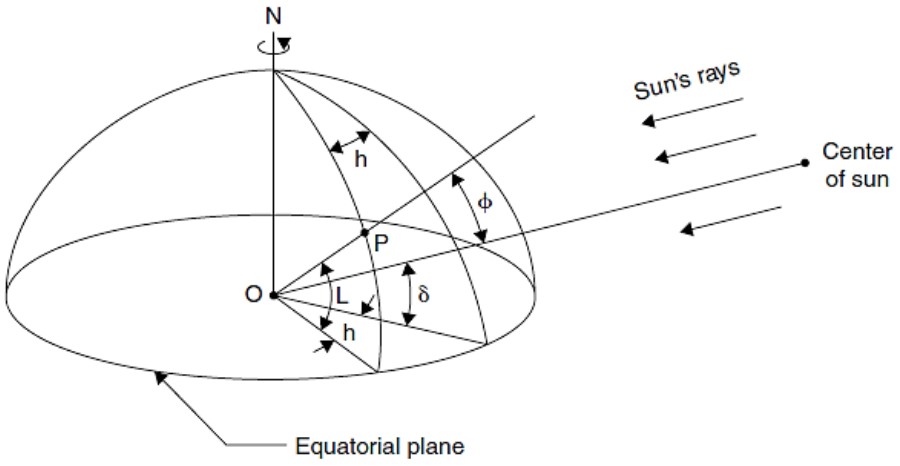

Figure 29: Illustration of latitude, hour angle and declination angle (Kalogirou, 2009)

The calculation of the cosine of the zenith angle takes also the parameters related to the solar geometry into account. Zenith angle is the angle between the sun's beams and a vertical line to the sun. Moreover, it is the complementary angle of solar

altitude angle (α). It is defined mathematically in equation (49). Additionally, Figure 30 can be used to visualize the parameters used in solar geometry.

$$\cos\phi = \sin L \sin\delta + \cos L \cos\delta \cos h \tag{49}$$

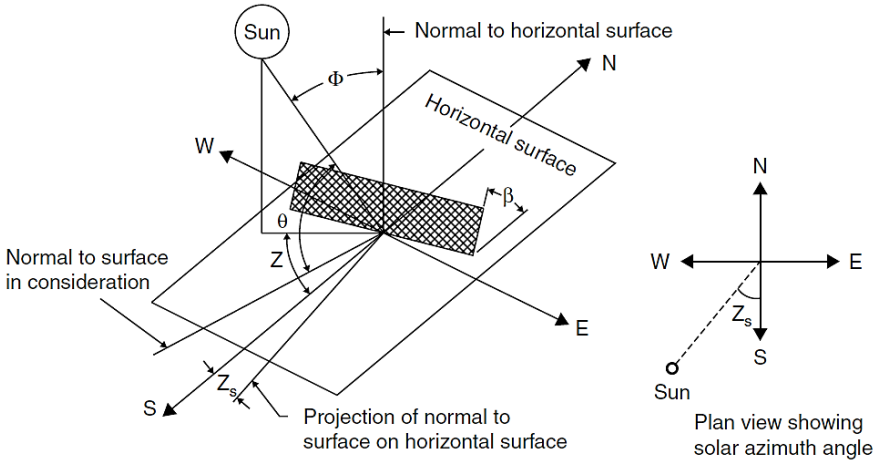

Figure 30: Representation of solar angles (Kalogirou, 2009)

Two 365x24 matrices are formed by using equations (47) and (49). The rows of these matrices represent the days in a year and the columns specify the hours in a day. So, parameters relying on solar geometry are indicated for every hour in a whole year. These equations are also used to determine the beam radiation tilt factor (R_B) as shown in equation (50).

$$R_B = \frac{\cos\theta}{\cos\phi} \tag{50}$$

Equation (50) is utilized in order to calculate the beam irradiance incident on the PV modules. The main aim at this point is to compute the global solar irradiance on the PV modules. This quantity has several components such as beam radiation tilt factor (R_B), beam irradiance on horizontal surface (G_B), diffuse irradiance on horizontal surface (G_D), albedo (ρ_G) and the PV module tilt angle ($\boldsymbol{\beta}$). Three major

components of the global irradiance on a tilted surface (G_t) are beam (direct), diffuse and ground reflected solar irradiance as illustrated in Figure 31.

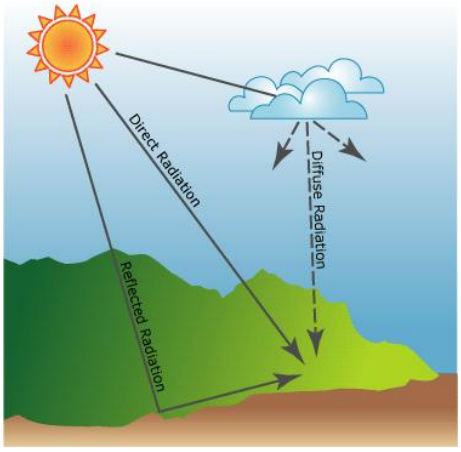

Figure 31: Beam, diffuse and ground reflected irradiance

The ground reflected irradiance depends on albedo which is a coefficient between zero and one. Albedo relies on the reflectivity of the ground. Hourly average values of the global horizontal irradiance can be obtained either by on-site measurements or from various meteorological databases such as Meteonorm, NASA, PVGIS etc. Once this data is gathered, the empirical approach indicated in equation (51) is used to estimate the diffuse irradiance on horizontal (Kalogirou, 2009).

$$G_D = G(1.39 - 4.027K_t + 5.531K_t^2 - 3.108K_t^3) \quad (51)$$

where K_t is the clearness index. It is the ratio of the global irradiance on a terrestrial horizontal surface to total irradiance on an extraterrestrial horizontal surface. The latitude dependent monthly average values of the clearness index can be obtained from different meteorological sources. The beam irradiance on horizontal is just the difference between the global horizontal and diffuse irradiance as shown in equation (52).

$$G_B = G - G_D \quad (52)$$

After obtaining and calculating all of the required data, the hourly average global solar irradiance falling on the tilted PV modules can be calculated by using equation (53).

$$G_t = R_B G_B + G_D \left(\frac{1+\cos \boldsymbol{\beta}}{2}\right) + G\rho_G \left(\frac{1-\cos \boldsymbol{\beta}}{2}\right) \tag{53}$$

The G_t values and the hourly average ambient temperature values (T_A) are used in equation (7) in order to calculate the module temperature (T_M). The actual power output of a PV module relies basically on G_t and T_M values. Additionally, other power reduction factors have to be considered while calculating the actual PV module output. These are; the shading factor (*saf*, %), soiling factor (*sof*, %) and yearly degradation in the module's output power (*d(y)*, %). The last value is provided by the PV module's manufacturer. Usually, the PV modules suffer from linear power loss in each year (*y*). Equation (54) modifies equation (6) by using the additional power loss factors for a PV module.

$$P_{M\_op} = \left(1-\frac{saf}{100}\right)\left(1-\frac{sof}{100}\right)\left(1 - y\frac{d(y)}{100}\right)\left(P_{M\_stc}\frac{G_t}{1000}\left(1+\gamma\frac{T_M-25}{100}\right)\right) \tag{54}$$

The equation above gives the power output of a single PV module. A PV array is the combination of modules connected in series across a string and strings connected in parallel to an inverter. Therefore, the power produced by a module is multiplied by the number of modules in the array. The additional losses such as the efficiency of the maximum power point tracker of the inverter (η_{mppt}), power losses across the

DC main cable (P_{L_dc}) and the string cables (P_{L_str}) have to be considered when computing the output power of a PV array.

$$P_{in} = \begin{cases} \boldsymbol{N_s N_p} \eta_{mppt} P_{M\_op} - P_{L\_dc} - P_{L\_str} \boldsymbol{N_p} & \text{, if } P_{M\_op} > 0 \\ 0 & \text{, else} \end{cases} \quad (55)$$

Depending on the layout of the PV power plant, DC combiner boxes may be used in order to combine a number of PV strings and then distribute the DC power through a DC main cable up to the inverters. In such cases power losses across the DC main cable must be calculated. If the layout of the power plant is chosen in such a way that the PV strings are connected to the inverters directly (decentralized inverter approach), the power loss regarding the DC main cable is eliminated. Equations (56) to (59) define the power losses on the DC side of the PV plant.

$$P_{L\_dc} = \frac{2 L_{dc} I_n^2}{1000 A_{dc} k_{dc}} \quad (56)$$

where L_{dc} is the simple wiring length (m), A_{dc} is the cross-sectional area and k_{dc} is the electrical conductivity $\left(\frac{\text{m}}{\Omega \cdot \text{mm}^2}\right)$ of the DC main cable. The nominal current of the PV array is shown as I_n and calculated in equation (57).

$$I_n = \boldsymbol{N_p} I_{M\_mpp} \quad (57)$$

The power loss across each string cable can be calculated similar to that across the DC main cable. Here L_{str} is the simple wiring length (m), A_{str} is the cross-sectional area and k_{str} is the electrical conductivity $\left(\frac{\text{m}}{\Omega \cdot \text{mm}^2}\right)$ of the string cables. Equation (58) can be used for the calculation of L_{str}, as it depends on $\boldsymbol{N_s}$ and the length of the PV modules (L_{PV}).

$$L_{str} = \boldsymbol{N_s} L_{PV} \quad (58)$$

Subsequently, L_{str} can be substituted in equation (59) to compute the power losses out across each PV string.

$$P_{L\_str} = \frac{2L_{str}I_{M\_mpp}^2}{1000A_{str}k_{str}} \tag{59}$$

The power produced by an inverter depends on efficiency of the inverter (η_i) and the power produced by the PV array.

$$P_{out} = \eta_i P_{in} \tag{60}$$

The power produced by the PV plant is determined by adding the power produced by each individual inverter. The additional loss factors to be considered in this stage are the efficiency of the medium voltage transformer (η_{tr}), power losses across the AC cables $\left(P_{L\_ac}\right)$ and the medium voltage cables $\left(P_{L\_MV}\right)$.

$$P_{pl} = \begin{cases} N_i\left(P_{out} - P_{L\_ac}\right)\eta_{tr} - P_{L\_MV}, & \text{if } P_{out} > 0 \\ 0, & \text{else} \end{cases} \tag{61}$$

The inverters in decentralized topology are distributed all around the PV power plant. Hence, the wiring length of the AC cables (L_{ac}) is subjected to vary for each inverter. In order to eliminate this uncertainty, the user is asked to enter an average value for L_{ac}. As number of PV modules connected to the inverters is same and the inverters are identical, assigning an average length for the AC cables simplifies the problem without changing the total power loss on the AC side.

$$P_{L\_ac} = \frac{3L_{ac}I_{i\_out}^2}{1000A_{ac}k_{ac}} \tag{62}$$

where L_{ac} is the wiring length (m), A_{ac} is the cross-sectional area and k_{ac} is the electrical conductivity $\left(\frac{\mathrm{m}}{\Omega \cdot \mathrm{mm}^2}\right)$ of the AC cables. The final power loss associated with cables is the loss across medium voltage cables. It can be calculated by using equation (63).

$$P_{L\_MV} = \frac{3 I_{MV}^2 L_{MV} R_{MV}}{1000} \tag{63}$$

where L_{MV} is the length up to the point of common coupling (km), R_{MV} is the resistivity $\left(\frac{\Omega}{km}\right)$ and I_{MV} is the current at the medium voltage cables. I_{MV} can be found directly from the transformation ratio of the transformer. Therefore, voltages at the low voltage (V_{LV}) and medium voltage (V_{MV}) sides are important.

$$I_{MV} = \boldsymbol{N_i} \frac{V_{LV}}{V_{MV}} I_{i\_out} \tag{64}$$

Hourly average PV energy generation of the power plant is calculated by using hourly P_{pl} values with the simulation time step $\Delta t = 1h$. Now, all the hourly average power values are converted into energy and represented in kWh.

$$E_{pl\_h} = P_{pl} \cdot \Delta t \tag{65}$$

The amount of net cash inflows is closely related with the yearly self-consumed energy. Therefore the PV energy that is self-consumed has to be calculated on hourly basis firstly. In order to evaluate the self-consumption, the consumption profile of the load must be identified. The injected energy into the grid has no value. Therefore, comparing the PV generation and consumption profiles on hourly basis is important for determining the self-consumed energy, thus the yearly cash inflows accurately.

Equations (66) and (67) are used to calculate the hourly and yearly self-consumed PV energy.

$$SC_h = \begin{cases} E_{pl\_h}, & \text{if } L_h > E_{pl\_h} \\ L_h, & \text{if } L_h \leq E_{pl\_h} \end{cases} \quad (66)$$

$$SC_y = \sum_{d=1}^{365} \sum_{h=0}^{23} SC_h \quad (67)$$

Hereby, the annual cash inflows based on the self-consumed PV energy can be calculated. It depends on price of the electricity in €/kWh (e_t), discount rate (*i*), annual growth rate of the electricity prices (g_e). A constant electricity pricing scheme is currently available in Northern Cyprus. Hence, decomposing the daily and seasonal self-consumed PV energy in different price periods is not required.

$$CIF(y) = e_t SC_y (1 + g_e)^y \quad (68)$$

The annual *CIF* is one of the components of the annual net cash flows. The other component is the annual operating and maintenance cost which refers to cash outflows. It is represented as a ratio (1% is used in this study) of the equipment cost (C_{EQ}). The equation of the operating and maintenance cost also takes the annual growth rate of the operating and maintenance expenditures (g_m) as shown in equation (69). The net cash flow in each year is calculated by considering all three components of it. Here, $C_{initial}$ only takes place in the year of the investment which is defined as year zero. Equation (70) is used to calculate the net cash flows.

$$C_{OM}(y) = 0.01 C_{EQ}(y)(1 + g_m)^y \quad (69)$$

$$NCF(y) = -C_{initial}(y) - C_{OM}(y) + CIF(y) \quad (70)$$

The second sub-branch of the equation tree for the objective functions involves the calculation of area occupied by the PV power plant. Besides, the initial cost of the PV plant investment is calculated in this sub-branch. The area used for PV power generation is based on the layout of the power plant. Therefore, geometrical computations are used to determine this area. The PV modules are mounted in such a way that they constitute the PV blocks. The number of PV module rows and columns in each PV block are defined as $\boldsymbol{N_r}$ and $\boldsymbol{N_c}$ respectively. Figure 32 illustrates the arrangement of PV blocks in the available PV area. Additionally, the other critical parameters which are used in the calculation of the occupied area are shown in Figure 32.

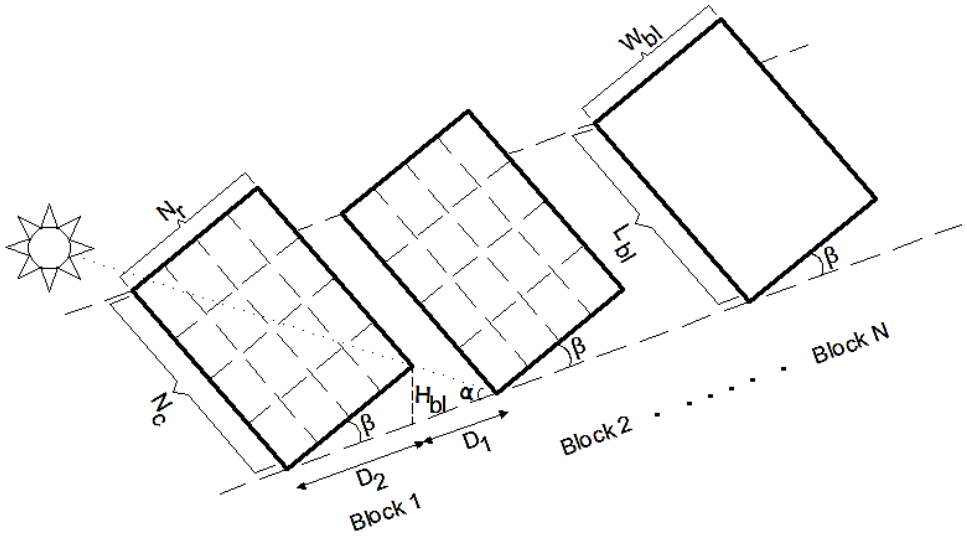

Figure 32: PV blocks installed in the available area

The total width of a PV block depends on the number of PV rows and the width of an individual PV module, W_{PV}, which is represented in meters. The latter can be obtained from the data sheet of the PV modules.

$$W_{bl} = \boldsymbol{N_r} W_{PV} + 0.02(\boldsymbol{N_r} - 1) \tag{71}$$

The constant, 0.02 (2 cm), is used in order to take the space between two rows into account. The center clamps which are located in between two rows require a space of 2 cm. The height and the depth of the PV block are calculated by using the sine and the cosine of the tilt angle. Equations (72) and (73) state this relation respectively.

$$H_{bl} = W_{bl} \cos \boldsymbol{\beta} \tag{72}$$

$$D_2 = W_{bl} \sin \boldsymbol{\beta} \tag{73}$$

Mounting support clearance is the distance between the pile of the front block and the rear block. The calculation of mounting support clearance takes the minimum solar altitude angle throughout a year. This angle is latitude specific and can be gathered from meteorological databases. The maximum solar energy harvesting period is around midday. The mounting support clearance distance must be calculated carefully, so that the front row does not cast shadow onto the second row even in the winter solstice.

$$D_1 = \frac{H_{bl}}{\tan \alpha} \tag{74}$$

The total distance between the blocks is just the summation of the PV block's depth and the mounting support clearance.

$$D = D_1 + D_2 \tag{75}$$

The total length of a PV block depends on the number of PV columns and the length of an individual PV module, L_{PV}, which is represented in meters. The latter can be obtained from the data sheet of the PV modules.

$$L_{bl} = \boldsymbol{N_c} L_{PV} + 0.02(\boldsymbol{N_c} - 1) \tag{76}$$

Similar to the case of row width, 2 cm is used in order to take the space between two columns into account. The center clamps which are located in between two columns require a space of 2 cm. The area occupied by a single PV block is calculated in equation (77).

$$A_{bl} = L_{bl}D \tag{77}$$

The total PV area is the sum of all the areas which are occupied by individual PV blocks. Therefore, number of PV blocks must be calculated beforehand. The total number of PV modules in the power plant is required to determine the number of PV blocks. Equation (78) shows the calculation of total number of PV modules in the power plant and equation (79) is used to define the number of PV blocks. Once these quantities are identified, the total area occupied by the PV plant, in m^2, can be calculated by using equation (80).

$$N_{PV\_t} = \boldsymbol{N_s N_p N_i} \tag{78}$$

$$N_{bl} = \frac{N_{PV\_t}}{\boldsymbol{N_r N_c}} \tag{79}$$

$$A_{tot} = N_{bl}A_{bl} \tag{80}$$

The total area is not only used to determine the size of the PV plant but also is a component in the calculation of the initial cost of the investment. Equation (19) defines the initial investment cost of the PV plant in general terms. This equation is further customized by establishing a relation between the cost components and the equipment cost that is actually the major expenditure. Equation (81) summarizes the customized initial investment cost used in this study.

$$C_{initial} = C_{EQ} + C_L A_{tot} + C_{TP} + C_{Lb} PV_{plant\_STC} + C_{per} \quad (81)$$

where C_{EQ} is the equipment cost (€), C_L is the land cost (€/m^2), C_{TP} is the transportation cost (€), C_{Lb} is the labor cost (€) and C_{per} is the connection permit cost to the national power grid. C_{TP}, C_{Lb} and C_{per} can be expressed in terms of the equipment cost for a more consistent and accurate cost calculation. The coefficients in equations (82), (83) and (84) actually serve as percentage values of the equipment cost (NREL, 2015). These percentage values are general and can be changed depending on the local conditions. Additionally the installed capacity of the PV plant is calculated in equation (85).

$$C_{TP} = 0.02 C_{EQ} \quad (82)$$

$$C_{Lb} = 0.1 C_{EQ} \quad (83)$$

$$C_{per} = 0.005 C_{EQ} \quad (84)$$

$$PV_{plant\_STC} = N_{PV\_t} P_{M\_STC} \quad (85)$$

The general definition of the equipment cost which is used in equation (20), is modified here in order to achieve a more sophisticated representation. The equipment cost is determined both by the decision variables used in the optimization algorithm and constant quantities such as the unit cost of the components used in the PV power plant.

$$\begin{aligned} C_{EQ} = {} & N_{PV\_t} C_{PV} P_{M\_STC} + \boldsymbol{N_i} C_i P_{i\_out} + C_{MS} PV_{plant\_STC} \\ & + \boldsymbol{N_p N_i} L_{str} C_{str} + 2 L_{dc} C_{dc} + \boldsymbol{N_i} L_{ac} C_{ac} + L_{MV} C_{MV} \\ & + (C_{PD} + C_{LPS}) PV_{plant\_STC} + C_{Tr} \end{aligned} \quad (86)$$

Table 14 summarizes the cost components along with their units and the weight in the equipment cost equation. The weights of these cost components are taken from (NREL, 2015).

Table 14: Cost components with definitions, units and weights

Cost Component	Definition	Unit	Weight in equation (86)
C_{PV}	Unit cost of PV modules	€/kW$_p$	60%
C_i	Unit cost of inverters	€/kW$_p$	11%
C_{MS}	Unit cost of mounting system	€/kW$_p$	15%
C_{str}	Unit cost of string cables	€/m	2%
C_{dc}	Unit cost of DC main cables	€/m	1%
C_{ac}	Unit cost of AC cables	€/m	3%
C_{MV}	Unit cost of medium voltage cables	€/m	2%
C_{PD}	Unit cost of over-current protection devices and the electric distribution boards	€/kW$_p$	3%
C_{LPS}	Unit cost of the lightning protection system	€/kW$_p$	1%
C_{Tr}	Total cost of the medium voltage transformer	€	2%

The overall unit cost of the equipment is the ratio of C_{EQ} to PV_{plant_STC}. It decreases with a rate of 8 €/kW$_p$ for each 50 kW$_p$ increment in the system size. Similarly, for each 50 kW$_p$ decrement in the system size, the unit cost of the equipment rises with a rate of 8 €/kW$_p$. This change in the general unit price is then reflected in the unit price of each component by means of its weight stated in Table 14. As the installed capacity increases the unit cost of the system decreases, however the amount of the PV energy injected to the grid increases. Since this energy has no value, the excessive installed capacity results in more energy injected into the grid free of charge. Therefore, this balance is very important while deciding the optimum capacity.

The payback period is calculated by combining $C_{initial}$ from equation (81) and $NCF(y)$ from equation (70). The result of this equation is the main target of the methodology that is proposed. The payback period is calculated for each iteration as the number of inverters, hence the PV plant size changes.

$$0 = -C_{initial} + \sum_{y=1}^{y=pbp} NCF(y)\left(\frac{1}{(1+i)^y}\right) \tag{87}$$

The step size of the iterations depends on the rated power of the selected inverter model. This may change from 10 kW to 100 kW for a decentralized PV power plant. Therefore, the payback period varies gradually. Net present value can be used as a second measure in order to choose the best project among the alternatives having very close or same payback periods.

$$NPV = -C_{initial} + \sum_{y=1}^{n} NCF(y)\left(\frac{1}{(1+i)^n}\right) \tag{88}$$

where n is the economic lifetime of the project. The other measures which are calculated for each PV plant size are the annual PV energy generation, annual energy injected into the grid and the energy from the grid. The solar energy generated by the plant in one year is calculated by using the equation (89).

$$E_{pl\_y} = \sum_{d=1}^{365}\sum_{h=0}^{23} E_{pl\_h} \tag{89}$$

The hourly average and the annual values of the energy injected into the grid are calculated in the following equations respectively.

$$EF_h = \begin{cases} 0, & \text{if } L_h \geq E_{pl\_h} \\ E_{pl\_h} - L_h, & \text{if } L_h < E_{pl\_h} \end{cases} \tag{90}$$

$$EF_y = \sum_{d=1}^{365} \sum_{h=0}^{23} EF_h \tag{91}$$

The hourly average and the annual values of the energy from grid are calculated in the following equations respectively.

$$EG_h = \begin{cases} L_h - E_{pl\_h}, & \text{if } L_h > E_{pl\_h} \\ 0, & \text{if } L_h \leq E_{pl\_h} \end{cases} \tag{92}$$

$$EG_y = \sum_{d=1}^{365} \sum_{h=0}^{23} EG_h \tag{93}$$

Chapter 5

CASE STUDY AND RESULTS

5.1 Structure of the Methodology

The proposed methodology is implemented by using the Global Optimization Toolbox in the MATLAB platform. Constrained nonlinear minimization solver is used for the predefined optimization problem in order to find a minimum point of the optimization problem using the interior point algorithm. The interior point algorithm is selected because it is especially useful for large-scale problems that have sparsity or structure, and tolerates user-defined objective and constraint function evaluation failures. It is based on a barrier function, and optionally keeps all iterations strictly feasible with respect to bounds during the optimization run.

The methodology is implemented in the campus of Cyprus International University that is located in Nicosia, Northern Cyprus. The electricity consumption was 3,860,230 kWh in 2011 while it reached 4,594,800 kWh in 2014. Figure 33 shows the consumption in the last three years and the first quarter of 2015. As it can be observed**,** the lowest consumption occurs in September when the University is partially closed. In hot regions such as Cyprus, highest electricity consumption always occurs during the summer period due to excessive use of air-conditioning systems. However, this is not valid for the University. The consumption in winter is higher than the consumption in summer because of the summer break.

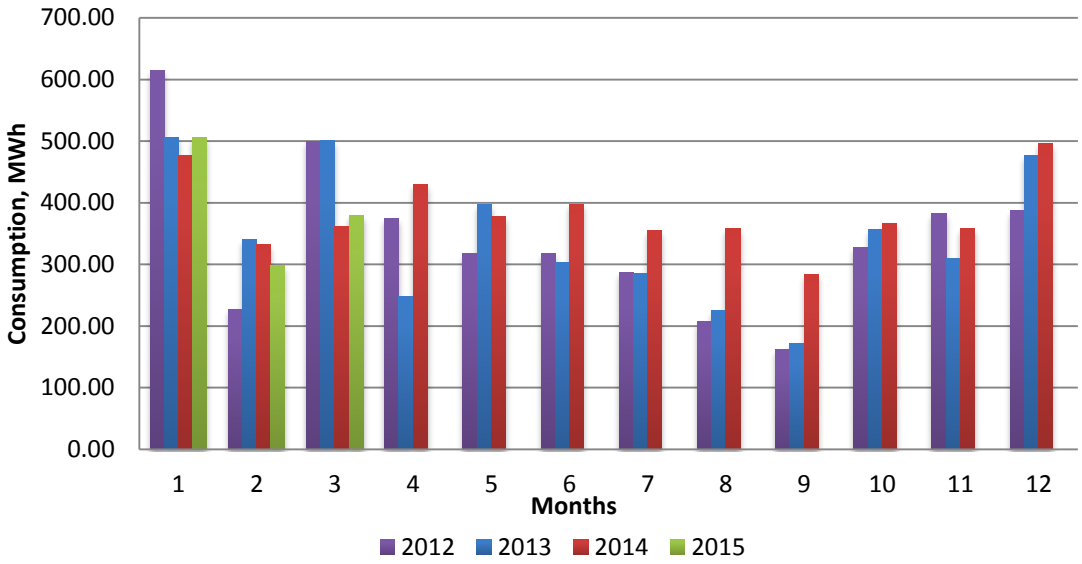

Figure 33: Electricity consumption of the University campus in years 2012-2015

The significance of the daily load profiles was emphasized in Section 3.2. Therefore, the daily electricity consumption of the University was measured during weekdays and weekends. These data were used to form the daily load profiles throughout the year. As both the educational and administrative works continue during all the year, it is assumed that the characteristic of the daily load profile stays unchanged in each academic semester. Figure 34 shows the daily load profiles of a typical weekday, Saturday and Sunday in December 2014. On the weekdays and Saturdays, electricity demand starts to increase in the early morning and reaches its peak value at 10 a.m. A wide demand plateau can be observed until the evening peak. The continuous educational and administrative works yield a wide consumption plateau in midday, but the evening peak is due to the dormitories and campus lighting.

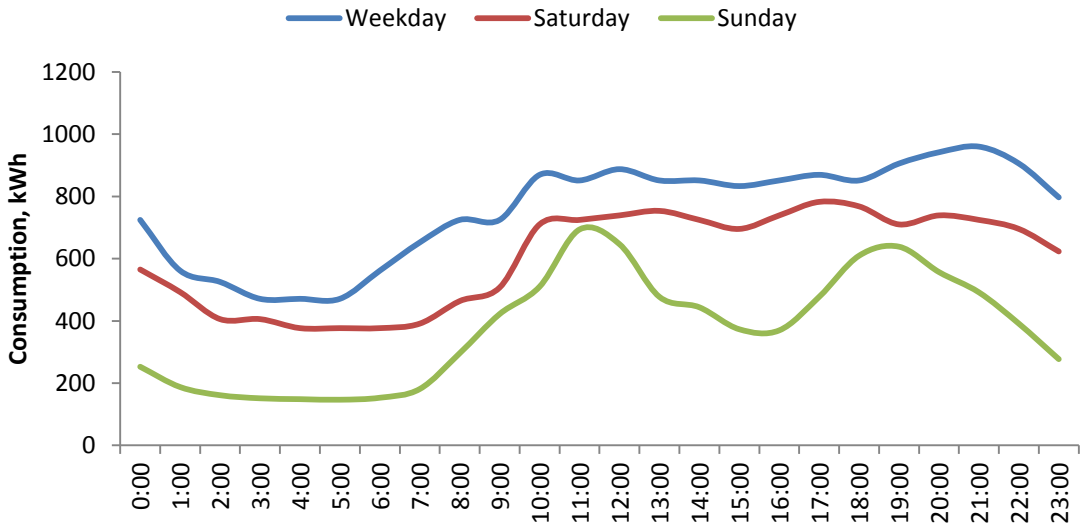

Figure 34: Daily electricity consumptions in a typical weekday, Saturday and Sunday

The universities in Northern Cyprus are enrolled in a constant electricity pricing scheme. The current electricity tariff for universities is 0.44 TL/kWh (KIB-TEK, 2015). TL is the Turkish currency unit and 1 Euro is equivalent to 3.5 TL on average in the last quarter of 2016. The evolution of the electricity tariffs for the universities between 2000 and 2016 is shown in Figure 35. It can be deduced that the average increase in the price of electricity is 20% p.a. in the last 17 years. To sum up, there is no need to correlate the consumption profile and the electricity tariffs as a single electrical tariff is to be discussed in this case study. The initial investment cost is expressed in Euro since all the equipment is imported. In order to ensure the consistency in the cash flow analysis, the electricity tariff is converted from TL to Euro. So, the tariff is taken as 0.126 €/kWh throughout the case study.

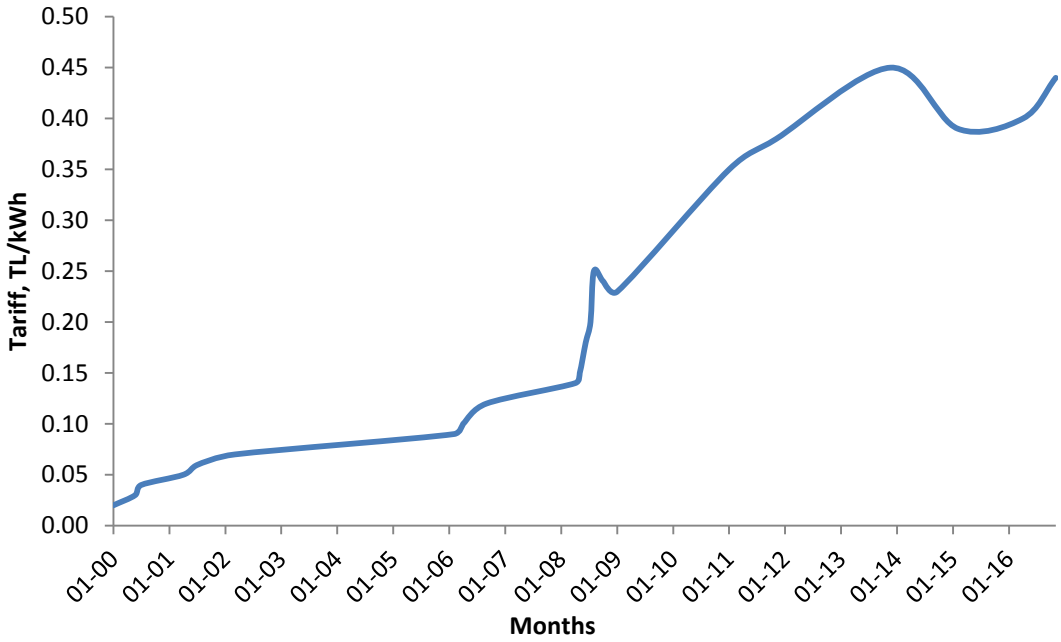

Figure 35: Evolution of electricity tariff for the universities in Northern Cyprus

The meteorological data set that includes hourly average values of the global horizontal irradiance (G) and the ambient temperature (T_A) is taken from PV*SOL Premium. PV*SOL Premium is a widely accepted PV system analysis and planning software. The meteorological data in PV*SOL Premium are originated from Meteonorm 7.0 which is a database that provides regional and global solar energy data. This meteorological data for Nicosia (35.19° N, 33.35° E) are the average of 20 years (1986-2005). 365x24 matrices are formed for G and T_A datasets. Each element in these matrices represents an hourly average value.

$$G = \begin{pmatrix} G_{11} & \cdots & G_{1m} \\ \vdots & \ddots & \vdots \\ G_{n1} & \cdots & G_{nm} \end{pmatrix} \tag{94}$$

$$T_A = \begin{pmatrix} T_{A_{11}} & \cdots & T_{A_{1m}} \\ \vdots & \ddots & \vdots \\ T_{A_{n1}} & \cdots & T_{A_{nm}} \end{pmatrix} \tag{95}$$

where *n* represents 365 days of a year and *m* represents 24 hours of a day.

The renewable energy law in Northern Cyprus states that; if total installed PV capacity is over 200 kW_p, then the PV system should be connected to the medium voltage grid. Furthermore, the law allows the consumers to connect a renewable energy unit with a capacity corresponding to ⅔ of their load demand to the grid over their own facility. The law only allows on-site generation. It means that the person who is going to install a renewable energy system must be a consumer and establish the connection over his/her metering unit. In addition to this, the stiffness ratio of the grid is calculated by KIB-TEK before giving the preliminary permission to the investors. The stiffness ratio is the ratio of the short circuit current (or power) of the grid at the Point of common coupling to the nominal current (or power) of the PV plant. This ratio must be above 100.

$$\text{Stiffness Ratio} = \frac{I''_{sc}}{I_n} \geq 100 \text{ or } \frac{S''_{sc}}{P_n} \geq 100 \tag{96}$$

The mathematical model applied in this study requires technical and economical parameters which are summarized in the methodology section. The specifications of the PV modules are summarized in Table 15.

Table 15: Specifications of the PV modules (Yingli Green Energy Holding Company)

Rated Power at STC (P_{M_STC})	0.31 kW_p
Module Efficiency (η_M)	15.9 %
Voltage at Maximum Power Point (V_{M_mpp})	36.3 V
Current a Maximum Power Point (I_{M_mpp})	8.53 A
Open Circuit Voltage (V_{M_oc})	45.6 V
Short Circuit Current (I_{M_sc})	8.99 A
NOCT	46 +/-2℃
Temperature Coefficient of P_{M_STC} (γ)	-0.42 %/℃
Temperature Coefficient of V_{M_oc} (β_{oc})	-0.32 %/℃
Temperature Coefficient of I_{M_sc} (α_{sc})	0.05 %/℃
Dimensions (L x W x H)	1970x990x50 mm^3
Weight	26 kg

The second important technical parameter is based on the inverter selection. The specifications of the inverters are summarized in Table 16.

Table 16: Specifications of the inverters (SMA Solar Technology AG)

Maximum DC power input (P_{i_max})	25.55 kW
Maximum DC Input Voltage (V_{i_max})	1000 V
Maximum MPP Voltage $(V_{i\_mpp\_max})$	800 V
Minimum MPP Voltage $(V_{i\_mpp\_min})$	390 V
Maximum Input Current (A/B) (I_{i_max})	33 A / 33 A
Rated AC Output Power (P_{i_out})	25 kW
Nominal AC Output Current (I_{i_out})	36.2 A
Nominal AC Output Voltage Range	160 – 280 V
Frequency	50 Hz
Conversion Efficiency (η_i)	98.3 %
MPPT Efficiency (η_{mppt})	99.0 %
Dimensions (W x H x D)	665x690x265 mm^3
Weight	61 kg

The miscellaneous parameters such as the unit cost of the power plant and the available area specifications are listed in Table 17. A reference equipment cost for a 1,000 kW_p PV plant is taken as 1,000,000 €. This makes the unit price for the equipment cost to be 1,000 €/kW_p. This unit cost is then distributed to the components of equipment cost with respect to their weights as stated in Table 14. The unit cost is dynamic in this study. It reduces in the steps of 8 €/kW_p for each 50 kW_p increase in the PV plant size. This rate is obtained after a PV market analysis based on operational and financial data for large-scale PV plants.

The first phase of the optimization algorithm is performed in order to calculate the decision variables which provide the minimum rate of energy injected into the grid. The decision variable vector $\mathbf{X} = \{\beta, N_p, N_s, N_i\}$ is decided as $\mathbf{X} = \{31.5,5,17,12\}$. The algorithm, $\min_{\mathbf{X}}\{\%E_{lost}(\mathbf{X})\}$, converges at 0% of energy lost (i.e. the amount of

energy injected into the grid for free of charge is zero). The variables obtained in the first phase are used in the second phase of the optimization algorithm. Here, the decision variable vector $\mathbf{Z} = \{N_r, N_c\}$ is calculated as $\mathbf{Z} = \{4,35\}$. The algorithm, $\mathbf{max}_{\mathbf{Z}}\{A_{tot}(\mathbf{Z})\}$, converges at 4042.2 m^2.

Table 17: Miscellaneous parameters of the PV system

Reference unit cost of the PV equipment	1,000 €/kW_p
Land Cost (L_A)	25 €/m^2
Maximum available area (A_{max})	14,000 m^2
Maximum permissible length of the southern side of the area (L_A)	70 m
Discount rate (i)	3%
Electricity tariff (e_t)	0.126 €
Growth rate of the electricity tariff (g_e)	10% pa.
Operating and maintenance cost (g_m)	1% of the equipment cost
Shading factor (*saf*)	3%
Soiling factor (*sof*)	1%
Annual PV degradation $(d(y))$	0.8%
Economic lifetime of the project	25 years
Albedo (ρ_G)	0.2
Azimuth angle of the PV modules (Z_s)	0^0

The calculated values of all six decision variables are used in the third phase of the algorithm in order to determine the PV plant size having the lowest payback period with an iterative approach. The inverter number is incremented from 9 (three less than the initial inverter number because of the reasons stated in Section 4.3) to 41 (this is the maximum inverter number that provides maximum system size within the limits of the available area). For each inverter number, PV plant size, number of PV modules, energy generated by the PV plant, self-consumed PV energy, energy injected into the grid, energy from the grid, payback period and the net present value are calculated. Table 18 summarizes the increments in the installed capacity of the PV plant from 237 to 1080 kW_p.

Table 18: Simulated PV plant sizes

Plant Size (kWp)	Number of Inverters	Number of PV Modules	Plant Size (kWp)	Number of Inverters	Number of PV Modules
237	9	765	**659**	25	2125
264	10	850	**685**	26	2210
290	11	935	**712**	27	2295
316	12	1020	**738**	28	2380
343	13	1105	**764**	29	2465
369	14	1190	**791**	30	2550
395	15	1275	**817**	31	2635
422	16	1360	**843**	32	2720
448	17	1445	**870**	33	2805
474	18	1530	**896**	34	2890
501	19	1615	**922**	35	2975
527	20	1700	**949**	36	3060
553	21	1785	**975**	37	3145
580	22	1870	**1001**	38	3230
606	23	1955	**1028**	39	3315
632	24	2040	**1054**	40	3400
			1080	41	3485

As the installed capacity increases the rates of energy fed into the grid, self-consumption and self-sufficiency change. Self-consumption rate is defined as the ratio of the self-consumed energy to the energy generated by the PV plant. Figure 13 and equation (1) in Section 3.2 can be used to visualize this rate. Self-sufficiency is the ratio of the self-consumed energy to the consumption. It shows how the on-site PV energy generation meets the consumption requirement sufficiently.

As it can be seen from Figure 36, the percent energy lost and the rate of self-sufficiency increase nonlinearly with each linear incrementation in the size of the PV plant. The energy lost rate goes up exponentially, while the rate of increase in the self-sufficiency declines as the plant size increases. This is mainly because of the mismatch between the electricity consumption and generation curves. The rate of increase in the self-sufficiency slows down because the power plant can never meet the amount of the load demanded at night without utilizing the energy units. On the

other hand, the rate of self-consumption falls from 100% to lower values as the plant size grows. Actually, the self-consumption rate and the energy lost rate are complementary. These rates are 100% and 0% respectively at the smallest plant size. Then, they are equal to 87.25% and 12.75% respectively at the largest power plant size.

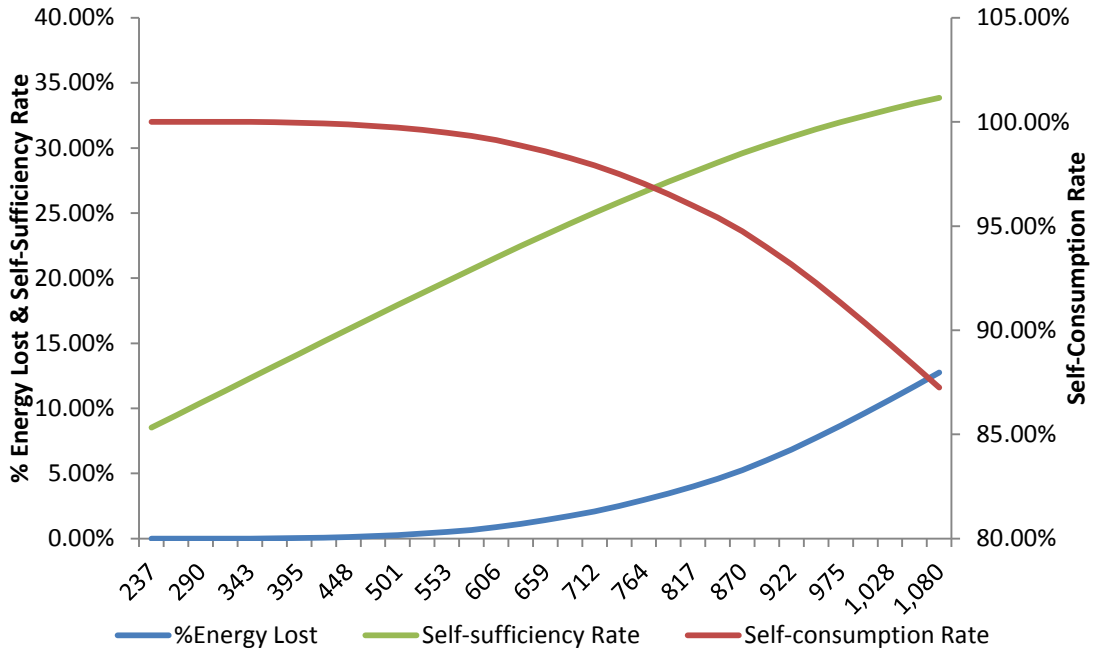

Figure 36: Percent energy lost, self-consumption and self-sufficiency rates

The initial investment cost of the project involves the equipment cost, land cost, transportation cost, labor cost and grid connection cost as stated both in Section 3.8 and Section 4.4. The PV system pricing data are obtained from various energy procurement companies. The cost per kW_p involves two main components. The first part includes equipment cost for low-voltage and medium-voltage sides (modules, inverters, mounting systems, cabling, protection devices and transformers), grid connection cost, transportation cost and labor cost. The second part includes the area cost. The unit cost of the entire power plant investment starts from 1580 €/kW_p for

237 kW_p system and ends at 1429 €/kW_p for 1080 kW_p system. The unit price of the initial investment cost excluding the land cost can be more comprehensible from the investor point of view. The land cost does not change remarkably with the selected combination of the equipment. The area requirement of the equally sized systems, which are composed of different equipment, is more or less the same. Therefore, the investor may want to see the unit price of the first part of the investment cost. The unit cost of the entire power plant investment excluding the expenses on the land starts from 1262 €/kW_p for 237 kW_p system and ends at 1111 €/kW_p for 1080 kW_p system.

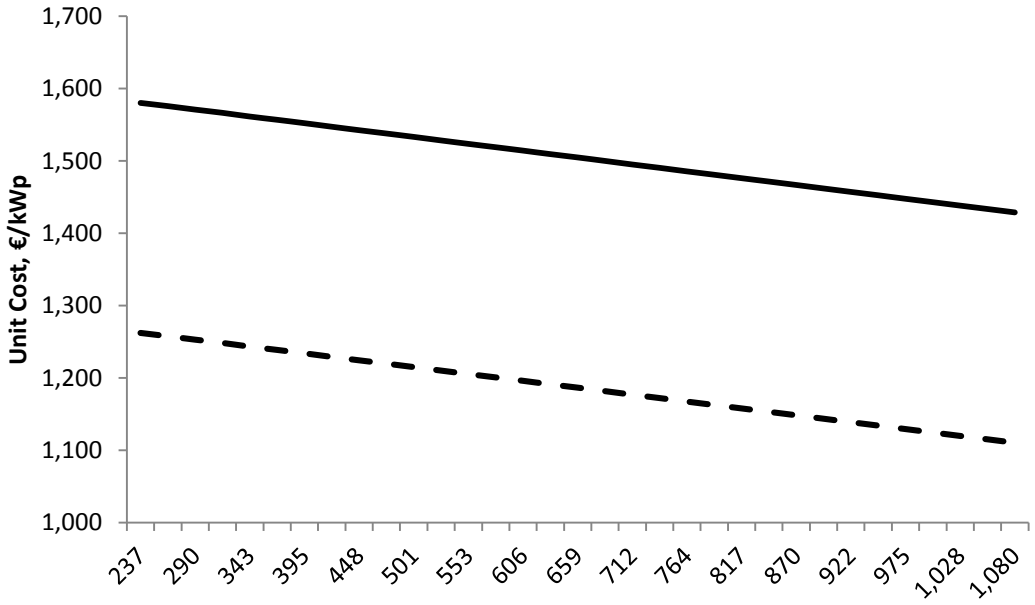

Figure 37: Trends in the unit cost of the PV power plant investment

The downward trends in the unit costs of the PV plant investment are compared in Figure 37. The solid line represents the unit cost of the entire investment while the dashed line stands for the unit cost excluding the expenditures on the land.

The payback period for each plant size is calculated in order to find out the system size having the lowest payback time. The decision variables obtained in the first two phases of the algorithm are utilized in this stage. The change in the payback period with the growth in the PV plant size is illustrated in Figure 38.

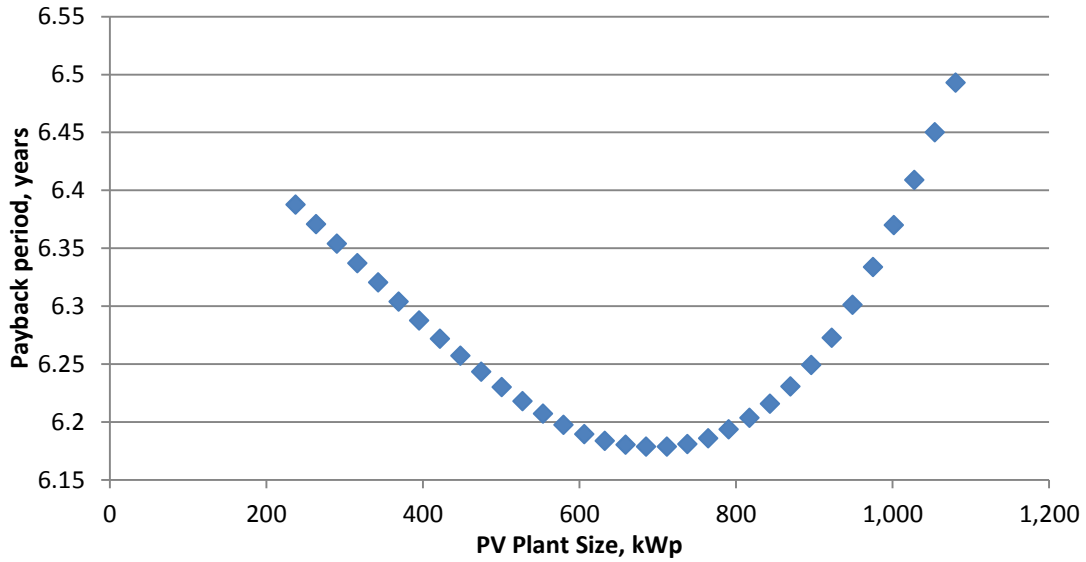

Figure 38: The change in PBP with respect to the installed PV capacity

The lowest payback period is achieved at 6.18 years with the total installed capacity of 712 kW_p. The payback time falls as the PV plant capacity increases from the smallest to its optimum size. The rise in the energy injected into the grid can be compensated by the drop in the unit cost of the overall investment up to the optimal PV plant capacity. After this point, the exponential growth in the energy lost rate surpasses the merits of the decline of the unit cost. At the same time, the rate of increase of the self-sufficiency cannot cope with the aggressive growth of the energy lost rate. Therefore, the payback period starts to escalate in the PV plants with higher capacity than the optimal size. Figure 39 shows the correlation between the increase in the PV capacity, the change in the payback period of the investment and the change in the PV energy injected to the grid with respect to the installed capacity.

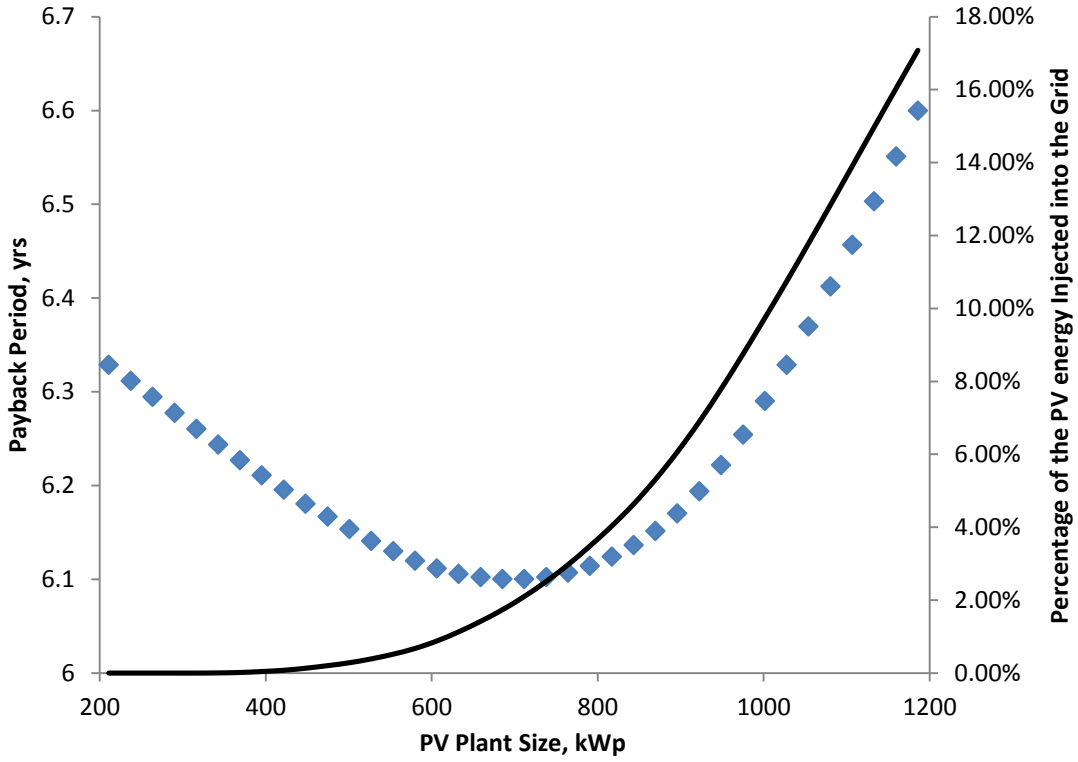

Figure 39: Amount of PV energy injected into the grid and the change in payback period with respect to the installed PV capacity

The land cost can be excluded from the total investment cost to observe the sole impact of the equipment and other miscellaneous costs on the payback period. The investors of the PV power plants may not necessarily pay for the land. The PV plant may be installed on pre-owned lands or roofs. The two parallel curves in Figure 40 indicate the change of the payback periods with and without the land cost. The lowest payback period of the PV plant without land cost is 5.03 years. This is achieved at 738 kW_p of installed capacity.

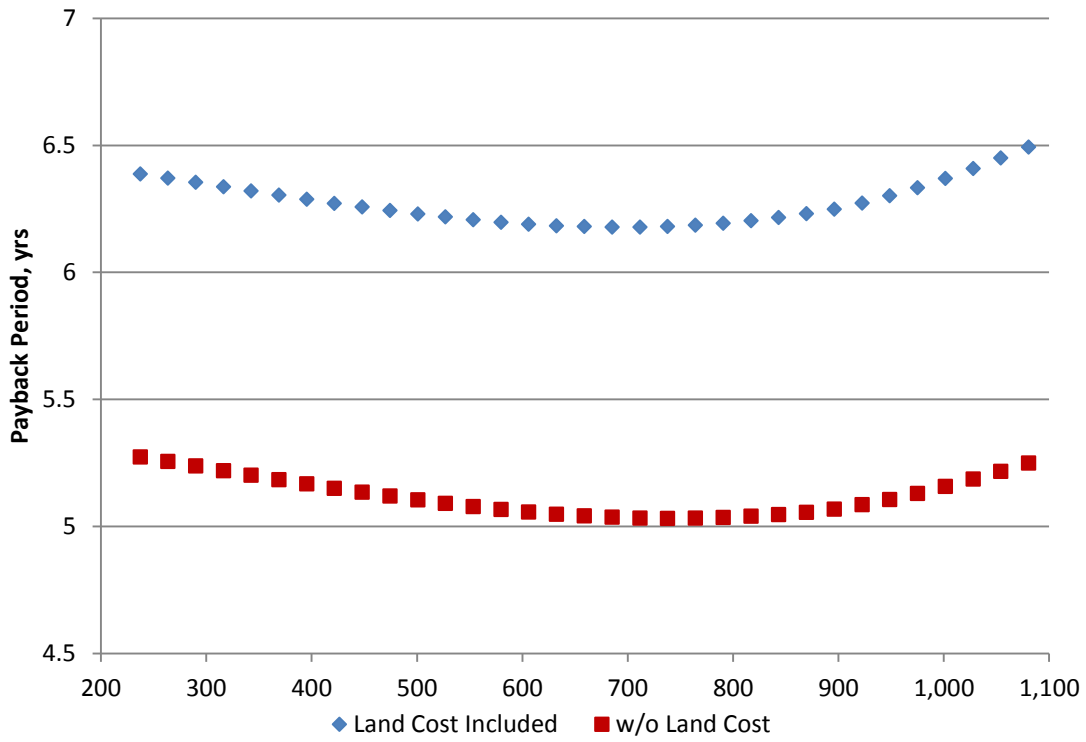

Figure 40: Comparison of the PBPs of the projects with and without the land cost

The decision variables obtained from the first two phases of the proposed algorithm are entered as input variables into PV*SOL Premium in order to calculate the payback period for each system size by a commercially available PV analysis and planning software. Figure 41 compares the payback period results calculated by the proposed algorithm and PV*SOL Premium for each increment in the PV plant size. The diamond data markers are used to illustrate the payback times calculated by the proposed algorithm. The square markers are used to show the payback times calculated in PV*SOL Premium. PV*SOL expresses the payback times up to one tenth of a number. However, the resolution of the results returned by the algorithm is much higher. This is the reason of having many payback period points lying in the same position.

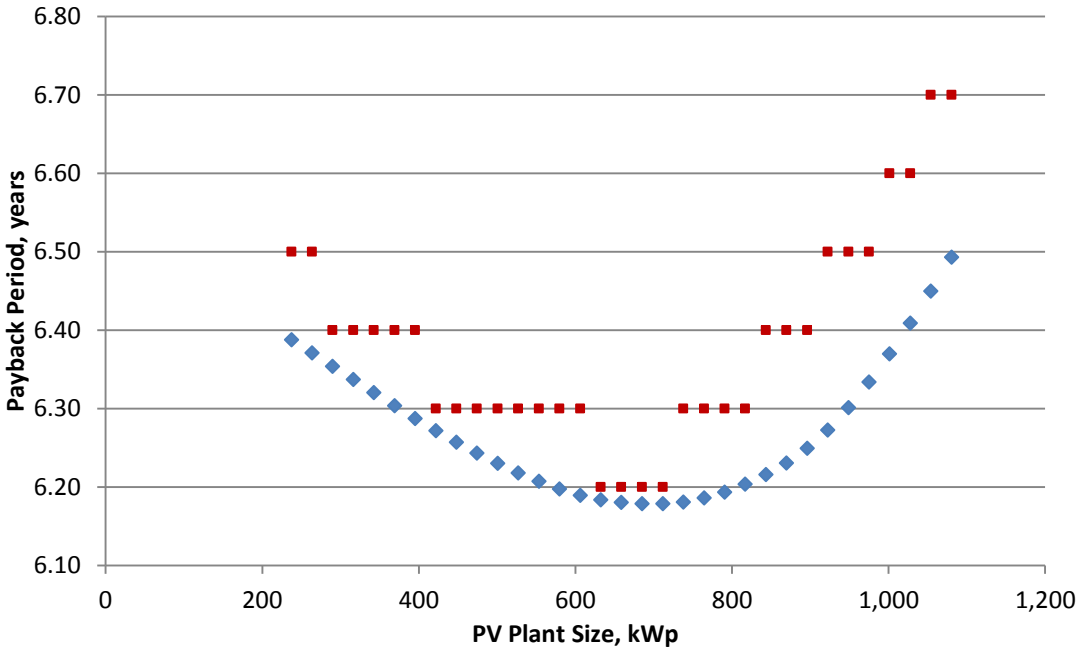

Figure 41: Comparison of payback periods obtained from the proposed algorithm and PV*SOL Premium

The difference between the payback periods obtained from the proposed algorithm and PV*SOL Premium is 1.8% on average. This is equivalent to one tenth of a year or approximately a month. Moreover, the two curves are parallel to each other. This indicates that the proposed algorithm operates with a great proximity to PV*SOL Premium.

The payback period analysis is used to make quick judgements about a particular investment. However, on its own it may not be enough to decide whether or not to make an investment. Therefore, payback analysis is used as a first-cut evaluation tool in conjunction with the net present value analysis. Furthermore, the payback period changes by fractions of a year. This may cause difficulties when selecting the right PV plant size.

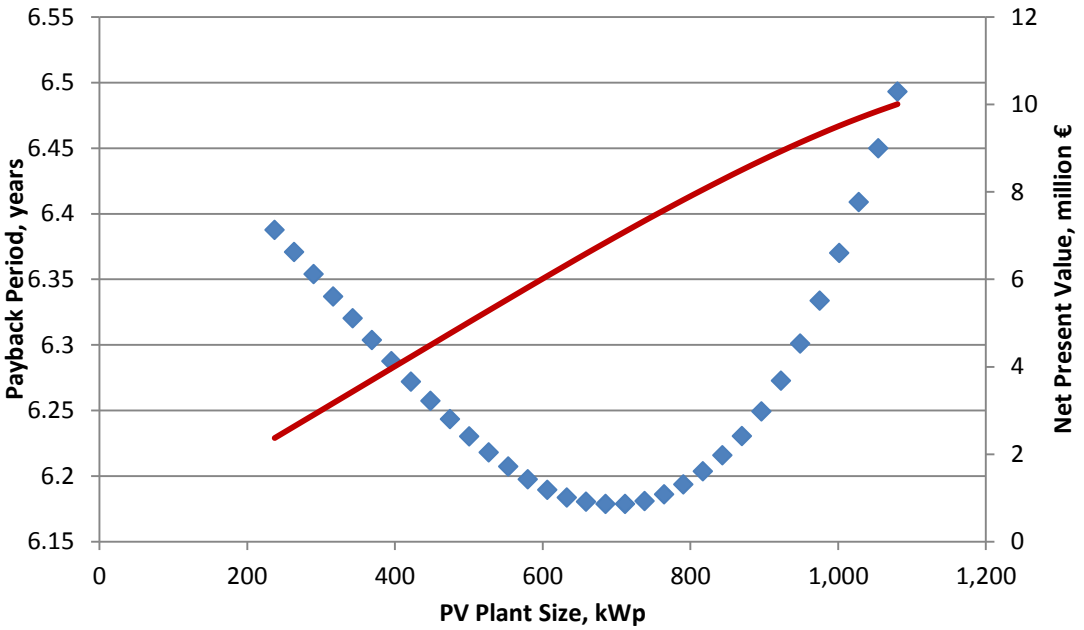

Figure 42: Net present value and payback period

The payback period falls to its lowest value that is 6.18 years, at a plant size of 712 kW_p. The net present value of this plant size is calculated as € 7,091,000. However, the payback periods of other plant sizes, which are close to 712 kW_p are only higher by one thousandth. These fractional variations may not have a significant impact on the judgment of the project. For instance, the payback period vector $PBP = [6.1894 \quad 6.1837 \quad 6.1804 \quad 6.1788 \quad 6.1788 \quad 6.1810 \quad 6.1860 \quad 6.1936]$ is calculated for the plant sizes $P = [606 \quad 632 \quad 659 \quad 685 \quad 715 \quad 738 \quad 764 \quad 791]$ and the corresponding net present values are presented in € in the vector $NPV = [6.073 \quad 6.332 \quad 6{,}588 \quad 6{,}841 \quad 7{,}091 \quad 7{,}338 \quad 7{,}580 \quad 7{,}818] \times 10^6$. The investor may choose the PV plant having the highest net present value among the lowest payback periods depending on his/her approach to the project.

Chapter 6

CONCLUSIONS AND FUTURE WORK

6.1 Conclusions

This study proposes a methodology on installing a large-scale PV plant with self-consumption support scheme. The main objective of this methodology is to find out optimum power capacity to be installed by considering technical and economic aspects. A flowchart of the process, that uses site survey, system components, associated costs, meteorological data, load analysis, is created. A three-step algorithm is developed in order to solve the optimization problem that searches for the PV plant size having the lowest payback period. The optimization algorithm is modelled in such a way that the number, ratings and the arrangement of the selected components have a direct impact on the goal. Four decision variables such as the tilt angle of the PV modules, number of PV modules connected in series across a string, number of strings connected to an inverter and the number of inverters are obtained from the first phase of the algorithm. The optimum combination of these decision variables gives the minimum energy injected into the grid for free of charge. The second phase of the optimization algorithm is used to determine the number of rows and the columns in a PV block for the maximum area occupied by the PV plant. The decision variables obtained from the first phase are used here to determine the area of the PV plant. Then, the results of all six decision variables are substituted in the third phase of the algorithm. Here, an iterative approach is applied to calculate the economic parameters such as payback period and net present value of various PV

plant sizes. Large-scale PV power plants take advantage of the lower prices in the wholesale market. Therefore, they provide a reduction in the PV plant cost per nominal system size. This ratio is known as the unit price. The unit price of the equipment cost decreases with a rate of 8 €/kW_p for each 50 kW_p increment in the system size. Similarly, for each 50 kW_p decrement in the system size, the unit cost of the equipment rises with a rate of 8 €/kW_p The parameters such as the annual PV energy generation, annual self-consumed energy, annual energy injected into the grid and the energy from the grid are calculated to assess a large-scale PV power plant investment by considering all of the aspects.

According to the proposed methodology, a case study is carried out in a university campus located in Nicosia, Northern Cyprus. The lowest payback period is achieved at 6.10 years with the total installed capacity of 712 kW_p. The payback period results calculated by the proposed algorithm and PV*SOL Premium for each increment in the PV plant size are compared. The difference between the payback periods obtained from the proposed algorithm and PV*SOL Premium is 1.8% on average. This is equivalent to one fifth of a year or approximately two and a half months. Additionally, the payback curves obtained from these two different approaches are parallel to each other. This validates the high accuracy of the proposed method in energy-based and economic calculations.

According to the case study, a 712 kW_p self-consumption PV plant can be installed on 9055 m^2 of land area. The system can consume 97.92% of its own annual production while only 2.09% of the annual PV energy generation is exported to the grid. The system reaches a self-sufficiency ratio of 25.02%. The net present value is

calculated as 7,091,000 €. Projected CO_2 emission of 678.134 ton/yr is factored into the design.

6.2 Future Work

In this research, a methodology is used to find the optimum size of a large-scale PV power plant having the lowest payback period under the non-incentivized self-consumption support scheme. The algorithm, which is used in this study, can be further developed and implemented on PV systems which are subjected to different regulatory frameworks. The algorithm can be modified so that the impact of the demand side management and energy storage systems on the economic analyses can be observed. Moreover, sensitivity analysis can be performed in order to determine the reaction of the payback period to the variations of different independent input variables such as the climate or costs. The technical and economic analysis can also be done for different physical and environmental conditions. The impact of higher altitudes, partial shading and soiling both on the energy production of the PV system and the economic parameters can be investigated.

REFERENCES

ABB. (2010). *Technical Application Papers No.10: Photovoltaic Plants.* Bergamo: ABB.

Abbasoğlu, S. (2011). Techno-economic and environmental analysis of PV power plants in Northern Cyprus. *Energy Education Science and Technology Part A: Energy Science and Research, 28*(1), 357-368.

Adedeji, M., Abbasoğlu, S., & Şenol, M. (2015). Determination of Optimum Tilt and Azimuth Angles for Photovoltaic Systems in Northern Cyprus. Proceedings of SolarTR Conference (pp. 554-560). İzmir: GUNDER.

Agarwal, A., Vashishtha, V. K., & Mishra, S. N. (2012). Comparative approach for the optimization of tilt angle to receive maximum radiation. *IJERT, 1*(5).

Agathokleous, R. A., & Kalogirou, S. A. (2016). Double skin facades (DSF) and building integrated photovoltaics (BIPV): A review of configurations and heat transfer characteristics. *Renewable Energy, 89*, 743-756.

Bakas, P., Papastergiou, K., & Norrga, S. (2011). Solar PV array-inverter matching considering impact of environmental conditions. 37th IEEE Photovoltaic Specialists Conference (PVSC) (pp. 1779-1784). Seattle: IEEE.

Bakirci, K. (2012). General Models for Optimum Tilt Angles of Solar Panels: Turkey Case Study. *Renewable and Sustainable Energy Reviews, 16*, 6149-6159.

Barbose, G., & Darghouth, N. (2015). *Tracking the Sun VIII.* CA, United States: Lawrence Berkeley National Laboratory.

Benghanem, M. (2011). Optimization of tilt angle for solar panel Case study for Madinah, Saudi Arabia. *Applied Energy, 88*, 1427-1433.

Blank, L., & Tarquin, A. (2005). *Engineering Economy* (6. ed.). NY, United States: McGraw Hill.

BP. (2015). *BP Energy Outlook 2035 Technical Report.* London: BP.

BP. (2016). *BP Energy Outlook 2016.* London: BP.

BP. (2016). *Statistical Review of World Energy 2016.* London: BP.

BS 7671:2008, Amendment 3: 2015. (2015). *The IET Wiring Regulations.* London: The Institution of Engineering and Technology.

Charalambous, C. A., Kokkinos, N. D., & Christofides, N. (2013). External Lightning Protection and Grounding in Large-Scale PV Applications. *IEEE Transactions on Electromagnetic Compatibility, 56*(2), 427-434.

CLC/TS 50539-12:2013. (2013). *Low-voltage surge protective devices - surge protective devices for specific application including d.c. - part 12: selection and application principles - SPDs connected to photovoltaic installations.* Brussels: Belgium: CENELEC.

Coster, E. J., Myrzik, J. M., Kruimer, B., & Kling, W. L. (2011). Integration Issues of Distributed Generation in Distribution Grids. Proceedings of the IEEE, 99(1), 28-39.

Dehler, J., Keles, D., Telsnig, T., Fleischer, B., Baumann, M., Fraboulet, D., . . . Fichtner, W. (2015, June). Self-consumption of Electricity from Renewable Sources. *Insight_E*.

DEHN + SÖHNE. (2014). *Lightning Protection Guide* (3. ed.). Neumarkt, Germany: DEHN + SÖHNE.

Deutsche Bank AG. (2015). *Deutche Bank Solar Market Research Report*. Deutsche Bank AG.

DGS LV Berlin BRB. (2008). *Planning and Installing Photovoltaic Systems* (2. ed.). London: Earhscan.

Dusonchet, L., & Telaretti, E. (2015). Comparative economic analysis of support policies for solar PV in the most representative EU countries. *Renewable and Sustainable Energy Reviews, 42*, 986-998.

Eke, R., & Senturk, A. (2012). Performance comparison of a double-axis sun tracking versus fixed PV system. *Solar Energy, 86*, 2665-2672.

Emery, K., & Smith, R. (2011). Monitoring System Performance. *Photovoltaic Module Reliability Workshop 2011* (pp. 163-186). Colarado: USA: NREL.

EN 50380. (2003). *Datasheet and nameplate information of PV modules.* Brussels: Belgium: European Committee for Electrotechnical Standardization.

EPIA. (2013). *Self-Consumption of PV Electricity.* Brussels: EPIA.

EPIA. (2015). *Global Market Outlook for Solar Power 2015 - 2019.* Brussels: EPIA.

EPIA. (2016). *Global Market Outlook for Solar Power 2016 - 2020.* Brussels: EPIA.

European Commission. (2013). *European Commission Guidance for the Design of Renewables Support Schemes.* Brussels: European Commission.

European Commission. (2015). *Best Practices on Renewable Energy Self-Consumption.* Brussels: European Commission.

Fraunhofer ISE. (2014). *Recent Facts about Photovoltaics in Germany.* Freiburg: Fraunhofer ISE.

Fraunhofer ISE. (2015). *Photovoltaics Report 2015.* Freiburg: Fraunhofer ISE.

Ghosh, H. R., Bhowmik, N. C., & Hussain, M. (2010). Determining seasonal optimum tilt angles, solar radiations on variously oriented, single and double axis tracking surfaces at Dhaka. *Renewable Energy, 35*, 1292-1297.

Gorji, N. E., Zandi, M. H., Houshmand, M., Abrari, M., & Abaei, B. (2011). Concentration effects on the efficiency, thickness and J–V characteristics of the intermediate band solar cells. *Physica E, 43*(4), 989-993.

Hernandez, J., Vidal, P. G., & Jurado, F. (2008). Lightning and Surge Protection in Photovoltaic Installations. *IEEE Transactions on Power Delivery, 23*(4), 1961-1971.

Houshmand, M., Zandi, H. M., & Gorji, N. E. (2015). SCAPS Modeling for Degradation of Ultrathin CdTe Films: Materials Interdiffusion. *JOM, 67*(9), 2062-2070.

Hussein, H. S., Ahmad, G. E., & El-Ghetany, H. H. (2004). Performance evaluation of photovoltaic modules at different tilt angles and orientations. *Energy Conversion & Management, 45*, 2441-2452.

IEA. (2014). *World Energy Outlook.* Paris: IEA.

IEA. (2015). *Key World Energy Statistics.* Paris: IEA.

IEA. (2016). *Energy and Air Pollution.* Paris: IEA.

IEA-ETSAP and IRENA. (2013). *Solar Photovoltaic Technology Brief E11*. IEA-ETSAP and IRENA.

IEA-PVPS. (2014). *Characterisation of Performance of Thin-film Photovoltaic Technologies.* Paris: IEA.

IEA-PVPS. (2014). *Transition From Uni-Directional to Bi-directional Distribution Grids.* Paris: IEA.

IEA-PVPS. (2015). *Trends in Photovoltaic Applications.* Paris: IEA.

IEA-PVPS. (2016). *A Methodology for the Analysis of PV Self-Consumption Policies.* Paris: IEA.

IEA-PVPS. (2016). *Review and Analysis of PV Self-Consumption Policies.* Paris: IEA.

IEC 60269-6:2010. (2010). *Low-voltage fuses - Part 6: Supplementary requirements for fuse-links for the protection of solar photovoltaic energy systems.* Geneva: Switzerland: International Electrotechnical Commission.

IEC 60364-4-41:2005. (2005). *Low-voltage electrical installations - Part 4-41: Protection for safety - Protection against electric shock.* Geneva: Switzerland: International Electrotechnical Commission.

IEC 60634-7-712:2002. (2002). *Electrical installations of buildings - Part 7-712: Requirements for special installations or locations - Solar photovoltaic (PV) power supply systems.* Geneva:Switzerland: International Electrotechnical Commission.

IEC 60755. (2008). *General requirements for residual current operated protective devices.* Geneva: Switzerland: International Electrotechnical Commission.

IEC 61724:1998. (1998). *Photovoltaic system performance monitoring - Guidelines for measurement, data exchange and analysis.* Geneva: Switzerland: International Electrotechnical Commission.

IEC 61730-2:2016. (2016). *Photovoltaic (PV) module safety qualification - Part 2: Requirements for testing.* Geneva: Switzerland: International Electrotechnical Commission.

IEC 62305:2013. (2013). *Protection against lightning.* Geneva: Switzerland: International Electrotechnical Commission.

International Finance Corporation. (2012). *Utility Scale Solar Power Plants: A Guide For Developers and Investors.* New Delhi: International Finance Corporation.

IPCC. (2014). *Climate Change 2014: Mitigation of Climate Change. Contribution of Working Group III to the Fifth Assessment.* Cambridge, United Kingdom and New York, NY, USA: Cambridge University Press.

IPCC. (2015). *Climate Change 2014: Synthesis Report.* Geneva, Switzerland: IPCC.

IRENA. (2016). *G20 Toolkit for Renewable Energy Deployment: Country Options for Sustainable Growth Based on REmap.* Abu Dhabi: IRENA.

ISO 9060:1990. (1990). *Solar energy - Specification and classification of instruments for measuring hemispherical solar and direct solar radiation.* Geneva: Switzerland: ISO.

JRC. (2014). *Cost Maps for Unsubsidised Photovoltaic Electricity.* Ispra, Italy: JRC.

JRC. (2014). *PV Status Report 2014.* Ispra, Italy: JRC.

Kacira, M., Simsek, M., Babur, Y., & Demirkol, S. (2004). Determining Optimum Tilt Angles and Orientations of Photovoltaic Panels in Sanliurfa. *Renewable Energy, 29,* 1265-1275.

Kaldellis, J., & Zafirakis, D. (2012). Experimental investigation of the optimum Photovoltaic panels' tilt angle during the summer period. *Energy, 38,* 305-314.

Kalogirou, S. A. (2009). *Solar Energy Engineering: Processes and Systems.* Elsevier.

Kerekes, T., Koutroulis, E., Sera, D., Teodorescu, R., & Katsanevakis, M. (2013). An Optimization Method for Designing Large PV Plants. *IEEE Journal of Photovoltaics, 3*(2), 814-822.

KIB-TEK, 2015. Tarifeler. Retrieved 2 February 2016 from www. kibtek. com/ tarifeler/

Kondrashov, A., & Booth, T. (2015, March/April). Distribution and Substation Transformers. *SolarPro Magazine*, pp. 18-30.

Kumar, K. A., & Eichner, J. (2013). *Guidance on proper residual current device selection for solar inverters.* Schneider Electric.

Kurtz, S., Whitfield, K., Miller, D., Joyce, J., Wohlgemuth, J., Kempe, M., . . . Zgonena, T. (2009). Evaluation of high-temperature exposure of rack-mounted photovoltaic modules. 34 IEEE Photovoltaic Specialists Conference (PVSC) (pp. 2399-2404). Philadelphia, PA: IEEE.

Liserre, M., Sauter, T., & Hung, J. Y. (2010). Future Energy Systems: Integrating Renewable Energy Sources into the Smart Power Grid Through Industrial Electronics. *IEEE Industrial Electronics Magazine, 4*(1), 18-37.

Luthander, R., Widén, J., Nilsson, D., & Palm, J. (2015). Photovoltaic Self-Consumption in Buildings: A Review. *Applied Energy, 142*, 80-94.

Maranda, W., & Piotrowicz, M. (2014). Sizing of Photovoltaic Array for Low Feed-in Tariffs. 21st International Conference of Mixed Design of Integrated Circuits and Systems (MIXDES) (pp. 405-408). Dublin: IEEE.

Markides, G., Zinsser, B., Norton, M., Georghiou, G. E., Schubert , M., & Werner , J. H. (2010). Potential of photovoltaic systems in countries with high solar irradiation. *Renewable and Sustainable Energy Reviews, 14*(2), 754-762.

Markides, G., Zinsser, B., Schubert, M., & Georghiou, G. E. (2014). Performance Loss Rate of Twelve Photovoltaic Technologies Under Field Conditions Using Statistical Techniques. *Solar Energy, 103*, 28-42.

MCS. (2012). *Guide to the Installation of Photovoltaic Systems.* London: Microgeneration Certification Scheme.

Mehleri, E. D., Zervas, P. L., Sarimveis, H., Palyvos, J. A., & Markatos, N. C. (2010). Determination of the Optimal Tilt Angle and Orientation for Solar PV Arrays. *Renewable Energy, 35*, 2468-2475.

Merei, G., Moshövel, J., Magnor, D., & Sauer, D. U. (2016). Optimization of self-consumption and techno-economic analysis of PV-battery systems in commercial applications. *Applied Energy*, *168*, 171-178.

Mondol, J. D., Yohanis, Y. G., & Norton, B. (2006). Optimal sizing of array and inverter for grid-connected photovoltaic systems. *Solar Energy, 80*(12), 1517-1539.

Mondol, J. D., Yohannis, Y. G., & Norton, B. (2007). The Impact of Array Inclination and Orientation on the Performance of a Grid-connected Photovoltaic Systems. *Renewable Energy, 32*, 118-140.

Muneer, W., Bhattacharya, K., & Cañizares, C. A. (2011). Large-Scale Solar PV Investment Models, Tools, and Analysis: The Ontario Case. *IEEE Transactions on Power Systems, 26*(4), 2547-2555.

Notton, G., Lazarov, V., Stoyanov, L., & Heraud, N. (2009). Grid-connected photovoltaic system: Optimization of the inverter size using an energy

approach. 8th International Symposium on Advanced Electromechanical Motion Systems & Electric Drives (pp. 1-7). Lille: IEEE.

NREL. (2012). *Impacts of Regional Electricity Prices and Building Type on the Economics of Commercial Photovoltaic Systems.* CO, United States: NREL.

NREL. (2012). *The Impact of Financial Structure on the Cost of Solar Energy.* CO, United States: NREL.

NREL. (2013). *Land-Use Requirements for Solar Power Plants in the United States.* CO, United States: NREL.

NREL. (2015). *U.S. Photovoltaic Prices and Cost Breakdowns: Q1 2015 Benchmarks for Residential, Commercial, and Utility-Scale Systems.* CO, United States: NREL.

OBO Betermann. (2015). *Transient and lightning protection systems.* Menden, Germany: OBO Bettermann.

Pons, E., & Tommasini, R. (2013). Lightning protection of PV systems. 4th International Youth Conference on Energy (IYCE) (pp. 1-5). IEEE.

Rajender, K., Rajapandiyan, K., & Vallisaranya. (2014). Transformer Rating for Solar PV Plants Based on Overloading Capability as per Guidelines. IEEE Region 10 Humanitarian Technology Conference (R10-HTC) (pp. 19-24). Chennai: IEEE.

REN21. (2015). *Renewables 2015: Global Status Report.* Paris: REN21.

REN21. (2016). *Renewables 2016: Global Status Report.* Paris: REN21.

Rhodes, J. D., Upshaw, C. R., Cole, W. J., Holcomb, C. L., & Webber, M. E. (2014). A multi-objective assessment of the effect of solar PV array orientation and tilt on energy production and system economics. *Solar Energy, 108*, 28-40.

Sadineni, S. B., Atallah, F., & Boehm, R. F. (2012). Impact of roof integrated PV orientation on the residential electricity peak demand. *Applied Energy, 92*, 204-210.

Sankar, A., & Kalathil, A. (2014). Qualitative validation of empirically observed higher generation in East-West orientated PV arrays over conventional South orientation. IEEE Region 10 Humanitarian Technology Conference (pp. 25-28). Chennai: IEEE.

Schletter Solar-Montagesysteme. (2014). *Lightning protection of photovoltaic plants: Tips and hints for the mounting system.* Germany: Schletter Solar-Montagesysteme.

Schneider Electric. (2015). *Electrical Installation Guide.* Rueil-Malmaison: Schneider Electric.

Şenol, M., Abbasoğlu, S., Kükrer, O., & Babatunde, A. A. (2016). A guide in installing large-scale PV power plant for self consumption mechanism. *Solar Energy,* 518-537.

Shah, R., Mithulananthan, N., Bansal, R. C., & Ramachandaramurthy, V. K. (2015). A Review of Key Power System Stability Challenges for Large-Scale PV Integration. *Renewable and Sustainable Energy Reviews, 41*, 1423-1436.

Sharaf Eldin, S. A., Abd-Elhady, M. S., & Kandil, H. A. (2016). Feasibility of solar tracking systems for PV panels in hot and cold regions. *Renewable Energy, 85*, 228-233.

Shu, N., Kameda, N., Kishida, Y., & Sonoda, H. (2006). Experimental and Theoretical Study on the Optimal Tilt Angle of Photovoltaic Panels. *Journal of Asian Architecture and Building Engineering, 5*(2), 399-405.

SMA Solar Technology AG. (2008). *SMA Advisory Guide: Decentralized Inverter Technology in Large-Scale PV Plants* (1.1. ed.). Niestetal: SMA Solar Technology AG.

SMA Solar Technology AG. Sunny Tripower 25000TL Datasheet.

Talavera, D. L., de la Casa, J., Muñoz-Cerón, E., & Almonacid, G. (2014). Grid parity and self-consumption with photovoltaic systems under the present regulatory framework in Spain: The case of the University of Jaén Campus. *Renewable and Sustainable Energy Reviews, 33*, 752-771.

Tiris, M., & Tiris, C. (1998). Optimum collector slope and model evaluation: Case study for Gebze, Turkey. *Energy Conversion & Management, 39*(3/4), 167-172.

UNEP. (2015). *Climate commitments of subnational actors and business: A quantitative assessment of their emission reduction impact.* Nairobi: United Nations Environment Programme (UNEP).

Velasco, G., Piqué, R., Guinjoan, F., Casellas, F., & de la Hoz, J. (2010). Power Sizing Factor Design of Central Inverter PV Grid-Connected Systems: A Simulation Approach. 14th International Power Electronics and Motion Control Conference (EPE/PEMC) (pp. 9.32-9.36). Ohrid: IEEE.

Vokas, G. A., Zoridis, G. C., & Lagogiannis, K. V. (2015). Single and dual axis PV energy production over Greece: Comparison between measured and predicted data. International Conference on Technologies and Materials for Renewable Energy, Environment and Sustainability. *74*, pp. 1490-1498. Beirut: Energy Procedia.

World Economic Form. (2013). *Energy Transitions: Past and Future.* World Economic Forum.

Yakup, M., & Malik, A. Q. (2001). Optimum tilt angle and orientation for solar collector in Brunei Darussalam. *Renewable Energy, 24*, 223-234.

Yılmaz, A., Kocer, A., Yaka, İ. F., & Güngör, A. (2016). Determination of Optimum Tilt Angle on Solar Thermal Collectors for Batman Province of Turkey. Proceedings of SolarTR Conference (pp. 669-673). İstanbul: GUNDER.

Yingli Green Energy Holding Company. YL310P-35b Data Sheet. *YGE 72 Cells HN Series*.